

Euler Obstructed Cooper Pairing in Twisted Bilayer Graphene: Nematic Nodal Superconductivity and Bounded Superfluid Weight

Jiabin Yu,^{1,*} Ming Xie,¹ Fengcheng Wu,^{2,3} and Sankar Das Sarma¹

¹*Condensed Matter Theory Center and Joint Quantum Institute,
Department of Physics, University of Maryland, College Park, MD 20742, USA*

²*School of Physics and Technology, Wuhan University, Wuhan 430072, China*

³*Wuhan Institute of Quantum Technology, Wuhan 430206, China*

Magic-angle twisted bilayer graphene (MATBG) hosts normal-state nearly-flat bands with nonzero Euler numbers and shows superconductivity. In this work, we study the effects of the nontrivial normal-state band topology on the intervalley $C_{2z}\mathcal{T}$ -invariant mean-field Cooper pairing order parameter in MATBG. We show that the pairing order parameter can always be split into a trivial channel and an Euler obstructed channel in all gauges for the normal-state basis, generalizing the previously-studied channel splitting in the Chern gauge. The nonzero normal-state Euler numbers require the pairing gap function of the Euler obstructed channel to have zeros, while the trivial channel can have a nonvanishing pairing gap function. When the pairing is spontaneously nematic, we find that a sufficiently-dominant Euler obstructed channel with two zeros typically leads to nodal superconductivity. Under the approximation of exactly-flat bands, we find that the mean-field zero-temperature superfluid weight is generally bounded from below, no matter whether the Euler obstructed channel is dominant or not, generalizing the previously-derived bound for the uniform s-wave pairing. We numerically verify these statements for pairings derived from a local attractive interaction. Our work suggests that Euler obstructed Cooper pairing may play an essential role in the superconducting MATBG.

I. INTRODUCTION

The normal state of MATBG (*i.e.*, twisted bilayer graphene with twist angle near 1.1° [1–3]) was theoretically shown to host topologically nontrivial nearly-flat bands near the charge neutrality, based on the Bistritzer-MacDonald (BM) model [3–7]. The nontrivial band topology is characterized by the $C_{2z}\mathcal{T}$ -protected nonzero Euler numbers [7] (or equivalently Wilson loop winding numbers [5]), where C_{nj} is the spinless part of the n -fold rotation about the j axis (with $j = z$ out of plane) and \mathcal{T} is the spinful time-reversal symmetry. When the nearly-flat bands are partially filled, superconductivity was observed in MATBG [2, 8–16], and the superconductivity may be nematic [12] (despite some debate [17]) and nodal [14, 15] when there are 2~3 holes per moiré unit cell. Here being nematic means breaking C_{3z} . Various theoretical mechanisms [18–39] have been proposed to explain the observed superconductivity. Yet, it is still unclear whether the potential nematic nodal feature of the superconducting MATBG has any relation to the normal-state Euler numbers.

In this work, we reveal the relation by studying the intervalley $C_{2z}\mathcal{T}$ -invariant mean-field pairing order parameter that is either spin-singlet or spin-triplet with a momentum-independent spin direction, which is energetically possible in MATBG [24, 26, 27]. By generalizing the theory for 3D semimetals in Ref. [40], we find that regardless of the gauge for the normal-state basis, the pairing order parameter can always be split into one trivial

channel and one nontrivial channel. The nonzero normal-state Euler numbers require the pairing gap function of the nontrivial channel to have zeros, and determine the total winding number of the zeros, whereas the trivial channel is allowed to have a nonvanishing pairing gap function. Then, the nontrivial channel is called the Euler obstructed pairing channel. Our gauge-independent formalism of the Euler obstructed Cooper pairing is a generalization of the known channel splitting in the Chern gauge [29, 41–44] (or for the Chern bands [45–47]); our gauge-independent formalism is more convenient for numerical calculations as it saves us from explicit gauge fixing.

When the considered $C_{2z}\mathcal{T}$ -invariant pairing is spontaneously nematic, we find that a sufficiently-dominant Euler obstructed channel with two zeros typically leads to nodal superconductivity. This serves as a mechanism that connects the nematic pairing to nodal superconductivity, although a nematic pairing in general does not necessarily lead to nodal superconductivity [48] (especially in multi-band cases like MATBG). Our mechanism roots in the normal-state Euler numbers, and our mechanism is general in the sense that it is independent of the specific interaction that accounts for the considered pairing form. We would like to mention that the role of nematicity in the Euler-obstructed-pairing-induced nodal superconductivity revealed in the current work is absent in Ref. [40].

We further provide analytic and numerical supports for the potential existence of a spontaneously-nematic dominant Euler obstructed pairing in MATBG. First, we use the formalism of Euler obstructed pairing to analytically derive a lower bound of the mean-field zero-temperature superfluid weight for the considered $C_{2z}\mathcal{T}$ -

* jiabinyu@umd.edu

invariant pairing, under the exact-flat-band approximation. Our bound generalizes the previously-derived bound for time-reversal invariant uniform s-wave pairing in Ref. [49]. Thus, under the exact-flat-band approximation, the superfluid weight is bounded from below even for pairings with a dominant Euler obstructed channel, regardless of the specific interaction that accounts for the pairing form. Second, we numerically verify the above statements for the pairings given by a local attractive interaction; the interaction has a similar form as that mediated by acoustic phonons [24, 26, 27]. In particular, we find that a spontaneously-nematic pairing with a dominant Euler obstructed channel can arise from the local interaction, which, together with the bounded superfluid weight, implies the potential existence of a spontaneously-nematic dominant Euler obstructed pairing in MATBG.

II. EULER OBSTRUCTED COOPER PAIRING IN MATBG

We start by introducing the Euler obstructed Cooper pairing in MATBG. The BM model contains two decoupled valley \pm related by the C_{2z} or \mathcal{T} symmetries, and within each valley, the model has $C_{2z}\mathcal{T}$, C_{3z} and spin-charge $U(2)$ symmetries. Because of the normal-state global spin $SU(2)$ symmetry, we only need to consider the spinless parts for C_{nz} , as mentioned above. The model has other exact and approximate symmetries [5, 50], but they are not required for the discussion below. With the twist angle θ near 1.1° , BM model captures the normal state of MATBG (that is not aligned with the hBN substrate [47]), and has two nearly-flat bands with additional spin degeneracy near the charge neutrality in each valley. We use $|u_{\pm, \mathbf{k}, a}\rangle \otimes |s\rangle$ to label the periodic parts of the Bloch basis for the nearly-flat bands, where $a = 1, 2$ labels the spinless basis of the two nearly-flat bands in one valley, and $s = \uparrow, \downarrow$ is the spin index. Defining $|u_{\pm, \mathbf{k}}\rangle = (|u_{\pm, \mathbf{k}, 1}\rangle, |u_{\pm, \mathbf{k}, 2}\rangle)$, the nontrivial topology of $|u_{\pm, \mathbf{k}}\rangle$ is manifested by the nonzero Euler number or Wilson loop winding number $\mathcal{N}_{\pm} = 1$ [5, 7, 40].

For the superconductivity in MATBG, we only consider the pairing between the nearly-flat bands, owing to the large normal-state band gaps ($\sim 20\text{meV}$) above and below the nearly-flat bands. We consider the following mean-field Cooper pairing operator

$$H_{\text{pairing}} = \sum_{\mathbf{k} \in \text{MBZ}} c_{+, \mathbf{k}}^\dagger \Delta(\mathbf{k}) \otimes \Pi(c_{-, -\mathbf{k}}^\dagger)^T + h.c., \quad (1)$$

where $c_{\pm, \mathbf{k}}^\dagger = (\dots, c_{\pm, \mathbf{k}, a, s}^\dagger, \dots)$ and $c_{\pm, \mathbf{k}, a, s}^\dagger$ is the creation operator for the Bloch state of $|u_{\pm, \mathbf{k}, a}\rangle \otimes |s\rangle$, and MBZ is short for moiré Brillouin zone. We have chosen and will always choose the pairing to be intervalley, since only the intervalley pairing can couple electrons with exactly the same energy and opposite momenta. Throughout the work, we also choose the pairing to be $C_{2z}\mathcal{T}$ -invariant

and to have a momentum-independent spin part Π . In particular, we consider two cases for Π , (i) spin-singlet $\Pi = is_y$ and (ii) spin-triplet $\Pi = i(\hat{n} \cdot \mathbf{s})is_y$ with \hat{n} any real momentum-independent unit vector, where $s_{x,y,z}$ are Pauli matrices for the spin index. For spin-triplet, we can always choose the spin index of the basis to keep $\hat{n} = (0, -1, 0)$, *i.e.*, $\Pi = s_0$. The chosen pairing form is satisfied by certain solutions of the mean-field linearized gap equation owing to the $C_{2z}\mathcal{T}$ and spin $SU(2)$ symmetries in the normal state [24, 26, 27], but remains an assumption at zero temperature. $\Delta(\mathbf{k})$ in Eq. (1) is the spinless part of the pairing gap function, which is the focus of our work.

Before our work, there were related discussions [29, 41–44, 47, 51] on how the normal-state band topology affects $\Delta(\mathbf{k})$ in the Chern gauge [49, 52–54] for $|u_{\pm, \mathbf{k}}\rangle$, which we specify below for our chosen pairing form. In the Chern gauge, $|u_{\pm, \mathbf{k}, a}\rangle$ has well-defined Chern number $C_{\pm, a}$; we henceforth choose $C_{\pm, 1} = -C_{\pm, 2} = \mathcal{N}_{\pm} = 1$ and choose the following symmetry representations for the Chern gauge

$$\begin{aligned} (C_{2z}\mathcal{T})c_{\pm, \mathbf{k}}^\dagger(C_{2z}\mathcal{T})^{-1} &= c_{\pm, \mathbf{k}}^\dagger \tau_x \otimes is_y \\ C_{2z}c_{+, \mathbf{k}}^\dagger C_{2z}^{-1} &= c_{-, -\mathbf{k}}^\dagger, \end{aligned} \quad (2)$$

where τ 's are the Pauli matrices for the spinless basis. Based on the Chern numbers of the paired Chern states [44], we can split $\Delta(\mathbf{k})$ into two channels as

$$\Delta(\mathbf{k}) = \Delta_{\parallel}(\mathbf{k}) + \Delta_{\perp}(\mathbf{k}), \quad (3)$$

where Δ_{\parallel} (Δ_{\perp}) contains the pairings between Chern states with the same (opposite) Chern numbers (Fig. 1(a)). [55] Owing to $C_2\mathcal{T}$ symmetry, we have

$$\Delta_{\parallel}(\mathbf{k}) = \begin{pmatrix} d_{\parallel}^*(\mathbf{k}) & \\ & d_{\parallel}(\mathbf{k}) \end{pmatrix}, \quad \Delta_{\perp}(\mathbf{k}) = \begin{pmatrix} & d_{\perp}(\mathbf{k}) \\ d_{\perp}^*(\mathbf{k}) & \end{pmatrix}, \quad (4)$$

where $d_b(\mathbf{k}) = |\Delta_b(\mathbf{k})|e^{i\theta_b(\mathbf{k})}$ with $b = \perp, \parallel$, and $|\Delta_b(\mathbf{k})| = \sqrt{\text{Tr}[\Delta_b(\mathbf{k})\Delta_b^\dagger(\mathbf{k})]}/2$. If Δ_b has zeros (*i.e.*, $|\Delta_b|$ has zeros) but is not everywhere-vanishing, an integer winding number can naturally be defined for each isolated zero i of Δ_b as

$$\mathcal{W}_{b,i} = -\frac{(-1)^b}{2\pi} \int_{\gamma_{b,i}} d\mathbf{k} \cdot \nabla_{\mathbf{k}} \theta_b(\mathbf{k}) \quad (5)$$

where $(-1)^\perp = 1$, $(-1)^\parallel = -1$, and $\gamma_{b,i}$ is a circle around the zero i of Δ_b . Then, Ref. [45, 46] (which studied the pairing between Chern states) suggests that

$$\begin{aligned} \sum_i \mathcal{W}_{\perp,i} &= C_{+,1} + C_{-,2} = 0, \\ \sum_i \mathcal{W}_{\parallel,i} &= -C_{+,2} - C_{-,2} = 2. \end{aligned} \quad (6)$$

(See SM for details.) As the total winding number $\sum_i \mathcal{W}_{b,i}$ is by definition zero if Δ_b has no zeros, Eq. (6)

suggests that Δ_{\parallel} must have zeros, while Δ_{\perp} can be non-vanishing [44–46]. According to the terminology defined in Ref. [45], Eq. (4) and Eq. (6) suggest that each element of Δ_{\parallel} in the Chern gauge is a monopole Cooper pairing, since the nonzero total winding indicates that the monopole Harmonics [56] are required for the full description of Δ_{\parallel} in the Chern gauge. Thus, Δ_{\parallel} in the Chern gauge can be viewed as a $C_{2z}\mathcal{T}$ -protected double version of monopole Cooper pairing.

The relation between Δ_{\parallel} and the monopole Cooper pairing relies on the Chern gauge, because the monopole Cooper pairing is only defined between Chern states. Nevertheless, as a generalization of Ref. [40] (generalization from sphere-like Fermi surfaces in Ref. [40] to torus-like MBZ here), we find that the channel splitting into trivial Δ_{\perp} and nontivial Δ_{\parallel} can be done for all gauges (even beyond the Chern gauge) by using the Wilson line and the gauge-invariant operator $P_{\Delta}(\mathbf{k}) = |u_{+,\mathbf{k}}\rangle\Delta(\mathbf{k})\langle u_{-,-\mathbf{k}}|$, where $|u_{\pm,\mathbf{k}}\rangle = C_{2z}\mathcal{T}|u_{\pm,\mathbf{k}}\rangle$. The gauge transformations of the generally defined Δ_{\parallel} and Δ_{\perp} are the same as the gauge transformation of Δ , meaning that $|\Delta_b(\mathbf{k})|$ and the zeros of $\Delta_b(\mathbf{k})$ are gauge invariant. Then, we can define the gauge-invariant winding number $W_{b,i}$ for the i th zero of $\Delta_b(\mathbf{k})$, and have

$$\sum_i W_{b,i} = \mathcal{N}_+ - (-1)^b \mathcal{N}_- = 1 - (-1)^b. \quad (7)$$

(See SM for details.) It means that the zeros of Δ_{\parallel} are generally enforced by the Euler numbers \mathcal{N}_{\pm} for any gauges of the normal-state basis, even when the normal-state gauges do not have well-defined Chern numbers. In other words, Eq. (6) in Chern gauge is just a special case of the gauge-independent Eq. (7). Therefore, Δ_{\parallel} is called the Euler obstructed pairing channel.

Typically, the parity-even inter-sublattice pairing tends to have a dominant Δ_{\parallel} , where the parity is equal (opposite) to the C_{2z} eigenvalue for the spin-singlet (spin-triplet) pairings. To show this, we can use the Chern gauge since $|\Delta_b|$ is gauge-invariant. Based on Eq. (2) and Eq. (4), we find that $|\Delta_{\parallel}| = 0$ for parity-odd pairing, and thus only the parity-even pairing can have a dominant Δ_{\parallel} . Then, since the states in the Chern gauge are polarized to the sublattice A or B of the BM model [41, 57] (see also Fig. 1(b)), the parity-even Δ_{\parallel} (Δ_{\perp}) mainly corresponds to inter-sublattice (intra-sublattice) pairing.

III. NEMATIC NODAL SUPERCONDUCTIVITY IN MATBG

Next we consider the case where the Euler obstructed pairing channel is sufficiently dominant, implying that $|\Delta_{\perp}|$ is perturbatively small compared to $|\Delta_{\parallel}|$ and the pairing is parity-even, and discuss the resultant nodal superconductivity. We only need to study the gapless nodes of the spin-up block of the Bogoliubov-de Gennes (BdG) Hamiltonian in $+$ valley, whose matrix representation is labelled as $\mathcal{H}(\mathbf{k})$ for basis $(c_{+,\mathbf{k},\uparrow}^{\dagger}, c_{-,\mathbf{k},\downarrow}^T)$ with

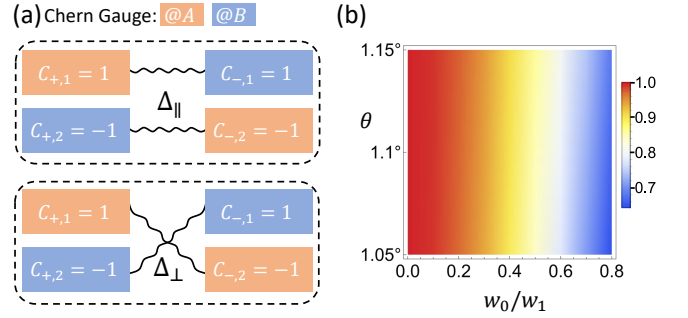


FIG. 1. (a) Schematic illustration of the two channels Δ_{\parallel} and Δ_{\perp} (Eq. (4)) in the Chern gauge. The blocks stand for the spinless basis for the nearly-flat bands in the Chern gauge, where \pm stand for the valleys. The orange and purple blocks stand for the normal states that are polarized to the sublattice A and B [57], respectively, though the polarization may not be complete [41]. (b) Plot of the probability of $|u_{+,1}(\mathbf{k})\rangle$ in the Chern gauge at sublattice A averaged over the MBZ, showing the sublattice polarization discussed in Ref. [41, 57]. w_0 and w_1 are the interlayer AB and AA tunneling strengths in the BM model, respectively.

$c_{\pm,\mathbf{k},s}^{\dagger} = (c_{\pm,\mathbf{k},1,s}^{\dagger}, c_{\pm,\mathbf{k},2,s}^{\dagger})$; it is because the BdG gapless nodes are the same for the spin-down block owing to the normal-state spin $SU(2)$ symmetry and the pairing form Eq. (1), and the BdG gapless nodes for the $-$ valley can be obtained from the particle-hole symmetry. As the presence or absence of BdG nodes is gauge-independent, we use the Chern gauge for convenience, resulting in

$$\mathcal{H}(\mathbf{k}) = \begin{pmatrix} h_+(\mathbf{k}) - \mu & \Delta_{\perp}(\mathbf{k}) + \Delta_{\parallel}(\mathbf{k}) \\ [\Delta_{\perp}(\mathbf{k}) + \Delta_{\parallel}(\mathbf{k})]^{\dagger} & -h_+^T(\mathbf{k}) + \mu \end{pmatrix}, \quad (8)$$

where μ is the chemical potential, $h_+(\mathbf{k}) = \epsilon(\mathbf{k}) + \text{Re}[f(\mathbf{k})]\tau_x + \text{Im}[f(\mathbf{k})]\tau_y$ describes the normal-state nearly-flat bands in valley $+$, the form of $\Delta_b(\mathbf{k})$ is in Eq. (4), and we choose the zero-point energy such that $\epsilon(K_M) = 0$.

Owing to the parity-even nature of the pairing, \mathcal{H} has an effective spinless $C_{2z}\mathcal{T}$ symmetry as $\rho_0\tau_x\mathcal{K}$ and a chiral symmetry $i\rho_y\tau_x$, belonging to the nodal class CI which can support stable zero-energy BdG gapless points protected by nonzero chiralities [58]. Here, \mathcal{K} is the complex conjugate, and ρ 's are the Pauli matrices for the particle-hole index. (See SM for details.) In the following, we will discuss the Δ_{\parallel} -guaranteed nodal superconductivity based on \mathcal{H} for both C_{3z} -invariant and spontaneously nematic pairings. We choose $\mu \in [\epsilon(\Gamma_M) - |f(\Gamma_M)|, \epsilon(\Gamma_M) + |f(\Gamma_M)|]$, which is typically true for 2~3 holes per moiré unit cell since the bottom and top of the set of nearly-flat bands are typically at Γ_M for realistic parameter values. (See SM for details.) We also choose the Euler obstructed Δ_{\parallel} (or equivalently $d_{\parallel}(\mathbf{k})$) to only have two zeros with winding 1, since more zeros typically require more complex pairing structure which tends to be physically unfavored.

A sufficiently-dominant Δ_{\parallel} guarantees \mathcal{H} to be gapless only if $\mathcal{H}^{(0)}$ (which is \mathcal{H} with $|\Delta_{\perp}| = 0$) is gapless. By diagonalizing $\mathcal{H}^{(0)}$, we find that $\mathcal{H}^{(0)}$ is gapless if and only if $\mu \in E(\Sigma)$, where Σ and $E(\Sigma)$ are defined in the following. Let us consider the following deformation

$$d_{\parallel}(\mathbf{k}) \pm \lambda f(\mathbf{k}), \quad (9)$$

where λ is gradually increased from 0 to 1. Owing to the normal-state Euler numbers, Eq. (9) must have zeros for all $\lambda \in [0, 1]$, since the deformation cannot merge the initial two zeros of $d_{\parallel}(\mathbf{k})$ that have the same winding. Then, the zeros of Eq. (9) for all $\lambda \in [0, 1]$ constitute Σ , and $E(\Sigma)$ consists of the values of $\epsilon(\mathbf{k}) \pm \sqrt{|f(\mathbf{k})|^2 - |d_{\parallel}(\mathbf{k})|^2}$ for all \mathbf{k} in Σ . (See SM for details.)

The difference between C_{3z} -invariant and spontaneously nematic pairings lies in the different shapes of Σ . $f(\mathbf{k})$ typically has two zeros at K_M and K'_M (Fig. 2(a)). For C_{3z} -invariant pairing, the two zeros of $d_{\parallel}(\mathbf{k})$ are also pinned at K_M and K'_M by the C_{3z} symmetry. Then, Eq. (9) is typically zero at K_M and K'_M , meaning that the initial two zeros of $d_{\parallel}(\mathbf{k})$ typically does not move during the deformation. As a result, Σ is typically localized in the neighborhood of K_M and K'_M (the simplest case shown in Fig. 2(b)), and $E(\Sigma)$ only contains energies close to zero, leading to gapped $\mathcal{H}^{(0)}$ for considerably large μ . Therefore, a sufficiently-dominant Δ_{\parallel} cannot always guarantee nodal superconductivity when the pairing is C_{3z} -invariant, even if fine-tuning cases are ruled out. (See SM for details.)

On the other hand, for spontaneously nematic pairing, only one of the two zeros of $d_{\parallel}(\mathbf{k})$ is constrained by the C_{3z} eigenvalues, and is pinned at Γ_M . Then, without invoking fine tuning, there must be continuous paths connecting Γ_M to zeros of $d_{\parallel}(\mathbf{k}) \pm i f(\mathbf{k})$ (Fig. 2(c)), resulting that $\mu \in [\epsilon(\Gamma_M) - |f(\Gamma_M)|, \epsilon(\Gamma_M) + |f(\Gamma_M)|] \subset E(\Sigma)$ and then $\mathcal{H}^{(0)}$ has gapless nodes with nonzero chiralities. Therefore, when the pairing is spontaneously nematic, a sufficiently-dominant Δ_{\parallel} can always guarantee nodal superconductivity unless invoking fine tuning. (See SM for details.)

The above mechanism for nematic nodal superconductivity is different from that discussed in Ref. [27] since the latter does not involve any normal-state band topology. More importantly, the mechanism in Ref. [27] relies on a scalar pairing, which is not required in our work. (See SM for details.)

The statements in the above discussion are independent of the specific form of the interaction that accounts for the pairing form Eq. (1). Nevertheless, we use a local attractive interaction, which has a similar form as that mediated by the acoustic phonons [24, 26, 27], to verify these general statements. According to Ref. [26], by tuning the interaction strength, we can get two types of $C_{2z}\mathcal{T}$ -invariant intervalley parity-even pairings: C_{3z} -invariant intra-sublattice pairings and spontaneously-nematic inter-sublattice pairings. We obtain spin-triplet pairings of both types for 2.5 holes per moiré unit cell and $w_0/w_1 = 0.8$ by numerically solving the self-consistent

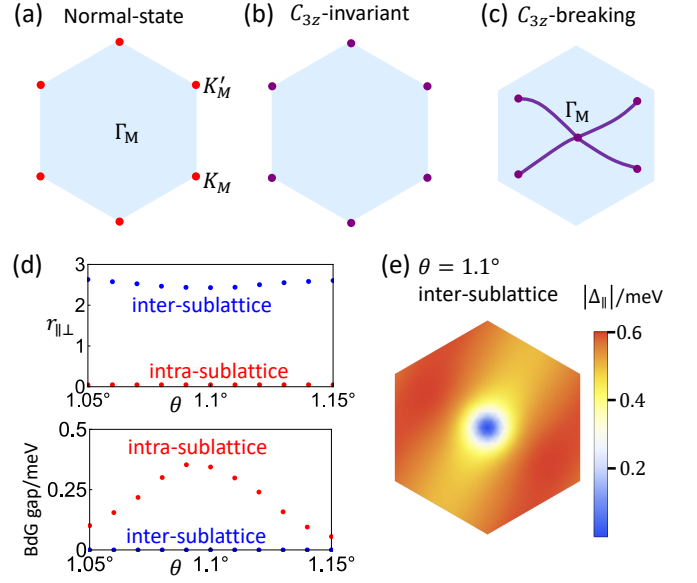


FIG. 2. (a) The normal-state Dirac cones (red dots, zeros of $f(\mathbf{k})$ in Eq. (8)) are typically located at K_M and K'_M in the MBZ (light blue). (b) Smallest Σ (defined below Eq. (9), purple) for C_{3z} -invariant pairing. (c) Illustrative Σ (purple) for spontaneously nematic pairing, when pinning both zeros of $\Delta_{\parallel}(\mathbf{k})$ at Γ_M . (d) Plots of the ratio $r_{\perp} = \langle |\Delta_{\perp}| \rangle / \max(|\Delta_{\perp}|)$ and the BdG gap for the intra-sublattice and inter-sublattice pairings induced by the local attractive interaction at zero temperature. θ is the twist angle, and $\langle |\Delta_b| \rangle$ and $\max(|\Delta_b|)$ are the averaged and maximum values of $|\Delta_b(\mathbf{k})|$ in the MBZ, respectively. (e) Plot of $|\Delta_{\parallel}|$ of the inter-sublattice pairing in the MBZ for $\theta = 1.1^\circ$ at zero temperature. $\Delta_{\parallel}(\mathbf{k})$ has two winding-1 zeros (or equivalently a winding-2 zero) at Γ_M , agreeing with the analogous discussion on the inter-Chern modes in Ref. [44].

equation, and find both the resultant intra-sublattice and inter-sublattice pairings have the form in Eq. (1). By using the gauge-invariant formalism, we find that the intra-sublattice and inter-sublattice pairings have dominant Δ_{\perp} and Δ_{\parallel} channels (Fig. 2(d)), respectively, agreeing with the above argument. Moreover, since the inter-sublattice pairing has two winding-1 zeros for Δ_{\parallel} (as exemplified in Fig. 2(e)), the corresponding BdG Hamiltonian must be nodal, which is also verified in Fig. 2(d). (See details in SM.) In short, the inter-sublattice pairing that we get from the local interaction is a spontaneously-nematic pairing that has an Euler obstructed channel dominant enough to guarantee nodal superconductivity.

Nodal superconductivity for the inter-valley inter-sublattice pairing was also shown in Ref. [59]. The 2D nodal superconductivity in Ref. [59] is enforced by the normal-state chiral-symmetry-protected winding numbers, but the normal-state chiral symmetry is not exact in the BM model with realistic parameter values. In contrast, our mechanism relies on the normal-state $C_{2z}\mathcal{T}$ -protected Euler numbers, which are exactly well-defined in the BM model with realistic parameter values.

IV. BOUNDED SUPERFLUID WEIGHT

We now discuss lower bound of superfluid weight within the mean-field approximation. We adopt the exact-flat-band approximation [49, 60–63], where we choose the normal-state flat bands to be exactly-flat. By using the formalism of Euler obstructed Cooper pairing, we obtain a lower bound for the trace of the zero-temperature superfluid weight for the $C_{2z}\mathcal{T}$ -invariant pairing in Eq. (1), which reads

$$\text{Tr}[D_{SF}] \geq \left\langle \frac{[|\Delta_{\perp}(\mathbf{k})| - |\Delta_{\parallel}(\mathbf{k})|]^2}{\sqrt{[|\Delta_{\perp}(\mathbf{k})| - |\Delta_{\parallel}(\mathbf{k})|]^2 + \mu^2}} \right\rangle_g \frac{4e^2}{\pi} \mathcal{N}_+, \quad (10)$$

where we have chosen the unit system in which $\hbar = c = 1$, e is the elementary charge,

$$\langle x(\mathbf{k}) \rangle_g = \frac{\int_{\text{MBZ}} d^2k x(\mathbf{k}) \text{Tr}[g(\mathbf{k})]}{\int_{\text{MBZ}} d^2k \text{Tr}[g(\mathbf{k})]}, \quad (11)$$

and $g_{ij}(\mathbf{k}) = \frac{1}{2} \text{Tr}[\partial_{k_i} P_+(\mathbf{k}) \partial_{k_j} P_+(\mathbf{k})]$ is the Fubini-Study metric for $P_+(\mathbf{k}) = |u_{+, \mathbf{k}}\rangle\langle u_{+, \mathbf{k}}|$. If we choose the time-reversal-invariant uniform s-wave pairing used in Ref. [49], Eq. (10) reproduces the lower bound presented in Ref. [49]; however our Eq. (10) holds for any pairing of the form Eq. (1), even if the pairing is not uniform s-wave (like the inter-sublattice pairing in Fig. 2). For MATBG with θ very close to 1.1° and with pair-

ings derived from the local attractive interaction mentioned above, the exact-flat-band approximation is valid for the study of the superfluid weight, and $\text{Tr}[D_{SF}]$ estimated from the bound in Eq. (10) is roughly 10^8 H^{-1} for both intra-sublattice and inter-sublattice pairings, similar to the values theoretically estimated in Ref. [49] and reported in Ref. [16], meaning that Eq. (10) is reasonably tight as a lower bound. (See details in SM.)

V. DISCUSSION

In summary, we have identified MATBG as a realistic superconductor that potentially hosts Euler obstructed Cooper pairing. In this work, we allow several symmetries (like C_{2x}) of the BM model to be broken either spontaneously or externally in the normal state. An interesting direction is to study the interplay between these symmetries and the Euler obstructed Cooper pairing.

VI. ACKNOWLEDGMENTS

J.Y. thanks B. Andrei Bernevig, Yang-Zhi Chou, Zhi-Da Song, and in particular Jie Wang for helpful discussions. This work is supported by Laboratory of Physical Science. F.W. is supported by start-up funds of Wuhan University.

-
- [1] Y. Cao, V. Fatemi, A. Demir, S. Fang, S. L. Tomarken, J. Y. Luo, J. D. Sanchez-Yamagishi, K. Watanabe, T. Taniguchi, E. Kaxiras, *et al.*, Correlated insulator behaviour at half-filling in magic-angle graphene superlattices, *Nature* **556**, 80 (2018).
 - [2] Y. Cao, V. Fatemi, S. Fang, K. Watanabe, T. Taniguchi, E. Kaxiras, and P. Jarillo-Herrero, Unconventional superconductivity in magic-angle graphene superlattices, *Nature* **556**, 43 (2018).
 - [3] R. Bistritzer and A. H. MacDonald, Moiré bands in twisted double-layer graphene, *Proceedings of the National Academy of Sciences* **108**, 12233 (2011).
 - [4] H. C. Po, L. Zou, A. Vishwanath, and T. Senthil, Origin of mott insulating behavior and superconductivity in twisted bilayer graphene, *Phys. Rev. X* **8**, 031089 (2018).
 - [5] Z. Song, Z. Wang, W. Shi, G. Li, C. Fang, and B. A. Bernevig, All magic angles in twisted bilayer graphene are topological, *Phys. Rev. Lett.* **123**, 036401 (2019).
 - [6] H. C. Po, L. Zou, T. Senthil, and A. Vishwanath, Faithful tight-binding models and fragile topology of magic-angle bilayer graphene, *Phys. Rev. B* **99**, 195455 (2019).
 - [7] J. Ahn, S. Park, and B.-J. Yang, Failure of nielsen-ninomiya theorem and fragile topology in two-dimensional systems with space-time inversion symmetry: Application to twisted bilayer graphene at magic angle, *Phys. Rev. X* **9**, 021013 (2019).
 - [8] M. Yankowitz, S. Chen, H. Polshyn, Y. Zhang, K. Watanabe, T. Taniguchi, D. Graf, A. F. Young, and C. R. Dean, Tuning superconductivity in twisted bilayer graphene, *Science* **363**, 1059 (2019).
 - [9] X. Lu, P. Stepanov, W. Yang, M. Xie, M. A. Aamir, I. Das, C. Urgell, K. Watanabe, T. Taniguchi, G. Zhang, A. Bachtold, A. H. MacDonald, and D. K. Efetov, Superconductors, orbital magnets and correlated states in magic-angle bilayer graphene, *Nature* **574**, 653 (2019).
 - [10] P. Stepanov, I. Das, X. Lu, A. Fahimniya, K. Watanabe, T. Taniguchi, F. H. L. Koppens, J. Lischner, L. Levitov, and D. K. Efetov, Untying the insulating and superconducting orders in magic-angle graphene, *Nature* **583**, 375–378 (2020).
 - [11] Y. Saito, J. Ge, K. Watanabe, T. Taniguchi, and A. F. Young, Independent superconductors and correlated insulators in twisted bilayer graphene, *Nature Physics* **16**, 926 (2020).
 - [12] Y. Cao, D. Rodan-Legrain, J. M. Park, N. F. Q. Yuan, K. Watanabe, T. Taniguchi, R. M. Fernandes, L. Fu, and P. Jarillo-Herrero, Nematicity and competing orders in superconducting magic-angle graphene, *Science* **372**, 264 (2021).
 - [13] F. K. de Vries, E. Portolés, G. Zheng, T. Taniguchi, K. Watanabe, T. Ihn, K. Ensslin, and P. Rickhaus, Gate-defined josephson junctions in magic-angle twisted bilayer graphene, *Nature Nanotechnology* **16**, 760 (2021).

- [14] M. Oh, K. P. Nuckolls, D. Wong, R. L. Lee, X. Liu, K. Watanabe, T. Taniguchi, and A. Yazdani, Evidence for unconventional superconductivity in twisted bilayer graphene, *Nature* **10.1038/s41586-021-04121-x** (2021).
- [15] G. D. Battista, P. Seifert, K. Watanabe, T. Taniguchi, K. C. Fong, A. Principi, and D. K. Efetov, Revealing the ultra-sensitive calorimetric properties of superconducting magic-angle twisted bilayer graphene (2021), [arXiv:2111.08735 \[cond-mat.supr-con\]](#).
- [16] H. Tian, S. Che, T. Xu, P. Cheung, K. Watanabe, T. Taniguchi, M. Randeria, F. Zhang, C. N. Lau, and M. W. Bockrath, Evidence for flat band dirac superconductor originating from quantum geometry (2021), [arXiv:2112.13401 \[cond-mat.supr-con\]](#).
- [17] T. Yu, D. M. Kennes, A. Rubio, and M. A. Sentef, Nematicity arising from a chiral superconducting ground state in magic-angle twisted bilayer graphene under in-plane magnetic fields, *Phys. Rev. Lett.* **127**, 127001 (2021).
- [18] C. Xu and L. Balents, Topological superconductivity in twisted multilayer graphene, *Phys. Rev. Lett.* **121**, 087001 (2018).
- [19] H. Guo, X. Zhu, S. Feng, and R. T. Scalettar, Pairing symmetry of interacting fermions on a twisted bilayer graphene superlattice, *Phys. Rev. B* **97**, 235453 (2018).
- [20] C.-C. Liu, L.-D. Zhang, W.-Q. Chen, and F. Yang, Chiral spin density wave and $d + id$ superconductivity in the magic-angle-twisted bilayer graphene, *Phys. Rev. Lett.* **121**, 217001 (2018).
- [21] H. Isobe, N. F. Q. Yuan, and L. Fu, Unconventional superconductivity and density waves in twisted bilayer graphene, *Phys. Rev. X* **8**, 041041 (2018).
- [22] D. M. Kennes, J. Lischner, and C. Karrasch, Strong correlations and $d + id$ superconductivity in twisted bilayer graphene, *Phys. Rev. B* **98**, 241407 (2018).
- [23] Y.-Z. You and A. Vishwanath, Superconductivity from valley fluctuations and approximate $so(4)$ symmetry in a weak coupling theory of twisted bilayer graphene, *npj Quantum Materials* **4**, 16 (2019).
- [24] F. Wu, A. H. MacDonald, and I. Martin, Theory of phonon-mediated superconductivity in twisted bilayer graphene, *Phys. Rev. Lett.* **121**, 257001 (2018).
- [25] B. Lian, Z. Wang, and B. A. Bernevig, Twisted bilayer graphene: A phonon-driven superconductor, *Phys. Rev. Lett.* **122**, 257002 (2019).
- [26] F. Wu, E. Hwang, and S. Das Sarma, Phonon-induced giant linear-in- t resistivity in magic angle twisted bilayer graphene: Ordinary strangeness and exotic superconductivity, *Phys. Rev. B* **99**, 165112 (2019).
- [27] F. Wu, Topological chiral superconductivity with spontaneous vortices and supercurrent in twisted bilayer graphene, *Phys. Rev. B* **99**, 195114 (2019).
- [28] D. V. Chichinadze, L. Classen, and A. V. Chubukov, Nematic superconductivity in twisted bilayer graphene, *Phys. Rev. B* **101**, 224513 (2020).
- [29] E. Khalaf, S. Chatterjee, N. Bultinck, M. P. Zaletel, and A. Vishwanath, Charged skyrmions and topological origin of superconductivity in magic-angle graphene, *Science advances* **7**, eabf5299 (2021).
- [30] Y. Wang, J. Kang, and R. M. Fernandes, Topological and nematic superconductivity mediated by ferro- $su(4)$ fluctuations in twisted bilayer graphene, *Phys. Rev. B* **103**, 024506 (2021).
- [31] M. Christos, S. Sachdev, and M. S. Scheurer, Superconductivity, correlated insulators, and wess–zumino–witten terms in twisted bilayer graphene, *Proceedings of the National Academy of Sciences* **117**, 29543 (2020).
- [32] L. Classen, A. V. Chubukov, C. Honerkamp, and M. M. Scherer, Competing orders at higher-order van hove points, *Phys. Rev. B* **102**, 125141 (2020).
- [33] V. Kozii, M. P. Zaletel, and N. Bultinck, Superconductivity in a doped valley coherent insulator in magic angle graphene: Goldstone-mediated pairing and kohn-luttinger mechanism (2020), [arXiv:2005.12961 \[cond-mat.str-el\]](#).
- [34] S. Chatterjee, M. Ippoliti, and M. P. Zaletel, Skyrmion superconductivity: Dmrg evidence for a topological route to superconductivity (2020), [arXiv:2010.01144 \[cond-mat.str-el\]](#).
- [35] E. Khalaf, P. Ledwith, and A. Vishwanath, Symmetry constraints on superconductivity in twisted bilayer graphene: Fractional vortices, $4e$ condensates or non-unitary pairing (2020), [arXiv:2012.05915 \[cond-mat.supr-con\]](#).
- [36] T. Cea and F. Guinea, Coulomb interaction, phonons, and superconductivity in twisted bilayer graphene, *Proceedings of the National Academy of Sciences* **118**, 10.1073/pnas.2107874118 (2021).
- [37] G. Shavit, E. Berg, A. Stern, and Y. Oreg, Theory of correlated insulators and superconductivity in twisted bilayer graphene, *Phys. Rev. Lett.* **127**, 247703 (2021).
- [38] C. Huang, N. Wei, W. Qin, and A. MacDonald, Pseudospin paramagnons and the superconducting dome in magic angle twisted bilayer graphene (2021), [arXiv:2110.13351 \[cond-mat.mes-hall\]](#).
- [39] Y. H. Kwan, G. Wagner, N. Bultinck, S. H. Simon, and S. A. Parameswaran, Skyrmions in twisted bilayer graphene: stability, pairing, and crystallization (2021), [arXiv:2112.06936 \[cond-mat.str-el\]](#).
- [40] J. Yu, Y.-A. Chen, and S. D. Sarma, Euler obstructed cooper pairing: Nodal superconductivity and hinge majorana zero modes (2021), [arXiv:2109.02685 \[cond-mat.supr-con\]](#).
- [41] N. Bultinck, E. Khalaf, S. Liu, S. Chatterjee, A. Vishwanath, and M. P. Zaletel, Ground state and hidden symmetry of magic-angle graphene at even integer filling, *Phys. Rev. X* **10**, 031034 (2020).
- [42] J. Kang and O. Vafek, Non-abelian dirac node braiding and near-degeneracy of correlated phases at odd integer filling in magic-angle twisted bilayer graphene, *Phys. Rev. B* **102**, 035161 (2020).
- [43] T. Soejima, D. E. Parker, N. Bultinck, J. Hauschild, and M. P. Zaletel, Efficient simulation of moiré materials using the density matrix renormalization group, *Phys. Rev. B* **102**, 205111 (2020).
- [44] E. Khalaf, N. Bultinck, A. Vishwanath, and M. P. Zaletel, Soft modes in magic angle twisted bilayer graphene (2020), [arXiv:2009.14827 \[cond-mat.str-el\]](#).
- [45] Y. Li and F. D. M. Haldane, Topological nodal cooper pairing in doped weyl metals, *Phys. Rev. Lett.* **120**, 067003 (2018).
- [46] S. Murakami and N. Nagaosa, Berry phase in magnetic superconductors, *Phys. Rev. Lett.* **90**, 057002 (2003).
- [47] N. Bultinck, S. Chatterjee, and M. P. Zaletel, Mechanism for anomalous hall ferromagnetism in twisted bilayer graphene, *Phys. Rev. Lett.* **124**, 166601 (2020).

- [48] L. Fu, Odd-parity topological superconductor with nematic order: Application to $\text{Cu}_x\text{Bi}_2\text{Se}_3$, *Phys. Rev. B* **90**, 100509 (2014).
- [49] F. Xie, Z. Song, B. Lian, and B. A. Bernevig, Topology-bounded superfluid weight in twisted bilayer graphene, *Phys. Rev. Lett.* **124**, 167002 (2020).
- [50] Z.-D. Song, B. Lian, N. Regnault, and B. A. Bernevig, Twisted bilayer graphene. ii. stable symmetry anomaly, *Phys. Rev. B* **103**, 205412 (2021).
- [51] S. Chatterjee, N. Bultinck, and M. P. Zaletel, Symmetry breaking and skyrmionic transport in twisted bilayer graphene, *Phys. Rev. B* **101**, 165141 (2020).
- [52] F. N. Ünal, A. Bouhon, and R.-J. Slager, Topological euler class as a dynamical observable in optical lattices, *Phys. Rev. Lett.* **125**, 053601 (2020).
- [53] A. Bouhon, Q. Wu, R.-J. Slager, H. Weng, O. V. Yazyev, and T. Bzdušek, Non-abelian reciprocal braiding of weyl points and its manifestation in zrte, *Nature Physics* **16**, 1137 (2020).
- [54] F. Xie, A. Cowsik, Z.-D. Song, B. Lian, B. A. Bernevig, and N. Regnault, Twisted bilayer graphene. vi. an exact diagonalization study at nonzero integer filling, *Phys. Rev. B* **103**, 205416 (2021).
- [55] Channel splitting based on a different band topology in a different symmetry class was studied in Ref. [64].
- [56] T. T. Wu and C. N. Yang, Dirac monopole without strings: Monopole harmonics, *Nuclear Physics B* **107**, 365 (1976).
- [57] G. Tarnopolsky, A. J. Kruchkov, and A. Vishwanath, Origin of magic angles in twisted bilayer graphene, *Phys. Rev. Lett.* **122**, 106405 (2019).
- [58] T. c. v. Bzdušek and M. Sigrist, Robust doubly charged nodal lines and nodal surfaces in centrosymmetric systems, *Phys. Rev. B* **96**, 155105 (2017).
- [59] C. F. B. Lo, H. C. Po, and A. H. Nevidomskyy, Inherited topological superconductivity in two-dimensional dirac semimetals, *arXiv:2108.12416* (2021).
- [60] S. Peotta and P. Törmä, Superfluidity in topologically nontrivial flat bands, *Nature Communications* **6**, 8944 (2015).
- [61] L. Liang, T. I. Vanhala, S. Peotta, T. Siro, A. Harju, and P. Törmä, Band geometry, berry curvature, and superfluid weight, *Phys. Rev. B* **95**, 024515 (2017).
- [62] J. Herzog-Arbeitman, V. Peri, F. Schindler, S. D. Huber, and B. A. Bernevig, Superfluid weight bounds from symmetry and quantum geometry in flat bands (2021), *arXiv:2110.14663* [cond-mat.mes-hall].
- [63] P. Törmä, S. Peotta, and B. A. Bernevig, Superfluidity and quantum geometry in twisted multilayer systems (2021), *arXiv:2111.00807* [cond-mat.supr-con].
- [64] C. Sun and Y. Li, z_2 topologically obstructed superconducting order, *arXiv:2009.07263* (2020).
- [65] R. Yu, X. L. Qi, A. Bernevig, Z. Fang, and X. Dai, Equivalent expression of F_2 topological invariant for band insulators using the non-abelian berry connection, *Phys. Rev. B* **84**, 075119 (2011).
- [66] J. Ahn, D. Kim, Y. Kim, and B.-J. Yang, Band topology and linking structure of nodal line semimetals with Z_2 monopole charges, *Phys. Rev. Lett.* **121**, 106403 (2018).
- [67] C. Brouder, G. Panati, M. Calandra, C. Mourougane, and N. Marzari, Exponential localization of wannier functions in insulators, *Phys. Rev. Lett.* **98**, 046402 (2007).
- [68] Y.-Q. Ma, S.-J. Gu, S. Chen, H. Fan, and W.-M. Liu, The euler number of bloch states manifold and the quantum phases in gapped fermionic systems, *EPL (Europhysics Letters)* **103**, 10008 (2013).
- [69] P. A. Frigeri, D. F. Agterberg, A. Koga, and M. Sigrist, Superconductivity without inversion symmetry: MnSi versus CePt_3Si , *Phys. Rev. Lett.* **92**, 097001 (2004).
- [70] X. Hu, T. Hyart, D. I. Pikulin, and E. Rossi, Geometric and conventional contribution to the superfluid weight in twisted bilayer graphene, *Phys. Rev. Lett.* **123**, 237002 (2019).
- [71] A. Julku, T. J. Peltonen, L. Liang, T. T. Heikkilä, and P. Törmä, Superfluid weight and berezinskii-kosterlitz-thouless transition temperature of twisted bilayer graphene, *Phys. Rev. B* **101**, 060505 (2020).
- [72] L. Balents, C. R. Dean, D. K. Efetov, and A. F. Young, Superconductivity and strong correlations in moiré flat bands, *Nature Physics* **16**, 725 (2020).

CONTENTS

I. Introduction	1
II. Euler Obstructed Cooper Pairing in MATBG	2
III. Nematic Nodal Superconductivity in MATBG	3
IV. Bounded Superfluid Weight	5
V. Discussion	5
VI. Acknowledgments	5
References	5
A. Conventions	8
B. Euler Obstructed Cooper Pairing in 2D Systems with $C_{2z}\mathcal{T}$ Symmetry	8

1. General Formalism	8
a. Normal State	8
b. Euler Obstructed Cooper Pairing	12
c. Comments on the Gauge Invariance	14
2. Chern Gauge	15
C. Superfluid Weight in 2D Systems with $C_{2z}\mathcal{T}$ Symmetry	16
1. Review of General Formalism for Mean-field Superfluid Weight	17
2. Superfluid Weight in 2D systems that satisfy Asm. 1-7	18
3. Bounded zero-temperature superfluid weight in 2D systems that satisfy Asm. 1-7	19
D. Euler Obstructed Cooper Pairing in MATBG at Zero Temperature	21
1. BM Model	21
2. Euler Obstructed Cooper Pairing in MATBG	22
3. Symmetry Classification of the Pairing in Eq. (D12)	24
4. General Discussion on the Possible Nodal Superconductivity	25
5. Nodal Superconductivity Guaranteed by Sufficiently-Dominant Δ_{\parallel} in MATBG	27
a. C_{3z} -Invariant	29
b. Spontaneously Nematic Pairing	29
6. Bounded Zero-temperature superfluid weight in MATBG	30
E. Euler Obstructed Cooper Pairing Induced by Attractive Local Interaction in MATBG	30

Appendix A: Conventions

We use C_{nj} to label the spinless part of a n -fold rotation along axis j , and use \bar{C}_{nj} to label the corresponding spinful operation.

We only consider the spinless part of any operation g when acting g on any spinless state.

We use the unit system in which $\hbar = 1$, unless specified otherwise.

We always imply $\mathbf{k} \in \mathbb{R}^2$ unless specifying $\mathbf{k} \in 1\text{BZ}$, where 1BZ is short for the first Brillouin zone.

Appendix B: Euler Obstructed Cooper Pairing in 2D Systems with $C_{2z}\mathcal{T}$ Symmetry

In this section, we will follow Ref. [40] to introduce the Euler obstructed Cooper pairing in 2D systems with $C_{2z}\mathcal{T}$ symmetry. We start with the general formalism and then focus on the Chern gauge.

1. General Formalism

In this part, we will introduce the gauge-invariant formalism for the Euler obstructed Cooper pairing in 2D systems. In most the discussions of this part, we will not choose any specific gauge; but in certain cases, we might use choose convenient gauges to prove a gauge-independent statement.

a. Normal State

The normal-state that we consider is a 2D (effectively) noninteracting fermionic Hamiltonian \tilde{H} that satisfies the following assumptions.

Assumption 1. \tilde{H} has 2D lattice translation symmetries and $\bar{C}_{2z}\mathcal{T}$ symmetry, with z perpendicular to the 2D system.

Assumption 2.

$$\tilde{H} = \tilde{H}_+ + \tilde{H}_- \quad (\text{B1})$$

The basis of \tilde{H}_α is created by $\psi_{\alpha,\mathbf{k},i,s}^\dagger$ with $\alpha = \pm$ the valley index, \mathbf{k} the momentum, s the spin index, and i labelling all other degrees of freedom. $\{\psi_{\alpha,\mathbf{k},i,s}^\dagger, \psi_{\alpha',\mathbf{k}',i',s'}\} = \delta_{\alpha\alpha'}\delta_{ii'}\delta_{ss'}\delta_{\mathbf{k}\mathbf{k}'}$. $e^{-i\mathbf{k}\cdot\mathbf{r}}\psi_{\alpha,\mathbf{k}}^\dagger e^{i\mathbf{k}\cdot\mathbf{r}} = \psi_{\alpha,0}^\dagger \forall \mathbf{k} \in 1\text{BZ}$, and

$e^{-i\mathbf{G}\cdot\mathbf{r}}\psi_{\alpha,0}^\dagger e^{i\mathbf{G}\cdot\mathbf{r}} = \psi_{\alpha,0}^\dagger S_{\alpha,\mathbf{G}} \otimes s_0$, where $s_{0,x,y,z}$ are the Pauli matrices for the spin index, $\psi_{\alpha,\mathbf{k}}^\dagger = (\dots, \psi_{\alpha,\mathbf{k},i,s}^\dagger, \dots)$, \mathbf{G} is an arbitrary reciprocal lattice vector, and $S_{\alpha,\mathbf{G}}$ is a unitary matrix with $S_{\alpha,\mathbf{G}+\mathbf{G}'} = S_{\alpha,\mathbf{G}} S_{\alpha,\mathbf{G}'}$.

Assumption 3. $\bar{C}_{2z}\mathcal{T}$ does not change the valley index α . \tilde{H}_α has its own spin-charge U(2) symmetry for $\alpha \in \{+, -\}$.

Then, we have $\bar{C}_{2z}\mathcal{T}\psi_{\pm,\mathbf{k}}^\dagger(\bar{C}_{2z}\mathcal{T})^{-1} = \psi_{\pm,\mathbf{k}}^\dagger \tilde{U}_\pm \otimes (-is_x) \forall \mathbf{k} \in 1\text{BZ}$, meaning that $[\bar{C}_{2z}\mathcal{T}, \tilde{H}_\alpha] = 0$.

$$\tilde{H}_\pm = \sum_{\mathbf{k} \in 1\text{BZ}} \psi_{\pm,\mathbf{k}}^\dagger \tilde{h}_\pm(\mathbf{k}) \otimes s_0 \psi_{\pm,\mathbf{k}} , \quad (\text{B2})$$

meaning that $[C_{2z}\mathcal{T}, \tilde{H}_\alpha] = 0$. In the following, we will use $C_{2z}\mathcal{T}$ more often.

We can extend the domain from $\psi_{\pm,\mathbf{k}}^\dagger$ from 1BZ to \mathbb{R}^2 by $\psi_{\pm,\mathbf{k}}^\dagger = e^{i\mathbf{k}\cdot\mathbf{r}}\psi_{\pm,0}^\dagger e^{-i\mathbf{k}\cdot\mathbf{r}} \forall \mathbf{k} \in \mathbb{R}^2$, and we have $S_{\alpha,\mathbf{G}}^\dagger \tilde{h}_\alpha(\mathbf{k} + \mathbf{G}) S_{\alpha,\mathbf{G}} = \tilde{h}_\alpha(\mathbf{k})$.

Assumption 4. Each \tilde{H}_α (with $\alpha = \pm$) has an isolated set of two spin doubly degenerated bands at low energy.

We use Bloch basis $|\psi_{\alpha,\mathbf{k},a}\rangle \otimes |s\rangle$ to label the Bloch basis of the two spin doubly degenerated bands in valley α , where $a = 1, 2$ labelling the two spinless states. By defining $V_{\alpha,a}(\mathbf{k})$ as the orthonormal linear combinations of the eigenvectors of $\tilde{h}_\alpha(\mathbf{k})$ for the two bands in valley α , we have

$$|\psi_{\alpha,\mathbf{k},a}\rangle \otimes |s\rangle = c_{\alpha,\mathbf{k},a,s}^\dagger |\Omega\rangle , \quad (\text{B3})$$

where $c_{\alpha,\mathbf{k},a,s}^\dagger = \sum_i \psi_{\alpha,\mathbf{k},i,s}^\dagger [V_{\alpha,a}(\mathbf{k})]_i$. Then, the projected Hamiltonian for the isolated set of bands in valley α reads

$$H_\alpha = \sum_{\mathbf{k} \in 1\text{BZ}} c_{\alpha,\mathbf{k}}^\dagger h_\alpha(\mathbf{k}) \otimes s_0 c_{\alpha,\mathbf{k}} , \quad (\text{B4})$$

where

$$h_\alpha(\mathbf{k}) = V_\alpha^\dagger(\mathbf{k}) \tilde{h}_\alpha(\mathbf{k}) V_\alpha(\mathbf{k}) , \quad (\text{B5})$$

$c_{\alpha,\mathbf{k}}^\dagger = (\dots, c_{\alpha,\mathbf{k},a,s}^\dagger, \dots)$, and $V_\alpha(\mathbf{k}) = \begin{pmatrix} V_{\alpha,1}(\mathbf{k}) & V_{\alpha,2}(\mathbf{k}) \end{pmatrix}$

We can choose $V_\alpha(\mathbf{k} + \mathbf{G}) = S_{\alpha,\mathbf{G}} V_\alpha(\mathbf{k})$. Then, we have $|\psi_{\alpha,\mathbf{k},a}\rangle = |\psi_{\alpha,\mathbf{k}+\mathbf{G},a}\rangle$ and $c_{\alpha,\mathbf{k}+\mathbf{G},a,s}^\dagger = c_{\alpha,\mathbf{k},a,s}^\dagger$. We define $|u_{\alpha,\mathbf{k},a}\rangle = e^{-i\mathbf{k}\cdot\mathbf{r}} |\psi_{\alpha,\mathbf{k},a}\rangle$ with \mathbf{r} the position operator, and define $|u_{\alpha,\mathbf{k}}\rangle = (|u_{\alpha,\mathbf{k},1}\rangle, |u_{\alpha,\mathbf{k},2}\rangle)$, which satisfies

$$|u_{\alpha,\mathbf{k}+\mathbf{G}}\rangle = e^{-i\mathbf{G}\cdot\mathbf{r}} |u_{\alpha,\mathbf{k}}\rangle \forall \text{ reciprocal lattice vector } \mathbf{G} . \quad (\text{B6})$$

Then, we have

$$C_{2z}\mathcal{T}|u_{\alpha,\mathbf{k}}\rangle = |u_{\alpha,\mathbf{k}}\rangle U_\alpha(\mathbf{k}) , \quad (\text{B7})$$

$|u_{\alpha,\mathbf{k}}\rangle$ has a U(2) gauge freedom

$$|u_{\alpha,\mathbf{k}}\rangle \rightarrow |u_{\alpha,\mathbf{k}}\rangle R_{\alpha,\mathbf{k}} \quad (\text{B8})$$

with $R_{\alpha,\mathbf{k}} \in \text{U}(2)$ and $R_{\alpha,\mathbf{k}+\mathbf{G}} = R_{\alpha,\mathbf{k}}$. By gauge invariant, we mean invariant under Eq. (B8).

The Wilson line matrix [65] is crucial for our later discussions. The Wilson line matrix is defined as

$$W_\alpha(\mathbf{k}_0 \xrightarrow{\gamma} \mathbf{k}) = \lim_{L \rightarrow \infty} \langle u_{\alpha,\mathbf{k}_0} | P_\alpha(\mathbf{k}_1) P_\alpha(\mathbf{k}_2) \dots P_\alpha(\mathbf{k}_L) | u_{\alpha,\mathbf{k}} \rangle , \quad (\text{B9})$$

where γ is a continuous path from \mathbf{k}_0 to \mathbf{k} , $\mathbf{k}_1, \dots, \mathbf{k}_L$ are sequentially arranged on γ with $|\mathbf{k}_{i+1} - \mathbf{k}_i| = O\left(\frac{\text{length of } \gamma}{L}\right)$, and $P_\alpha(\mathbf{k}) = |u_{\alpha,\mathbf{k}}\rangle \langle u_{\alpha,\mathbf{k}}|$. Moreover, for any $\mathbf{k}_0, \mathbf{k} \in \mathbb{R}^2$, $\det[W_\pm(\mathbf{k}_0 \xrightarrow{\gamma} \mathbf{k})] = \det[W_\pm(\mathbf{k}_0, \mathbf{k})]$ is independent of the path γ .

In particular, we define the continuous γ to be effectively-closed if and only if $\mathbf{k} - \mathbf{k}_0$ is a reciprocal lattice vector. Then, owing to the $C_{2z}\mathcal{T}$ symmetry, $\det[W_\alpha(\mathbf{k} \xrightarrow{\gamma} \mathbf{k} + \mathbf{G})] = \pm 1$ for any effectively-closed γ , which can be derived based on $C_{2z}\mathcal{T}P_\alpha(\mathbf{k})(C_{2z}\mathcal{T})^\dagger = P_\alpha(\mathbf{k})$. Then, we choose the following assumption for the normal-state Hamiltonian H_\pm .

Assumption 5. $\exists \mathbf{k}_{0,\beta} \in \mathbb{R}^2$ such that $\det[W_\pm(\gamma_\beta)] = 1$, where γ_β is the straight path from $\mathbf{k}_{0,\beta}$ to $\mathbf{k}_{0,\beta} + \mathbf{b}_\beta$, $\beta = 1, 2$, and $\mathbf{b}_{1,2}$ are the basis vectors of the reciprocal lattice.

This assumption implies that $\det[W_\pm(\mathbf{k} \xrightarrow{\gamma} \mathbf{k} + \mathbf{G})] = 1$ for all effectively-closed γ , since we can always express $\det[W_\pm(\mathbf{k} \xrightarrow{\gamma} \mathbf{k} + \mathbf{G})]$ in terms of the products of $\det[W_\pm(\gamma_1)]$ and $\det[W_\pm(\gamma_2)]$.

With the properties of the Wilson line, we can define the following path-independent η factor

$$\eta_{\alpha, \mathbf{k}_0}(\mathbf{k}) = \sqrt{\det \left(\langle u_{\alpha, \mathbf{k}_0}^{C_{2z}\mathcal{T}} | u_{\alpha, \mathbf{k}_0} \rangle \right)} \det[W_\alpha(\mathbf{k}_0, \mathbf{k})] , \quad (\text{B10})$$

where \mathbf{k}_0 is treated as a base point, and $|u_{\alpha, \mathbf{k}}^{C_{2z}\mathcal{T}}\rangle = C_{2z}\mathcal{T}|u_{\alpha, \mathbf{k}}\rangle$. Then, we can define

$$\begin{aligned} Q_{\alpha, \mathbf{k}_0}(\mathbf{k}) &= \frac{\eta_{\alpha, \mathbf{k}_0}^*(\mathbf{k})}{\sqrt{2}} |u_{\alpha, \mathbf{k}}\rangle (-i\tau_y) \langle u_{\alpha, \mathbf{k}}^{C_{2z}\mathcal{T}} | \\ \Phi_{\alpha, \mathbf{k}_0}(\mathbf{k}) &= \frac{1}{\sqrt{2}} \text{Tr}[Q_{\alpha, \mathbf{k}_0}(\mathbf{k}) \partial_{k_x} P_\alpha(\mathbf{k}) \partial_{k_y} P_\alpha(\mathbf{k})] - (\partial_{k_x} \leftrightarrow \partial_{k_y}) \\ \mathcal{N}_{\alpha, \mathbf{k}_0} &= \frac{1}{2\pi} \int_{\text{1BZ}} d^2k \Phi_{\alpha, \mathbf{k}_0}(\mathbf{k}) \\ \mathcal{N}_\alpha &= |\mathcal{N}_{\alpha, \mathbf{k}_0}| , \end{aligned} \quad (\text{B11})$$

where (and also for the rest of the work) the square root is always fixed in the principle branch as

$$\sqrt{e^{i\theta}} = e^{i(\theta+2\pi n)/2} \text{ for } n \in \mathbb{Z} \text{ such that } \theta + 2\pi n \in (-\pi, \pi] . \quad (\text{B12})$$

Among the quantities defined above, \mathcal{N}_α is invariant under the gauge transformation Eq. (B8) and the shift of the base point \mathbf{k}_0 , since both the gauge transformation Eq. (B8) and the shift of the base point \mathbf{k}_0 can only change $Q_{\alpha, \mathbf{k}_0}(\mathbf{k})$, $\Phi_{\alpha, \mathbf{k}_0}(\mathbf{k})$ and $\mathcal{N}_{\alpha, \mathbf{k}_0}$ by the same sign factor.

Now we show $\mathcal{N}_{\alpha, \mathbf{k}_0} \in \mathbb{Z}$ and $\mathcal{N}_\alpha \in \mathbb{N}$ for any gauges and base points. All we need to show is that $\mathcal{N}_{\alpha, \mathbf{k}_0} \in \mathbb{Z}$ holds for one gauge and one choice of base point. It is because if it is true, then $\mathcal{N}_{\alpha, \mathbf{k}_0} \in \mathbb{Z}$ and $\mathcal{N}_\alpha \in \mathbb{N}$ holds for all gauges and all choices of base points, since the gauge transformation and the base point shift can only change $\mathcal{N}_{\alpha, \mathbf{k}_0}$ by a sign. Then, we will use a special gauge to show $\mathcal{N}_{\alpha, \mathbf{k}_0} \in \mathbb{Z}$, which is the real oriented gauge [7, 66] as described in the following. First, there exists a gauge

$$|\tilde{u}_{\alpha, \mathbf{k}}\rangle = |u_{\alpha, \mathbf{k}}\rangle \tilde{R}_\alpha(\mathbf{k}) \sqrt{\Lambda_\alpha(\mathbf{k})} , \quad (\text{B13})$$

which satisfies $C_{2z}\mathcal{T}|\tilde{u}_{\alpha, \mathbf{k}}\rangle = |\tilde{u}_{\alpha, \mathbf{k}}\rangle$. Here $\tilde{R}_\alpha(\mathbf{k})$ is an orthogonal real matrix that satisfies

$$[\tilde{R}_\alpha(\mathbf{k})]^T U_\alpha(\mathbf{k}) \tilde{R}_\alpha(\mathbf{k}) = \Lambda_\alpha(\mathbf{k}) \quad (\text{B14})$$

with $\Lambda_\alpha(\mathbf{k})$ diagonal, and the square roots in $\sqrt{\Lambda_\alpha(\mathbf{k})}$ act on the diagonal elements [53]. Furthermore, we ensure $|\tilde{u}_{\alpha, \mathbf{k}+\mathbf{G}}\rangle = e^{-i\mathbf{G}\cdot\mathbf{r}}|\tilde{u}_{\alpha, \mathbf{k}}\rangle$. $|\tilde{u}_{\alpha, \mathbf{k}}\rangle$ is called a real gauge. The real gauge is not unique: $|\tilde{u}_{\alpha, \mathbf{k}}\rangle \rightarrow |\tilde{u}_{\alpha, \mathbf{k}}\rangle R_{\alpha, \mathbf{k}}$ with $R_{\alpha, \mathbf{k}} \in \text{O}(2)$ and $R_{\alpha, \mathbf{k}+\mathbf{G}} = R_{\alpha, \mathbf{k}}$ gives another real gauge. If the $C_{2z}\mathcal{T}$ -protected topology of the nearly flat bands is nontrivial, it is impossible to make $|\tilde{u}_{\alpha, \mathbf{k}}\rangle$ smooth everywhere in \mathbb{R}^2 . However, owing to Asm. 5, we can choose patches that cover \mathbb{R}^2 as Fig. 3, and we can make $|\tilde{u}_{\alpha, \mathbf{k}}\rangle$ to be smooth in each patch, noted as $|\tilde{u}_{\alpha, \mathbf{k}}^A\rangle$ where $A = I, II, II + \mathbf{b}_1, II + \mathbf{b}_2, II + \mathbf{b}_1 + \mathbf{b}_2, \dots$ labels the patches. Note that for any reciprocal lattice vector \mathbf{G} , $|\tilde{u}_{\alpha, \mathbf{k}+\mathbf{G}}^I\rangle = e^{-i\mathbf{G}\cdot\mathbf{r}}|\tilde{u}_{\alpha, \mathbf{k}}^I\rangle$ if $\mathbf{k} + \mathbf{G}, \mathbf{k} \in I$, and $|\tilde{u}_{\alpha, \mathbf{k}+\mathbf{G}}^{II+\mathbf{G}}\rangle = e^{-i\mathbf{G}\cdot\mathbf{r}}|\tilde{u}_{\alpha, \mathbf{k}}^{II}\rangle$ if $\mathbf{k} \in II$. For any $\mathbf{k} \in A \cap A'$, $\langle \tilde{u}_{\alpha, \mathbf{k}}^A | \tilde{u}_{\alpha, \mathbf{k}}^{A'} \rangle \in \text{O}(2)$. As shown in Fig. 3, the intersection only occurs between I and copies of II , and then we further choose the proper $\tilde{u}_{\alpha, \mathbf{k}}^A$ with $A = II, II + \mathbf{b}_1, II + \mathbf{b}_2, \dots$ to realize

$$\langle \tilde{u}_{\alpha, \mathbf{k}}^A | \tilde{u}_{\alpha, \mathbf{k}}^{A'} \rangle \in \text{SO}(2) \quad \forall \text{ any } \mathbf{k} \in A \cap A' . \quad (\text{B15})$$

As a result, $|\tilde{u}_{\alpha, \mathbf{k}}^A\rangle$ is a patchwise-smooth real oriented gauge, and the real oriented gauge for $|u_{\alpha, \mathbf{k}}\rangle$ is $|u_{\alpha, \mathbf{k}}^{RO}\rangle = |\tilde{u}_{\alpha, \mathbf{k}}^{A_{\mathbf{k}}}\rangle$, where $A_{\mathbf{k}}$ is the unique patch chosen for \mathbf{k} . We emphasize that the existence of the smooth real $|\tilde{u}_{\alpha, \mathbf{k}}^I\rangle$ in I , as well as the existence of both the patchwise-smooth real oriented gauge $|\tilde{u}_{\alpha, \mathbf{k}}^A\rangle$ and the real oriented gauge $|u_{\alpha, \mathbf{k}}^{RO}\rangle$, relies on Asm. 5, which makes the real vector bundle given by $|\tilde{u}_{\alpha, \mathbf{k}}\rangle$ orientable.

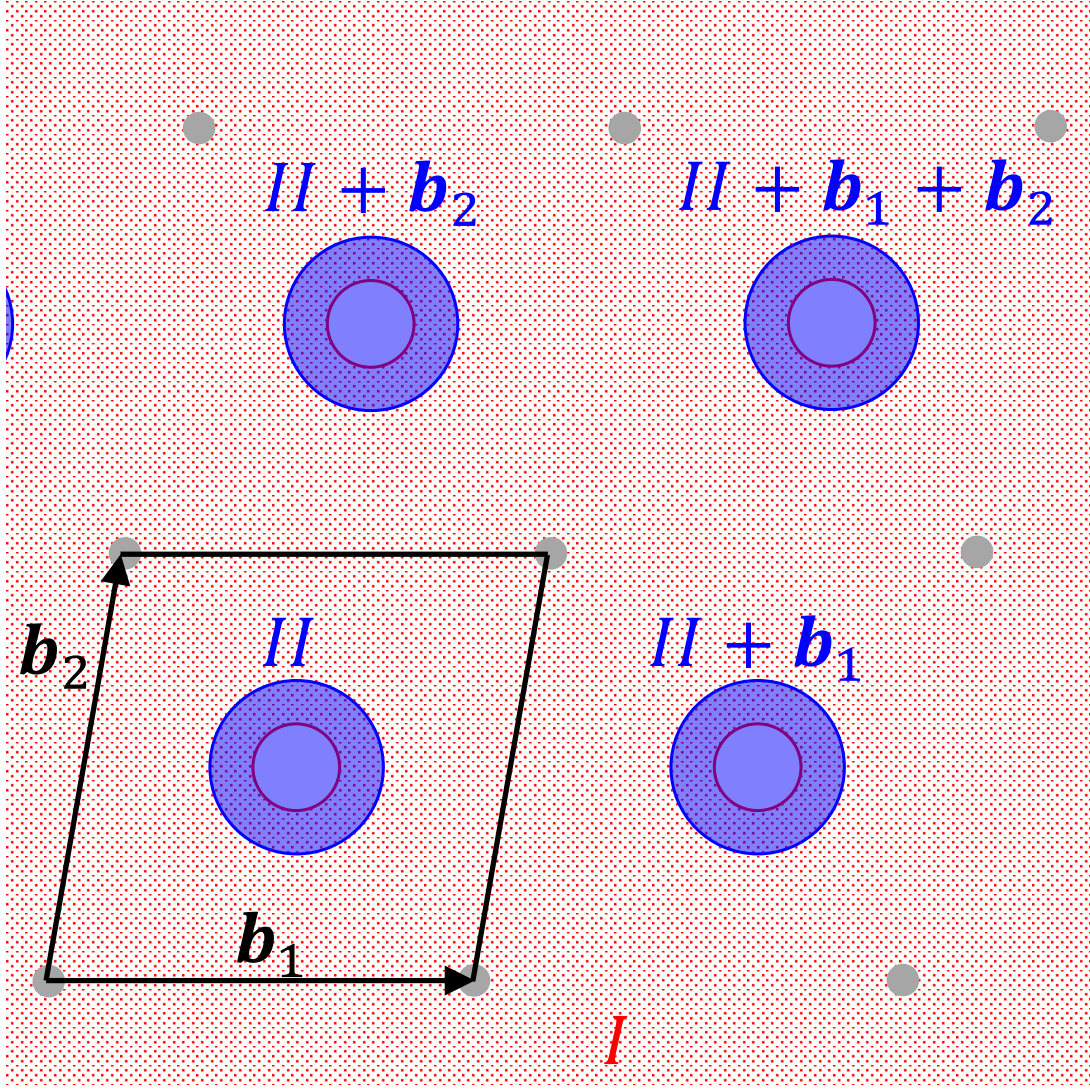


FIG. 3. This shows the patches that we choose for the patchwise-smooth real oriented gauge. The gray dots are reciprocal lattice points, $\mathbf{b}_{1,2}$ are the basis vectors of the reciprocal lattice, and the tetragon marked by the black lines is the unit cell of the reciprocal lattice. Patch I (red dotted) covers \mathbb{R}^2 except holes that form a reciprocal lattice, and the holes are covered by the patch II (blue) and its copies given by shifts along the reciprocal lattice vectors. This choice of patches is allowed by Asm. 5, which makes the corresponding real vector bundle orientable.

For the real oriented gauge $|u_{\alpha,\mathbf{k}}^{RO}\rangle$, we have

$$\begin{aligned} \eta_{\alpha,\mathbf{k}_0}(\mathbf{k}) &= 1, \\ Q_{\alpha,\mathbf{k}_0}(\mathbf{k}) &= \frac{1}{\sqrt{2}} |u_{\alpha,\mathbf{k}}^{RO}\rangle (-i\tau_y) \langle u_{\alpha,\mathbf{k}}^{RO}|, \end{aligned} \quad (\text{B16})$$

which leads to

$$\Phi_{\alpha,\mathbf{k}_0}(\mathbf{k}) = f_{\alpha}(\mathbf{k}) = \langle \partial_{k_x} u_{\alpha,\mathbf{k},1}^{RO} | \partial_{k_y} u_{\alpha,\mathbf{k},2}^{RO} \rangle - (\partial_{k_x} \leftrightarrow \partial_{k_y}), \quad (\text{B17})$$

where $f_{\alpha}(\mathbf{k})$ is the real curvature for the real oriented gauge $|u_{\alpha,\mathbf{k}}^{RO}\rangle$ [7]. Then,

$$\mathcal{N}_{\alpha,\mathbf{k}_0} = \frac{1}{2\pi} \int_{\text{1BZ}} d^2k \Phi_{\alpha,\mathbf{k}_0}(\mathbf{k}) = \frac{1}{2\pi} \int_{\text{1BZ}} d^2k f_{\alpha}(\mathbf{k}) = e_{2,\alpha} \in \mathbb{Z}, \quad (\text{B18})$$

where $e_{2,\alpha}$ is the integer Euler class for the real oriented gauge $|u_{\alpha,\mathbf{k}}^{RO}\rangle$. As a result, we know $\mathcal{N}_{\alpha,\mathbf{k}_0} \in \mathbb{Z}$ and $\mathcal{N}_{\alpha} \in \mathbb{N}$ for any gauges and base points. Since $\mathcal{N}_{\alpha} = |e_{2,\alpha}|$ for any real oriented gauge and \mathcal{N}_{α} is gauge-independent, \mathcal{N}_{α} is called the Euler number [40], which is distinguished from the Euler class $e_{2,\alpha}$ [7] that relies on the real oriented gauges.

In the following, we will introduce an extra assumption on the normal-state Hamiltonian.

Assumption 6. $\mathcal{N}_\pm \neq 0$

With this assumption, we can define

$$\begin{aligned} Q_\alpha(\mathbf{k}) &= \frac{\mathcal{N}_{\alpha, \mathbf{k}_0}}{\mathcal{N}_\alpha} Q_{\alpha, \mathbf{k}_0}(\mathbf{k}) \\ \Phi_\alpha(\mathbf{k}) &= \frac{\mathcal{N}_{\alpha, \mathbf{k}_0}}{\mathcal{N}_\alpha} \Phi_{\alpha, \mathbf{k}_0}(\mathbf{k}) , \end{aligned} \quad (\text{B19})$$

which are independent of the gauge and the choice of the base point. The $C_{2z}\mathcal{T}$ symmetry requires

$$C_{2z}\mathcal{T}Q_\alpha(\mathbf{k})(C_{2z}\mathcal{T})^{-1} = Q_\alpha(\mathbf{k}) , \quad \Phi_\alpha(\mathbf{k}) \in \mathbb{R} . \quad (\text{B20})$$

Moreover, $Q_\alpha(\mathbf{k})$ is smooth everywhere in \mathbb{R}^2 since it is smooth for real oriented gauges and is gauge invariant, which means $\Phi_\alpha(\mathbf{k})$ is smooth everywhere in \mathbb{R}^2 since $P_\alpha(\mathbf{k})$ must be globally smooth. These properties are useful in the following discussion.

b. Euler Obstructed Cooper Pairing

Now we discuss the Euler obstructed Cooper pairing. The normal state that we consider satisfies Asm. 1-6. We consider the zero-temperature $C_{2z}\mathcal{T}$ intervalley mean-field pairing operator among the low-energy isolated sets of bands in Asm. 4, and we choose it to satisfy the following condition.

Assumption 7.

$$H_{\text{pairing}} = \sum_{\mathbf{k} \in 1BZ} c_{+, \mathbf{k}}^\dagger \Delta(\mathbf{k}) \otimes \Pi(c_{-, -\mathbf{k}}^\dagger)^T + h.c. , \quad (\text{B21})$$

where $c_{\pm, \mathbf{k}}^\dagger = (\dots, c_{\pm, \mathbf{k}, a, s}^\dagger, \dots)$, $\Delta(\mathbf{k})$ is for spinless index a , Π is for the spin index s , $s_y \Pi^* s_y = \Pi$, and $\Pi^\dagger \Pi = s_0$. Moreover, $[C_{2z}\mathcal{T}, H_{\text{pairing}}] = 0$, and

$$\sum_{a, a'} [\Delta(\mathbf{k})]_{aa'} |u_{+, \mathbf{k}, a}\rangle |u_{-, -\mathbf{k}, a'}\rangle \quad (\text{B22})$$

is smooth everywhere in \mathbb{R}^2 .

The spinless part of the pairing $\Delta(\mathbf{k})$ is the focus of this work. We first discuss how to split $\Delta(\mathbf{k})$ into two channels in a gauge independent way. To do so, we define an operator

$$P_\Delta(\mathbf{k}) = |u_{+, \mathbf{k}}\rangle \Delta(\mathbf{k}) \langle u_{-, -\mathbf{k}}^{C_{2z}\mathcal{T}}| , \quad (\text{B23})$$

which is invariant under the gauge transformation Eq. (B8), since $\Delta(\mathbf{k})$ transforms as $\Delta(\mathbf{k}) \rightarrow R_{+, \mathbf{k}}^\dagger \Delta(\mathbf{k}) R_{-, -\mathbf{k}}^*$ under Eq. (B8). Then, $P_\Delta(\mathbf{k})$ should be smooth everywhere in \mathbb{R}^2 . It is because the $C_{2z}\mathcal{T}$ symmetry restricts the total Chern number of $|u_{\alpha, \mathbf{k}}\rangle$ to zero, and thus $|u_{\alpha, \mathbf{k}}\rangle$ has complex gauge that is smooth everywhere in \mathbb{R}^2 [67]. Then, $\Delta(\mathbf{k})$ is smooth for any globally smooth complex gauges of $|u_{\alpha, \mathbf{k}}\rangle$, resulting that $P_\Delta(\mathbf{k})$ is smooth everywhere in \mathbb{R}^2 for any complex smooth gauges of $|u_{\alpha, \mathbf{k}}\rangle$. As $P_\Delta(\mathbf{k})$ is gauge invariant, $P_\Delta(\mathbf{k})$ is smooth everywhere in \mathbb{R}^2 for all gauges.

The gauge-independent way of splitting $\Delta(\mathbf{k})$ is achieved by defining

$$P_b(\mathbf{k}) = \frac{1}{2} P_\Delta(\mathbf{k}) - (-1)^b Q_{+, \mathbf{k}} P_\Delta(\mathbf{q}) Q_{-, -\mathbf{k}} = |u_{+, \mathbf{k}}\rangle \Delta_b(\mathbf{k}) \langle u_{-, -\mathbf{k}}^{C_{2z}\mathcal{T}}| , \quad (\text{B24})$$

which is gauge invariant and is smooth everywhere in \mathbb{R}^2 . Here $b \in \{\perp, \parallel\}$, $(-1)^\perp = 1$, and $(-1)^\parallel = -1$. Then, clearly,

$$\Delta(\mathbf{k}) = \Delta_\perp(\mathbf{k}) + \Delta_\parallel(\mathbf{k}) . \quad (\text{B25})$$

Next, we discuss the winding of the possible zeros of $\Delta_b(\mathbf{k})$. First,

$$|\Delta_b(\mathbf{k})| = \sqrt{\frac{1}{2} \text{Tr}[\Delta_b(\mathbf{k}) \Delta_b^\dagger(\mathbf{k})]} = \sqrt{\frac{1}{2} \text{Tr}[P_b(\mathbf{k}) P_b^\dagger(\mathbf{k})]} \quad (\text{B26})$$

is gauge invariant and is smooth at where $|\Delta_b(\mathbf{k})| \neq 0$. Then, for any \mathbf{k} such that $|\Delta_b(\mathbf{k})| \neq 0$, we can define

$$\mathbf{v}_b(\mathbf{k}) = \frac{1}{\sqrt{2}} \text{Tr}[Q_+(\mathbf{k})\hat{P}_b(\mathbf{k})\nabla_{\mathbf{k}}\hat{P}_b^\dagger(\mathbf{k})] , \quad (\text{B27})$$

where $\hat{P}_b(\mathbf{k}) = P_b(\mathbf{k})/|\Delta_b(\mathbf{k})|$. Clearly, $\mathbf{v}_b(\mathbf{k})$ and $\hat{P}_b(\mathbf{k})$ are gauge invariant and are smooth at any \mathbf{k} such that $|\Delta_b(\mathbf{k})| \neq 0$. Owing to the $C_{2z}\mathcal{T}$ invariance of the pairing operator, we have $C_{2z}\mathcal{T}P_\Delta(\mathbf{k})(C_{2z}\mathcal{T})^{-1} = P_\Delta(\mathbf{k})$. Combined with Eq. (B20), we know that the $C_{2z}\mathcal{T}$ symmetry requires $\mathbf{v}_b(\mathbf{k})$ to be real.

The zeros of $\Delta_b(\mathbf{k})$ are the zeros of $|\Delta_b(\mathbf{k})|$, and the winding numbers of the possible zeros of $\Delta_b(\mathbf{k})$ are defined by $\mathbf{v}_b(\mathbf{k})$ and $\Phi_\alpha(\mathbf{k})$. Since $\Delta_b(\mathbf{k})$, $\mathbf{v}_b(\mathbf{k})$ and $\Phi_\alpha(\mathbf{k})$ are periodic in \mathbf{G} , *i.e.*,

$$\Delta_b(\mathbf{k} + \mathbf{G}) = \Delta_b(\mathbf{k}) , \quad \mathbf{v}_b(\mathbf{k} + \mathbf{G}) = \mathbf{v}_b(\mathbf{k}) , \quad \Phi_\alpha(\mathbf{k} + \mathbf{G}) = \Phi_\alpha(\mathbf{k}) \quad \forall \text{ reciprocal lattice vector } \mathbf{G} , \quad (\text{B28})$$

we can focus on the reciprocal unit cell and treat it as a torus for the study of winding numbers of pairing zeros. Before defining the winding numbers of the pairing zeros, let us first define a winding number for $\Delta_b(\mathbf{k})$ associated with a closed connected region D_b that is a subset of the reciprocal unit cell (with boundary), when $|\Delta_b(\mathbf{k})|$ that is not everywhere zero in \mathbb{R}^2 . Specifically, we require the boundary ∂D_b does not touch any zeros of Δ_b , and then the winding number reads

$$\mathcal{W}_b(D_b) = \frac{1}{2\pi} \int_{\partial D_b} d\mathbf{k} \cdot \mathbf{v}_b(\mathbf{k}) + \frac{1}{2\pi} \int_{D_b} d^2k [\Phi_+(\mathbf{k}) - (-1)^b \Phi_-(-\mathbf{k})] . \quad (\text{B29})$$

We emphasize that ∂D_b is chosen as if the reciprocal unit cell is a torus as schematically shown in Fig. 4(a). $\mathcal{W}_b(D_b)$ is gauge invariant. More importantly, $\mathcal{W}_b(D_b)$ is an integer, as discussed in the following. First, we consider the case where D_b is the same as the reciprocal unit cell, which makes $\partial D_b = \emptyset$, resulting in $\mathcal{W}_b(D_b) = \mathcal{N}_+ - (-1)^b \mathcal{N}_- \in \mathbb{Z}$. Then, we turn to the case where D_b is a proper subset of the reciprocal unit cell. In this case, we can choose the patch I in Fig. 3 to fully cover D_b , and then choose a real oriented gauge $|u_{\pm,\mathbf{k}}^{RO}\rangle$ that is smooth in I and has $e_{2,\pm} > 0$. For this real oriented gauge $|u_{\pm,\mathbf{k}}^{RO}\rangle$, we have

$$\hat{P}_b(\mathbf{k}) = |u_{+,\mathbf{k}}^{RO}\rangle \begin{pmatrix} 1 & \\ & (-1)^b \end{pmatrix} e^{i\theta_b(\mathbf{k})\tau_y} \langle u_{-,\mathbf{k}}^{RO}| , \quad (\text{B30})$$

resulting in

$$\mathbf{v}_b = -(-1)^b \nabla_{\mathbf{k}} \theta_b(\mathbf{k}) - (-1)^b \langle u_{-,-\mathbf{k},1}^{RO} | \nabla_{-\mathbf{k}} | u_{-,-\mathbf{k},2}^{RO} \rangle - \langle u_{+,\mathbf{k},1}^{RO} | \nabla_{\mathbf{k}} | u_{+,\mathbf{k},2}^{RO} \rangle . \quad (\text{B31})$$

Combined with

$$\Phi_{\pm,\mathbf{k}} = \langle \partial_{k_x} u_{\pm,\mathbf{k},1}^{RO} | \partial_{k_y} u_{\pm,\mathbf{k},2}^{RO} \rangle - (\partial_{k_x} \leftrightarrow \partial_{k_y}) , \quad (\text{B32})$$

we have

$$\mathcal{W}_b(D_b) = -(-1)^b \frac{1}{2\pi} \int_{\partial D_b} d\mathbf{k} \cdot \nabla_{\mathbf{k}} \theta_b(\mathbf{k}) \in \mathbb{Z} \text{ for this real oriented gauge.} \quad (\text{B33})$$

Since $\mathcal{W}_b(D_b)$ is gauge-invariant, $\mathcal{W}_b(D_b) \in \mathbb{Z}$ is an integer for all gauges.

Now we are ready to define the winding number for the possible zeros of $|\Delta_b(\mathbf{k})|$, given that $|\Delta_b(\mathbf{k})|$ is not everywhere-vanishing in \mathbb{R}^2 . For each isolated connected region i of zeros of $|\Delta_b(\mathbf{k})|$ in the reciprocal unit cell, we choose a closed connected subset of the reciprocal unit cell, $D_{b,i}$, such that (i) i is in the interior of $D_{b,i}$ and (ii) $D_{b,i}$ does not contain any other zeros of $|\Delta_b(\mathbf{k})|$. Then, since $D_{b,i}$ satisfies the requirements for D_b in Eq. (B29), the winding number of the zero i of $|\Delta_b(\mathbf{k})|$ is defined as

$$\mathcal{W}_{b,i} = \mathcal{W}_b(D_{b,i}) , \quad (\text{B34})$$

which is an integer as discussed above. Here we emphasize that the above discussion holds for i being a point zero (0D), a line of zeros (1D), or an area of zeros (2D), as schematically shown in Fig. 4(b).

At the end of this part, we show the main result for the Euler obstructed Cooper pairing. If $|\Delta_b(\mathbf{k})|$ is not everywhere zero in \mathbb{R}^2 , we have

$$\sum_i \mathcal{W}_{b,i} = \mathcal{N}_+ - (-1)^b \mathcal{N}_- , \quad (\text{B35})$$

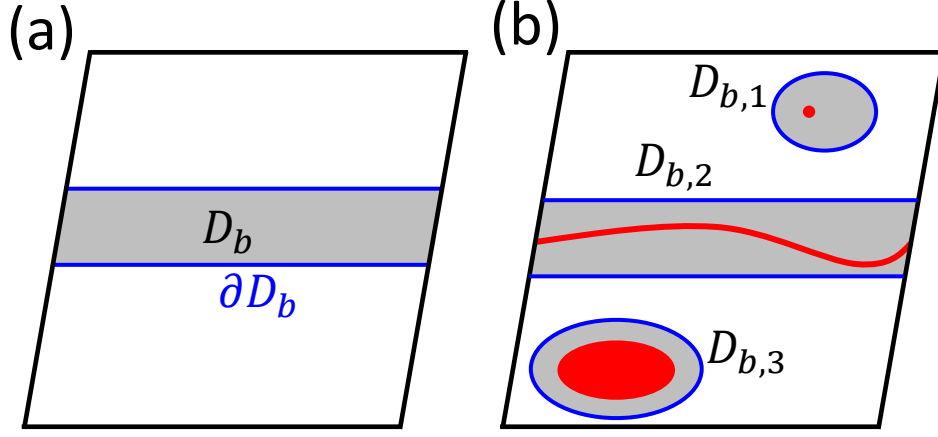


FIG. 4. In this figure, we show the D_b (Eq. (B29)) or $D_{b,i}$ (Eq. (B34)) regions in the reciprocal unit cell, whose boundary is marked by the black lines. In (a), we show a generic D_b (gray area) that is a closed connected proper subset of the reciprocal unit cell. The boundary ∂D_b (blue lines) is chosen as if the reciprocal unit cell is a torus with parallel opposite edges being identified. In (b), we choose three closed connected regions $D_{b,i}$ (gray areas) that include isolated zeros (red) of Δ_b in their interior. $D_{b,1}$ contains a point zero, $D_{b,2}$ contains a line of zeros, and $D_{b,3}$ contains an area of zeros. Again, the boundaries (blue lines) of $D_{b,i}$'s are determined as if the reciprocal unit cell is a torus.

where i ranges over all isolated points, lines or areas of zeros of $\Delta_b(\mathbf{k})$, and $\sum_i \mathcal{W}_{b,i} = 0$ if $\Delta_b(\mathbf{k})$ has no zeros. To show this, we first consider the case where $\Delta_b(\mathbf{k})$ has zeros. In this case, we can continuously deform $D_{b,i}$ such that $\cup_i D_{b,i}$ covers the reciprocal unit cell and $D_{b,i}$'s at most intersect at boundaries. After the deformation, we have $\sum_i \int_{D_{b,i}} d\mathbf{k} \cdot \mathbf{v}_b(\mathbf{k}) = 0$, meaning that Eq. (B35) holds after the deformation. To show Eq. (B35) holds for the generic case before the deformation, note that we can keep all $\partial D_{b,i}$'s not touching any zeros of $\Delta_b(\mathbf{k})$ in the process, since all zeros of $\Delta_b(\mathbf{k})$ are included inside $D_{b,i}$'s, meaning that $\int_{\partial D_{b,i}} d\mathbf{k} \cdot \mathbf{v}(\mathbf{k})$ is continuously changing during the deformation. Then, combined with the fact that $\Phi_{\pm}(\mathbf{k})$ is smooth everywhere in \mathbb{R}^2 , the deformation cannot cause any discontinuous change of $\mathcal{W}_{b,i}$, and thus cannot change $\mathcal{W}_{b,i}$. Thus, Eq. (B35) holds for the generic case before the deformation.

We now consider the case where $\Delta_b(\mathbf{k})$ has no zeros. In this case, we know $\sum_i \mathcal{W}_{b,i} = 0$, and thus we only need to show $\mathcal{N}_+ - (-1)^b \mathcal{N}_- = 0$. Since $\Delta_b(\mathbf{k})$ has no zeros, $\mathbf{v}_b(\mathbf{k})$ is smooth everywhere in \mathbb{R}^2 . Then, $\mathcal{W}_b(D_b)$ is the same for any closed connected subset D_b of the reciprocal unit cell, since continuously deforming D_b cannot cause any singular behavior of $\mathbf{v}_b(\mathbf{k})$ on ∂D_b and thus cannot cause any discontinuous change of $\mathcal{W}_b(D_b)$. As a result, we have $\mathcal{W}_b(D_b) = 0$ for any closed subset D_b of the reciprocal unit cell, since we can make D_b infinitesimal and have $|\mathcal{W}_b(D_b)| \ll 1$. Then, choosing D_b to be the same as the reciprocal unit cell gives $\mathcal{N}_+ - (-1)^b \mathcal{N}_- = 0$.

In sum, Eq. (B35) holds as long as $|\Delta_b(\mathbf{k})|$ is not everywhere-vanishing in \mathbb{R}^2 , no matter whether $\Delta_b(\mathbf{k})$ has zeros or not. In particular, we know if $\mathcal{N}_+ - (-1)^b \mathcal{N}_- \neq 0$, $\Delta_b(\mathbf{k})$ must have zeros, since no zeros mean $\mathcal{N}_+ - (-1)^b \mathcal{N}_- = 0$. In other words, when $\mathcal{N}_+ - (-1)^b \mathcal{N}_- \neq 0$ occurs, the nonzero normal-state Euler numbers prevent the corresponding pairing channel to have a nonvanishing pairing gap function Δ_b . Therefore, when $\mathcal{N}_+ - (-1)^b \mathcal{N}_- \neq 0$ occurs, Δ_b is called an Euler obstructed pairing channel.

c. Comments on the Gauge Invariance

In the last part of this section, we would like to comment on the gauge invariance of the formalism proposed above. The key quantities \mathcal{N}_{\pm} (Eq. (B11)), $\mathbf{Q}_{\alpha}(\mathbf{k})$ (Eq. (B19)), $\Phi_{\alpha}(\mathbf{k})$ (Eq. (B19)), $P_b(\mathbf{k})$ (Eq. (B24)), $\mathbf{v}_b(\mathbf{k})$ (Eq. (B27)) and $\mathcal{W}_{b,i}$ (Eq. (B34)) in the above formalism are manifestly gauge-invariant, in the sense that (i) they take the same values for all gauges, and (ii) no special gauges are chosen in their expressions. However, the sense of gauge invariance here is weaker than the gauge invariance of the Berry curvature, as discussed in the following.

To derive the Berry curvature at any momentum \mathbf{k} , we only need to know the states near \mathbf{k} , and the resultant Berry curvature is gauge invariant. However, to get $\mathbf{Q}_{\alpha}(\mathbf{k})$, $\Phi_{\alpha}(\mathbf{k})$, $P_b(\mathbf{k})$ or $\mathbf{v}_b(\mathbf{k})$, knowing the states near \mathbf{k} is not enough, since there is a Wilson line matrix embedded in their definitions which connect \mathbf{k} to a base point \mathbf{k}_0 . So $\mathbf{Q}_{\alpha}(\mathbf{k})$, $\Phi_{\alpha}(\mathbf{k})$, $P_b(\mathbf{k})$ or $\mathbf{v}_b(\mathbf{k})$ are not locally defined at \mathbf{k} . The Wilson line matrix is crucial for the gauge invariance of those

quantities, and what it does is to align the gauge of $|u_{\alpha,\mathbf{k}}\rangle(-i\tau_y)\langle u_{\alpha,\mathbf{k}}^{C_{2z}\mathcal{T}}|$ at \mathbf{k} to that at \mathbf{k}_0 . Therefore, although we have not chosen any special gauges in the expressions of \mathcal{N}_{\pm} , $\mathbf{Q}_{\alpha}(\mathbf{k})$, $\Phi_{\alpha}(\mathbf{k})$, $P_b(\mathbf{k})$, $\mathbf{v}_b(\mathbf{k})$ and $\mathcal{W}_{b,i}$, the gauges of $|u_{\alpha,\mathbf{k}}\rangle(-i\tau_y)\langle u_{\alpha,\mathbf{k}}^{C_{2z}\mathcal{T}}|$ have been implicitly aligned by the Wilson line embedded in their expression. On the other hand, there are no gauge alignments in the expression of the Berry curvature, and thus the sense of gauge invariance here is weaker than the gauge invariance of the Berry curvature.

Nevertheless, no special gauges are chosen in the expressions of \mathcal{N}_{\pm} , $\mathbf{Q}_{\alpha}(\mathbf{k})$, $\Phi_{\alpha}(\mathbf{k})$, $P_b(\mathbf{k})$, $\mathbf{v}_b(\mathbf{k})$ and $\mathcal{W}_{b,i}$. Therefore, the numerical evaluation of them is very convenient, since we do not need to care about the random $U(2)$ rotations or $U(1)$ phases of the eigenvectors in numerical calculations.

2. Chern Gauge

In the above, we have introduced the gauge-invariant formalism for the Euler obstructed Cooper pairing, which is convenient for numerical calculations. In some cases, choosing certain special gauges may help understand the physics or help prove a gauge-invariant conclusion. In this part, we will discuss the Euler obstructed Cooper pairing in a class of special gauges, called Chern gauges, under Asm. 1-7. The Cooper pairings between Chern states (or in the Chern gauge) were discussed in Ref. [29, 44–46], and we will see the following discussion agrees with those previous discussions.

The Chern gauges for the bands with nonzero Euler numbers have been carefully discussed in Ref. [49, 52, 53]. Here we briefly review it. The Chern gauges for the set of two nearly flat bands in valley α are derived from the real oriented gauges. Specifically, given a real oriented gauge $|u_{\alpha,\mathbf{k}}^{RO}\rangle$ with real curvature $f_{\alpha}(\mathbf{k})$ and Euler class $e_{2,\alpha}$, we can get a complex gauge as

$$|u_{\alpha,\mathbf{k}}^{Ch}\rangle = |u_{\alpha,\mathbf{k}}^{RO}\rangle \frac{1}{\sqrt{2}} \begin{pmatrix} 1 & 1 \\ i & -i \end{pmatrix}. \quad (\text{B36})$$

$P_{Ch,\alpha,a}(\mathbf{k}) = |u_{\alpha,\mathbf{k},a}^{Ch}\rangle\langle u_{\alpha,\mathbf{k},a}^{Ch}|$ is smooth everywhere in \mathbb{R}^2 . It is because for any $\mathbf{k}' \in \mathbb{R}^2$, $|u_{\alpha,\mathbf{k}}^{RO}\rangle$ can be made smooth in a neighborhood of \mathbf{k}' by performing $|u_{\alpha,\mathbf{k}}^{RO}\rangle \rightarrow |u_{\alpha,\mathbf{k}}^{RO}\rangle e^{i\tau_y\phi_{\mathbf{k}}}$ with $\phi_{\mathbf{k}} \in \mathbb{R}$ around \mathbf{k}' , which means we can perform $|u_{\alpha,\mathbf{k}}^{Ch}\rangle \rightarrow |u_{\alpha,\mathbf{k}}^{Ch}\rangle e^{i\tau_z\phi_{\mathbf{k}}}$ around \mathbf{k}' to make $|u_{\alpha,\mathbf{k}}^{Ch}\rangle$ smooth in a neighborhood of \mathbf{k}' . Since $P_{Ch,\alpha,a}(\mathbf{k})$ is invariant under $|u_{\alpha,\mathbf{k}}^{Ch}\rangle \rightarrow |u_{\alpha,\mathbf{k}}^{Ch}\rangle e^{i\tau_z\phi_{\mathbf{k}}}$, $P_{Ch,\alpha,a}(\mathbf{k})$ must be smooth everywhere in \mathbb{R}^2 . Then, the globally smooth $P_{Ch,\alpha,a}(\mathbf{k})$ means $|u_{\alpha,\mathbf{k},a}^{Ch}\rangle$ is the basis of a rank-1 vector bundle, which has well-defined Berry curvature

$$F_{\alpha,a}(\mathbf{k}) = (-i) \text{Tr}[P_{Ch,\alpha,a}(\mathbf{k})\partial_{k_x}P_{Ch,\alpha,a}(\mathbf{k})\partial_{k_y}P_{Ch,\alpha,a}(\mathbf{k})] - (\partial_{k_x} \leftrightarrow \partial_{k_y}) \quad (\text{B37})$$

and well-defined Chern number.

$$C_{\alpha,a} = \frac{1}{2\pi} \int_{\text{1BZ}} d^2k F_{\alpha,a}(\mathbf{k}). \quad (\text{B38})$$

Therefore, $|u_{\alpha,\mathbf{k}}^{Ch}\rangle$ obtained from Eq. (B36) is called a Chern gauge. In particular, owing to Eq. (B36), the Berry curvatures and Chern numbers for the Chern gauges are related to the real curvature and the Euler class of the real oriented gauge as

$$\begin{aligned} F_{\alpha,1}(\mathbf{k}) &= -F_{\alpha,2}(\mathbf{k}) = f_{\alpha}(\mathbf{k}) \\ C_{\alpha,1} &= -C_{\alpha,2} = e_{2,\alpha}, \end{aligned} \quad (\text{B39})$$

where the opposite Berry curvatures and Chern numbers for the two components of the Chern gauge are guaranteed by the $C_{2z}\mathcal{T}$ symmetry, as

$$C_{2z}\mathcal{T}|u_{\pm,\mathbf{k}}^{Ch}\rangle = |u_{\pm,\mathbf{k}}^{Ch}\rangle\tau_x. \quad (\text{B40})$$

Since we can always choose the real oriented gauge such that $e_{2,\pm} = \mathcal{N}_{\pm}$, we can always choose a Chern gauge $|u_{\alpha,\mathbf{k}}^{Ch}\rangle$ such that

$$C_{\alpha,1} = -C_{\alpha,2} = \mathcal{N}_{\alpha}. \quad (\text{B41})$$

Then, we define an assumption for the Chern gauge as

Assumption 8. *Given any Chern gauge, we choose it to satisfy Eq. (B41).*

With Asm. 8, we know $\eta_{\pm, \mathbf{k}_0}^{Ch}(\mathbf{k}) = i$, and

$$\begin{aligned} Q_{\pm}(\mathbf{k}) &= -\frac{i}{\sqrt{2}} |u_{\pm, \mathbf{k}}^{Ch}\rangle \tau_z \langle u_{\pm, \mathbf{k}}^{Ch}| \\ \Phi_{\pm}(\mathbf{k}) &= F_{\pm, 1}(\mathbf{k}) . \end{aligned} \quad (\text{B42})$$

Combined with Eq. (B24), we have

$$\Delta_{\perp}^{Ch}(\mathbf{k}) = \begin{pmatrix} d_{\perp}(\mathbf{k}) \\ d_{\perp}^*(\mathbf{k}) \end{pmatrix}, \quad \Delta_{\parallel}^{Ch}(\mathbf{k}) = \begin{pmatrix} d_{\parallel}^*(\mathbf{k}) \\ d_{\parallel}(\mathbf{k}) \end{pmatrix} \quad (\text{B43})$$

with $d_b(\mathbf{k}) = |\Delta_b(\mathbf{k})| e^{i\theta_b(\mathbf{k})}$. Furthermore, combined with Eq. (B27) and Eq. (B34), we have

$$\begin{aligned} \mathbf{v}_b(\mathbf{k}) &= -(-1)^b \nabla_{\mathbf{k}} \theta_b(\mathbf{k}) - \mathbf{A}_{+, 1}(\mathbf{k}) - (-1)^b \mathbf{A}_{-, 1}(-\mathbf{k}) \\ \mathcal{W}_{b, i} &= -\frac{(-1)^b}{2\pi} \int_{\partial D_{b, i}} d\mathbf{k} \cdot \nabla_{\mathbf{k}} \theta_b(\mathbf{k}), \end{aligned} \quad (\text{B44})$$

where $\mathbf{A}_{\pm, a}(\mathbf{k}) = (-i) \langle u_{\pm, \mathbf{k}, a}^{Ch} | \nabla_{\mathbf{k}} u_{\pm, \mathbf{k}, a}^{Ch} \rangle$, and $\partial D_{b, i}$ encloses only the zero i of $|\Delta_b(\mathbf{k})|$ as defined in Eq. (B34). Eventually, combining Eq. (B41) and Eq. (B35), we have

$$\sum_i \mathcal{W}_{b, i} = -C_{+, 2} - (-1)^b C_{-, 1} = -C_{+, 2} + (-1)^b C_{-, 2}, \quad (\text{B45})$$

which has the same form as the monopole Cooper pairing in Ref. [45] if $\mathcal{N}_+ - (-1)^b \mathcal{N}_- \neq 0$, and also agrees with the discussion in Chern gauge in [29, 44]. Therefore, when choosing the Chern gauge for the normal-state basis, the Euler obstructed Cooper pairing can be treated as a $C_{2z}\mathcal{T}$ -protected double version of the monopole Cooper pairing. However, the whole discussion in the Chern gauge, including the connection between the Euler obstructed Cooper pairing and the monopole Cooper pairing, is just a special case for the general formalism discussed in the last part.

At last, we would like to describe how we can numerically choose a Chern gauge that satisfies Asm. 8. Numerically, it is straight forward to get a random gauge for $|u_{\alpha}(\mathbf{k})\rangle$, *e.g.*, by diagonalizing the Hamiltonian.

1. From $|u_{\alpha}(\mathbf{k})\rangle$, we can get a real gauge $|\tilde{u}_{\alpha}(\mathbf{k})\rangle$ from Eq. (B13).
2. Then, we pick a base point \mathbf{k}_0 in 1BZ, evaluate $\det(W_{\alpha}(\mathbf{k}_0, \mathbf{k}))$ for the real gauge $|\tilde{u}_{\alpha}(\mathbf{k})\rangle$ for every \mathbf{k} ; if $\det(W_{\alpha}(\mathbf{k}_0, \mathbf{k})) = -1$, perform $|\tilde{u}_{\alpha}(\mathbf{k})\rangle \rightarrow |\tilde{u}_{\alpha}(\mathbf{k})\rangle \tau_z$. After these operations, we have $\det(W_{\alpha}(\mathbf{k}, \mathbf{k}')) = 1$ for $|\tilde{u}_{\alpha}(\mathbf{k})\rangle$ and for any \mathbf{k}, \mathbf{k}' , and thus $|\tilde{u}_{\alpha}(\mathbf{k})\rangle$ becomes a real oriented gauge $|u_{\alpha}^{RO}(\mathbf{k})\rangle$.
3. Then, with Eq. (B36), we can get the Chern gauge $|u_{\alpha, a}^{Ch}(\mathbf{k})\rangle$ from $|u_{\alpha, a}^{RO}(\mathbf{k})\rangle$. If $C_{\alpha, 1} < 0$, $|u_{\alpha}^{Ch}(\mathbf{k})\rangle \rightarrow |u_{\alpha}^{Ch}(\mathbf{k})\rangle \tau_x$, resulting in a Chern gauge that satisfies Asm. 8.

In the above process, we use the fact that if a real gauge $|\tilde{u}_{\alpha}(\mathbf{k})\rangle$ has $\det(W_{\alpha}(\mathbf{k} \xrightarrow{\gamma} \mathbf{k}')) = 1$ for any \mathbf{k}, \mathbf{k}' and γ , then $|\tilde{u}_{\alpha}(\mathbf{k})\rangle$ is a real oriented gauge. The reasoning is the following. We can always have a patchwise-smooth real gauge $|\tilde{u}_{\alpha}^A(\mathbf{k})\rangle$ such that $|\tilde{u}_{\alpha}(\mathbf{k})\rangle = |\tilde{u}_{\alpha}^A(\mathbf{k})\rangle$. Then, for any $\mathbf{k} \in A \cap A'$, we have $\mathbf{k}_{initial} \in A$ and $\mathbf{k}_{final} \in A'$, and we can choose a path γ from $\mathbf{k}_{initial}$ through \mathbf{k} to \mathbf{k}_{final} . Then, $\det(W_{\alpha}(\mathbf{k}_{initial} \xrightarrow{\gamma} \mathbf{k}_{final})) = 1$ for $|\tilde{u}_{\alpha}(\mathbf{k})\rangle$ gives

$$\begin{aligned} 1 &= \lim_{L \rightarrow \infty} \det(\langle \tilde{u}_{\alpha}^A(\mathbf{k}_{initial}) | P_{\alpha}(\mathbf{k}_1) \dots P_{\alpha}(\mathbf{k}_L) | \tilde{u}_{\alpha}^A(\mathbf{k}) \rangle) \det(\langle \tilde{u}_{\alpha}^A(\mathbf{k}) | \tilde{u}_{\alpha}^{A'}(\mathbf{k}) \rangle) \det(\langle \tilde{u}_{\alpha}^{A'}(\mathbf{k}) | P_{\alpha}(\mathbf{k}_{L+1}) \dots P_{\alpha}(\mathbf{k}_{2L}) | \tilde{u}_{\alpha}^{A'}(\mathbf{k}_{final}) \rangle) \\ &= \det(\langle \tilde{u}_{\alpha}^A(\mathbf{k}) | \tilde{u}_{\alpha}^{A'}(\mathbf{k}) \rangle), \end{aligned} \quad (\text{B46})$$

meaning that $|\tilde{u}_{\alpha}^A(\mathbf{k})\rangle$ is a patchwise-smooth real oriented gauge and thus $|\tilde{u}_{\alpha}(\mathbf{k})\rangle$ is a real oriented gauge.

The above method of finding Chern gauges is equivalent to the method presented in Ref. [54].

Appendix C: Superfluid Weight in 2D Systems with $C_{2z}\mathcal{T}$ Symmetry

In this section, we will discuss the superfluid weight. We first review the general framework, and then focus on the case where Asm. 1-7 are satisfied. In this section, we will adopt the Lorentz-Heaviside unit system with $\hbar = c = 1$ unless specified otherwise.

1. Review of General Formalism for Mean-field Superfluid Weight

Let us first review the general formalism of the superfluid weight within the mean-field approximation following Ref. [49]. Consider a general mean-field Hamiltonian \tilde{H}_{MF} for a generic superconductor. The trick to derive superfluid weight is to put the superconductors in a constant vector field \mathbf{A} , resulting in the mean-field Hamiltonian

$$\tilde{H}_{MF}(\mathbf{A}) = \tilde{H}(\mathbf{A}) - \mu \hat{N}_\psi + \tilde{H}_{pairing} , \quad (C1)$$

where $\mathbf{A} = e\mathbf{A}^{phy}$ with \mathbf{A}^{phy} the physical U(1) vector field,

$$\tilde{H}(\mathbf{A}) = \sum_{\mathbf{k} \in 1\text{BZ}} \psi_{\mathbf{k}}^\dagger \tilde{h}(\mathbf{k} + \mathbf{A}) \psi_{\mathbf{k}} \quad (C2)$$

represents the normal state,

$$\tilde{H}_{pairing} = \sum_{\mathbf{k} \in 1\text{BZ}} \psi_{\mathbf{k}}^\dagger \tilde{\Delta}(\mathbf{k}) (\psi_{-\mathbf{k}}^\dagger)^T + h.c. \quad (C3)$$

represents the mean-field pairing operator, $\hat{N}_\psi = \sum_{\mathbf{k} \in 1\text{BZ}} \psi_{\mathbf{k}}^\dagger \psi_{\mathbf{k}}$, and $\psi_{\mathbf{k}}^\dagger = (\dots, \psi_{\mathbf{k},l}^\dagger, \dots)$ are the creation operators for the atomic Bloch basis. We can also interpret \mathbf{A} as a momentum shift caused by an in-homogeneous deformation of the pairing order parameter, since we treat \mathbf{A} to be independent of temporal and spatial coordinates.

Very often, we do not address the problem in the atomic Bloch basis, and instead, we need to project the system into a set of bands with creation operators

$$c_{\mathbf{k},\mathbf{A}}^\dagger = \psi_{\mathbf{k}}^\dagger V(\mathbf{k} + \mathbf{A}) , \quad (C4)$$

where $V(\mathbf{k})$ has orthonormal columns. Then, we care about the projected mean-field Hamiltonian

$$H_{MF}(\mathbf{A}) = H(\mathbf{A}) - \mu \hat{N}(\mathbf{A}) + H_{pairing}(\mathbf{A}) , \quad (C5)$$

where $\hat{N}(\mathbf{A}) = \sum_{\mathbf{k} \in 1\text{BZ}} c_{\mathbf{k},\mathbf{A}}^\dagger c_{\mathbf{k},\mathbf{A}}$,

$$H(\mathbf{A}) = \sum_{\mathbf{k} \in 1\text{BZ}} c_{\mathbf{k},\mathbf{A}}^\dagger h(\mathbf{k} + \mathbf{A}) c_{\mathbf{k},\mathbf{A}} \quad (C6)$$

with $h(\mathbf{k}) = V^\dagger(\mathbf{k}) \tilde{h}(\mathbf{k}) V(\mathbf{k})$, and

$$H_{pairing}(\mathbf{A}) = \sum_{\mathbf{k} \in 1\text{BZ}} c_{\mathbf{k},\mathbf{A}}^\dagger D(\mathbf{k}, \mathbf{A}) (c_{-\mathbf{k},\mathbf{A}}^\dagger)^T + h.c. \quad (C7)$$

with

$$D(\mathbf{k}, \mathbf{A}) = V^\dagger(\mathbf{k} + \mathbf{A}) \tilde{\Delta}(\mathbf{k}) V^*(-\mathbf{k} + \mathbf{A}) . \quad (C8)$$

Using $E_{\mathbf{k},m}(\mathbf{A})$ to label the eigenvalues of

$$\begin{pmatrix} h(\mathbf{k} + \mathbf{A}) - \mu & D(\mathbf{k}, \mathbf{A}) \\ D^\dagger(\mathbf{k}, \mathbf{A}) & -[h(-\mathbf{k} + \mathbf{A}) - \mu]^T \end{pmatrix} , \quad (C9)$$

we arrive at the mean-field Free energy of the system as

$$\Omega(\mathbf{A}) = \sum_{\mathbf{k} \in 1\text{BZ}} \left\{ \frac{1}{2} \text{Tr}[h(\mathbf{k} + \mathbf{A}) - \mu] - \frac{1}{\beta} \sum_m^{E_{\mathbf{k},m}(\mathbf{A}) > 0} \log \left[2 \cosh \left(\frac{\beta E_{\mathbf{k},m}(\mathbf{A})}{2} \right) \right] \right\} , \quad (C10)$$

where $\beta = 1/(k_B T)$ with T the temperature and k_B the Boltzmann constant. At zero temperature, the free energy equals to the ground state energy of $H_{MF}(\mathbf{A})$, which reads

$$\Omega_0(\mathbf{A}) = \lim_{T \rightarrow 0} \Omega(\mathbf{A}) = -\frac{1}{4} \sum_{\mathbf{k} \in 1\text{BZ}, m} |E_{\mathbf{k},m}(\mathbf{A})| + \frac{1}{2} \sum_{\mathbf{k} \in 1\text{BZ}} \text{Tr}[h(\mathbf{k} + \mathbf{A}) - \mu] . \quad (C11)$$

The superfluid weight then reads

$$[D_{SF}(T)]_{ij} = \frac{e^2}{\mathcal{V}} \frac{\partial^2 \Omega(\mathbf{A})}{\partial A_i \partial A_j} \Big|_{\mathbf{A} \rightarrow 0} \quad (C12)$$

with \mathcal{V} the volume of the system. Detailed derivations can be found in the supplementary materials of Ref. [49].

2. Superfluid Weight in 2D systems that satisfy Asm. 1-7

Now we derive the expression for the superfluid weight of the 2D systems that satisfy Asm. 1-7, generalizing the derivation for the uniform pairing in Ref. [49].

Owing to Asm. 1-7, we have $\psi_{\mathbf{k}}^\dagger = (\psi_{+, \mathbf{k}}^\dagger, \psi_{-, \mathbf{k}}^\dagger)$,

$$\tilde{h}(\mathbf{k}) = \begin{pmatrix} \tilde{h}_+(\mathbf{k}) \otimes s_0 & \\ & \tilde{h}_-(\mathbf{k}) \otimes s_0 \end{pmatrix} \quad (\text{C13})$$

$\tilde{h}_\pm(\mathbf{k})$ defined in Eq. (B2),

$$V(\mathbf{k}) = \begin{pmatrix} V_+(\mathbf{k}) \otimes s_0 & \\ & V_-(\mathbf{k}) \otimes s_0 \end{pmatrix} \quad (\text{C14})$$

with V_\pm defined above Eq. (B3), and

$$\tilde{\Delta}(\mathbf{k}) = V(\mathbf{k}) \begin{pmatrix} \Delta(\mathbf{k}) \otimes \Pi & \\ -\Delta^T(-\mathbf{k}) \otimes \Pi^T \end{pmatrix} V^T(-\mathbf{k}) \quad (\text{C15})$$

with $\Delta(\mathbf{k}) \otimes \Pi$ defined in Asm. 7. Then, we have

$$h(\mathbf{k}) = \begin{pmatrix} h_+(\mathbf{k}) \otimes s_0 & \\ & h_-(\mathbf{k}) \otimes s_0 \end{pmatrix} \quad (\text{C16})$$

with $h_\pm(\mathbf{k}) = V_\pm^\dagger(\mathbf{k}) \tilde{h}_\pm(\mathbf{k}) V_\pm(\mathbf{k})$, and

$$D(\mathbf{k}, \mathbf{A}) = \begin{pmatrix} D_{+, \mathbf{k}}(\mathbf{A}) \otimes \Pi & \\ -D_{+, -\mathbf{k}}^T(\mathbf{A}) \otimes \Pi^T \end{pmatrix} \quad (\text{C17})$$

with

$$D_{+, \mathbf{k}}(\mathbf{A}) = V_+^\dagger(\mathbf{k} + \mathbf{A}) V_+(\mathbf{k}) \Delta(\mathbf{k}) V_-^T(-\mathbf{k}) V_-^*(-\mathbf{k} + \mathbf{A}) . \quad (\text{C18})$$

Finally, by using Eq. (C10) and the fact that $\Pi^\dagger \Pi = s_0$, we arrive at

$$\Omega(\mathbf{A}) = \sum_{\mathbf{k} \in \text{1BZ}} \left\{ \sum_{\alpha} \text{Tr}[h_{\alpha}(\mathbf{k} + \mathbf{A}) - \mu] - \frac{2}{\beta} \sum_n^{E_{+, \mathbf{k}, n}(\mathbf{A}) > 0} \log \left[2 \cosh \left(\frac{\beta E_{+, \mathbf{k}, n}(\mathbf{A})}{2} \right) \right] \right\} , \quad (\text{C19})$$

where $E_{+, \mathbf{k}, n}(\mathbf{A})$ eigenvalues of

$$\mathcal{H}(\mathbf{k}, \mathbf{A}) = \begin{pmatrix} h_+(\mathbf{k} + \mathbf{A}) - \mu & D_{+, \mathbf{k}}(\mathbf{A}) \\ D_{+, \mathbf{k}}^\dagger(\mathbf{A}) & -h_-^T(-\mathbf{k} + \mathbf{A}) + \mu \end{pmatrix} . \quad (\text{C20})$$

The superfluid weight can be derived by substituting Eq. (C19) into Eq. (C12),

In 2D, the superconductivity transition is typically Berezinskii–Kosterlitz–Thouless (BKT) transition [49], and the corresponding BKT transition temperature can be estimated as

$$k_B T_{BKT} \approx \frac{\pi}{8e^2} \frac{\text{Tr}[D_{SF}(T_{BKT})]}{2} . \quad (\text{C21})$$

3. Bounded zero-temperature superfluid weight in 2D systems that satisfy Asm. 1-7

In the the remaining discussion, we will discuss the zero-temperature superfluid weight for superconductors that satisfies Asm. 1-7. Besides Asm. 1-7, we further impose the following extra assumption

Assumption 9. *The normal-state bands described by Eq. (B4) are exactly flat with zero energies, $\mu \neq 0$, and the normal state has C_{2z} symmetry with $C_{2z}c_{+,\mathbf{k}}^\dagger C_{2z}^{-1} = c_{-,-\mathbf{k}}^\dagger U_{C_{2z}}(\mathbf{k}) \otimes s_0$.*

Under Asm. 9, we can choose a Chern gauge that satisfies Asm. 8 and $C_{2z}c_{+,\mathbf{k}}^\dagger C_{2z}^{-1} = c_{-,-\mathbf{k}}^\dagger$. Let us first use this gauge to derive the bound for the superfluid weight. With this gauge, we have

$$D_{+,\mathbf{k}}(\mathbf{A}) = V_+^\dagger(\mathbf{k} + \mathbf{A})V_+(\mathbf{k})\Delta(\mathbf{k})V_+^T(\mathbf{k})V_+^*(\mathbf{k} - \mathbf{A}) , \quad (\text{C22})$$

resulting in

$$D_{+,\mathbf{k}}^*(\mathbf{A}) = \tau_x D_{+,\mathbf{k}}(\mathbf{A})\tau_x \Rightarrow D_{+,\mathbf{k}}(\mathbf{A}) = \begin{pmatrix} d_\parallel^*(\mathbf{k}, \mathbf{A}) & d_\perp(\mathbf{k}, \mathbf{A}) \\ d_\perp^*(\mathbf{k}, \mathbf{A}) & d_\parallel(\mathbf{k}, \mathbf{A}) \end{pmatrix} . \quad (\text{C23})$$

Combined with $h_\alpha(\mathbf{k}) = 0$ required by Asm. 9, we have $E_{+,\mathbf{k},n}(\mathbf{A})$ taking values in $\{\pm\sqrt{\mu^2 + \lambda_{+,\mathbf{k},a}(\mathbf{A})}|a = 1, 2\}$, resulting in the zero-temperature superfluid weight as

$$[D_{SF}]_{ij} = -\frac{2e^2}{\mathcal{V}} \sum_{\mathbf{k} \in \text{1BZ}} \sum_a \partial_{A_i} \partial_{A_j} \sqrt{\mu^2 + \lambda_{+,\mathbf{k},a}(\mathbf{A})} \Big|_{\mathbf{A} \rightarrow 0} , \quad (\text{C24})$$

where

$$\lambda_{+,\mathbf{k},a}(\mathbf{A}) = (|d_\perp(\mathbf{k}, \mathbf{A})| + (-1)^{a-1}|d_\parallel(\mathbf{k}, \mathbf{A})|)^2 . \quad (\text{C25})$$

Here both $d_\perp(\mathbf{k}, \mathbf{A})$ and $d_\parallel(\mathbf{k}, \mathbf{A})$ are complex, and $d_b(\mathbf{k}, 0) = d_b(\mathbf{k})$ with $d_b(\mathbf{k})$ in Eq. (B43).

In particular, $\sum_a \sqrt{\mu^2 + \lambda_{+,\mathbf{k},a}(\mathbf{A})}$ is a smooth function of (\mathbf{k}, \mathbf{A}) , because

$$\sum_a \sqrt{\mu^2 + \lambda_{+,\mathbf{k},a}(\mathbf{A})} = \sqrt{2(\mu + \delta_+(\mathbf{k}, \mathbf{A})) + 2\sqrt{\mu^4 + 2\mu^2\delta_+(\mathbf{k}, \mathbf{A}) + \delta_-^2(\mathbf{k}, \mathbf{A})}} \quad (\text{C26})$$

with $\delta_\pm(\mathbf{k}, \mathbf{A}) = |d_\perp(\mathbf{k}, \mathbf{A})|^2 \pm |d_\parallel(\mathbf{k}, \mathbf{A})|^2$, and $|d_b(\mathbf{k}, \mathbf{A})|^2$ is a smooth function of (\mathbf{k}, \mathbf{A}) since it is independent of the choice of Chern gauge (that satisfies the requirements) and we can always choose the Chern gauge to make $d_b(\mathbf{k}, \mathbf{A})$ in a neighborhood of any (\mathbf{k}, \mathbf{A}) . Furthermore, from the above equation, $\text{Tr}[D_{SF}]$ is solely determined by $\partial_{A_i}^{1,2}\delta_\pm(\mathbf{k}, \mathbf{A}) \Big|_{\mathbf{A} \rightarrow 0}$. Straightforward derivations give

$$\partial_{A_i} \delta_\pm(\mathbf{k}, \mathbf{A}) \Big|_{\mathbf{A} \rightarrow 0} = 0 , \quad (\text{C27})$$

and

$$\begin{aligned} \partial_{A_i}^2 \delta_+(\mathbf{k}, \mathbf{A}) \Big|_{\mathbf{A} \rightarrow 0} &= -[2\delta_+(\mathbf{k}, 0)g_{+,ii}(\mathbf{k}) + 4z_i(\mathbf{k})] \\ \partial_{A_i}^2 \delta_-(\mathbf{k}, \mathbf{A}) \Big|_{\mathbf{A} \rightarrow 0} &= -[2\delta_-(\mathbf{k}, 0)g_{+,ii}(\mathbf{k})] , \end{aligned} \quad (\text{C28})$$

where

$$\begin{aligned} g_{+,ij}(\mathbf{k}) &= \frac{1}{2} \text{Tr}[\partial_{k_i} P_{+,\mathbf{k}} \partial_{k_j} P_{+,\mathbf{k}}] \\ z_i(\mathbf{k}) &= \frac{1}{2} \text{Tr}[P_\perp(\mathbf{k})C_2] \text{Tr}[P_\parallel(\mathbf{k})C_2 \partial_{k_i} P_{+,\mathbf{k}} \partial_{k_i} P_{+,\mathbf{k}}] , \end{aligned} \quad (\text{C29})$$

$P_{+,\mathbf{k}} = |u_{+,\mathbf{k}}\rangle\langle u_{+,\mathbf{k}}|$, and $P_b(\mathbf{k})$ is defined in Eq. (B24). $g_+(\mathbf{k})$ is called the Fubini-Study metric [68] for the two normal-state bands in valley +, which is a positive semi-definite matrix.

By exploiting Eq. (C27) and Eq. (C28), we can simplify the expression of $\text{Tr}[D_{SF}]$ to

$$\text{Tr}[D_{SF}] = 4e^2 \int_{\text{1BZ}} \frac{d^2 k}{(2\pi)^2} \left[f_+(\mathbf{k}) \text{Tr}[g_+(\mathbf{k})] + \frac{f_-(\mathbf{k})}{|\Delta_\parallel(\mathbf{k})||\Delta_\perp(\mathbf{k})|} z_{\mathbf{k}} \right] , \quad (\text{C30})$$

where $z_{\mathbf{k}} = \sum_i z_i(\mathbf{k})$ and

$$f_{\pm}(\mathbf{k}) = \frac{1}{2} \left(\frac{(|\Delta_{\perp}(\mathbf{k})| + |\Delta_{\parallel}(\mathbf{k})|)^2}{\sqrt{\mu^2 + (|\Delta_{\perp}(\mathbf{k})| + |\Delta_{\parallel}(\mathbf{k})|)^2}} \pm \frac{(|\Delta_{\perp}(\mathbf{k})| - |\Delta_{\parallel}(\mathbf{k})|)^2}{\sqrt{\mu^2 + (|\Delta_{\perp}(\mathbf{k})| - |\Delta_{\parallel}(\mathbf{k})|)^2}} \right). \quad (\text{C31})$$

Here $\frac{f_{-}(\mathbf{k})}{|\Delta_{\parallel}(\mathbf{k})||\Delta_{\perp}(\mathbf{k})|}$ is continuous even at \mathbf{k} with $|\Delta_{\parallel}(\mathbf{k})||\Delta_{\perp}(\mathbf{k})| = 0$ since

$$\frac{f_{-}(\mathbf{k})}{|\Delta_{\parallel}(\mathbf{k})||\Delta_{\perp}(\mathbf{k})|} = \frac{2}{\sqrt{\mu^2 + (|\Delta_{\perp}(\mathbf{k})| + |\Delta_{\parallel}(\mathbf{k})|)^2} + \sqrt{\mu^2 + (|\Delta_{\perp}(\mathbf{k})| - |\Delta_{\parallel}(\mathbf{k})|)^2}} \times \left(1 + \frac{\mu^2}{\sqrt{\mu^2 + (|\Delta_{\perp}(\mathbf{k})| + |\Delta_{\parallel}(\mathbf{k})|)^2} \sqrt{\mu^2 + (|\Delta_{\perp}(\mathbf{k})| - |\Delta_{\parallel}(\mathbf{k})|)^2}} \right). \quad (\text{C32})$$

Although we derive Eq. (C30) in the Chern gauge, Eq. (C30) holds for all gauges since both sides are gauge-invariant.

Note that for any \mathbf{k} such that $|\Delta_{\parallel}(\mathbf{k})| \neq 0$,

$$|\text{Tr}[P_{\parallel}(\mathbf{k}) C_{2z} \partial_{k_i} P_{+}(\mathbf{k}) \partial_{k_i} P_{+}(\mathbf{k})] / |\Delta_{\parallel}(\mathbf{k})| \leq g_{+,ii}(\mathbf{k}). \quad (\text{C33})$$

Then, we have

$$\left| \frac{f_{-}(\mathbf{k})}{|\Delta_{\parallel}(\mathbf{k})||\Delta_{\perp}(\mathbf{k})|} z_{\mathbf{k}} \right| \leq |f_{-}(\mathbf{k})| \text{Tr}[g_{+}(\mathbf{k})] \quad (\text{C34})$$

for all \mathbf{k} since it trivially holds for $|\Delta_{\parallel}(\mathbf{k})||\Delta_{\perp}(\mathbf{k})| = 0 \Rightarrow z_{\mathbf{k}} = 0$ and follows from Eq. (C33) for $|\Delta_{\parallel}(\mathbf{k})||\Delta_{\perp}(\mathbf{k})| \neq 0$. As a result, we have

$$\begin{aligned} \text{Tr}[D_{SF}] &= 4e^2 \int_{\text{1BZ}} \frac{d^2 k}{(2\pi)^2} \left[f_{+}(\mathbf{k}) \text{Tr}[g_{+}(\mathbf{k})] + \frac{f_{-}(\mathbf{k})}{|\Delta_{\parallel}(\mathbf{k})||\Delta_{\perp}(\mathbf{k})|} z_{\mathbf{k}} \right] \\ &\geq 4e^2 \int_{\text{1BZ}} \frac{d^2 k}{(2\pi)^2} \left[f_{+}(\mathbf{k}) \text{Tr}[g_{+}(\mathbf{k})] - \left| \frac{f_{-}(\mathbf{k})}{|\Delta_{\parallel}(\mathbf{k})||\Delta_{\perp}(\mathbf{k})|} z_{\mathbf{k}} \right| \right] \\ &\geq 4e^2 \int_{\text{1BZ}} \frac{d^2 k}{(2\pi)^2} [f_{+}(\mathbf{k}) \text{Tr}[g_{+}(\mathbf{k})] - |f_{-}(\mathbf{k})| \text{Tr}[g_{+}(\mathbf{k})]] \\ &\geq 4e^2 \int_{\text{1BZ}} \frac{d^2 k}{(2\pi)^2} \frac{[|\Delta_{\perp}(\mathbf{k})| - |\Delta_{\parallel}(\mathbf{k})|]^2}{\sqrt{[|\Delta_{\perp}(\mathbf{k})| - |\Delta_{\parallel}(\mathbf{k})|]^2 + \mu^2}} \text{Tr}[g_{+}(\mathbf{k})], \end{aligned} \quad (\text{C35})$$

where we have used $|f_{-}(\mathbf{k})| = f_{-}(\mathbf{k})$. Then, combined with

$$\int_{\text{1BZ}} \frac{d^2 k}{(2\pi)^2} \text{Tr}[g_{+}(\mathbf{k})] \geq \frac{\mathcal{N}_{+}}{\pi} > 0 \quad (\text{C36})$$

derived in Ref. [49] for any isolated set of two bands with nonzero Euler number \mathcal{N}_{+} , we eventually get

$$\text{Tr}[D_{SF}] \geq \text{Tr}[D_{SF}^{\text{bound}}] = \left\langle \frac{[|\Delta_{\perp}(\mathbf{k})| - |\Delta_{\parallel}(\mathbf{k})|]^2}{\sqrt{[|\Delta_{\perp}(\mathbf{k})| - |\Delta_{\parallel}(\mathbf{k})|]^2 + \mu^2}} \right\rangle_{g_{+}} \frac{4e^2}{\pi} \mathcal{N}_{+}, \quad (\text{C37})$$

where

$$\langle x(\mathbf{k}) \rangle_{g_{+}} = \frac{\int_{\text{1BZ}} d^2 k x(\mathbf{k}) \text{Tr}[g_{+}(\mathbf{k})]}{\int_{\text{1BZ}} d^2 k \text{Tr}[g_{+}(\mathbf{k})]}. \quad (\text{C38})$$

Similar to Eq. (C30), Eq. (C37) also holds for all gauges since both sides are gauge-invariant.

If we choose the time-reversal-invariant uniform pairing for the flat bands in MATBG in Ref. [49], we would have $|\Delta_{\perp}(\mathbf{k})| = |\Delta|$ is momentum-independent and $|\Delta_{\parallel}(\mathbf{k})| = 0$. Then, Eq. (C37) reproduces the bound for the time-reversal-invariant uniform pairing in Ref. [49] as

$$\text{Tr}[D_{SF}] \geq \text{Tr}[D_{SF}^{\text{bound}}] = \frac{4e^2}{\pi} \mathcal{N}_{+} 2\sqrt{\nu(1-\nu)} |\Delta|, \quad (\text{C39})$$

where ν is the filling ratio of the normal-state flat bands with $\nu = 0$ meaning that the entire normal-state flat bands are empty.

Appendix D: Euler Obstructed Cooper Pairing in MATBG at Zero Temperature

In this section, we provide more details on the Euler obstructed Cooper pairing in MATBG. We start with the BM model that captures the normal state, then discuss the possible Euler obstructed Cooper pairing in MATBG and its relation to nematic nodal superconductivity, and finally address the bounded zero-temperature superfluid weight. All discussions in this section are at zero temperature, unless specified otherwise.

1. BM Model

In this part, we review the BM model [3] that describes the normal state of MATBG. If we rotate the top (bottom) layer by $-\theta/2$ ($\theta/2$) about the out of plane axis, the BM model reads

$$H_{BM} = \tilde{H}_+ + \tilde{H}_- \quad (D1)$$

with

$$\tilde{H}_+ = \int d^2r \psi_{\pm, \mathbf{r}}^\dagger \begin{pmatrix} -iv_0 \nabla_{\mathbf{r}} \cdot \boldsymbol{\sigma}_{\theta/2} & T(\mathbf{r}) \\ T^\dagger(\mathbf{r}) & -iv_0 \nabla_{\mathbf{r}} \cdot \boldsymbol{\sigma}_{-\theta/2} \end{pmatrix} \otimes s_0 \psi_{+, \mathbf{r}} \quad (D2)$$

and $\tilde{H}_- = \mathcal{T} \tilde{H}_+ \mathcal{T}^{-1}$. Here $\psi_{\pm, \mathbf{r}}^\dagger = (\psi_{\pm, \mathbf{r}, t, A}^\dagger, \psi_{\pm, \mathbf{r}, t, B}^\dagger, \psi_{\pm, \mathbf{r}, b, A}^\dagger, \psi_{\pm, \mathbf{r}, b, B}^\dagger)$, A/B labels the graphene sublattice (not confused with the patch index A for patchwise-smooth gauges in Appendix B), t/b labels the top and bottom layers (not confused with the $b = \perp, \parallel$ for the channel splitting in Eq. (B25)), $\psi_{\pm, \mathbf{r}, t/b, A/B}^\dagger$ has two spin components, and σ_x are Pauli matrices for the sublattice index. $\sigma_\theta = e^{-i\theta\sigma_z/2}(\sigma_x, \sigma_y)e^{i\theta\sigma_z/2}$.

$$T(\mathbf{r}) = \sum_{j=1}^3 e^{-i\mathbf{r} \cdot \mathbf{q}_j} T_j, \quad (D3)$$

$\mathbf{q}_1 = k_D(0, -1)^T$, $\mathbf{q}_2 = k_D(\sqrt{3}/2, 1/2)^T$, $\mathbf{q}_3 = k_D(-\sqrt{3}/2, 1/2)^T$, $k_D = \frac{4\pi}{3a_0} 2 \sin(\theta/2)$ and

$$T_j = w_0 \sigma_0 + w_1 \left[\sigma_x \cos\left(\frac{2\pi(j-1)}{3}\right) + \sigma_y \sin\left(\frac{2\pi(j-1)}{3}\right) \right]. \quad (D4)$$

All parameters v_0 , a_0 , w_0 and w_1 are real.

The symmetry group of the BM model Eq. (D1) is spanned by the spin-charge $U(2)$ rotation in each valley (in total $U(2) \times U(2)$), the Moiré lattice translation $T_{\mathbf{a}_{M,i}}$ with $i = 1, 2$ and $\mathbf{a}_{M,1} = \frac{4\pi}{3k_D}(\frac{\sqrt{3}}{2}, \frac{1}{2})$ and $\mathbf{a}_{M,2} = \frac{4\pi}{3k_D}(-\frac{\sqrt{3}}{2}, \frac{1}{2})$, $\overline{C}_{2z}\mathcal{T}$, \overline{C}_{3z} , \overline{C}_{2x} , and \mathcal{T} . Although we mention the \overline{C}_{2x} symmetry, we will not use \overline{C}_{2x} in the discussion of nodal superconductivity. Specifically,

$$\begin{aligned} T_{\mathbf{x}} \psi_{\pm, \mathbf{r}}^\dagger T_{\mathbf{x}}^{-1} &= \psi_{\pm, \mathbf{r}+\mathbf{x}}^\dagger \begin{pmatrix} e^{\mp i K_{-\theta/2} \cdot \mathbf{x} \sigma_0} & \\ & e^{\mp i K_{\theta/2} \cdot \mathbf{x} \sigma_0} \end{pmatrix} \otimes s_0 \\ \overline{C}_{3z} \psi_{\pm, \mathbf{r}}^\dagger \overline{C}_{3z}^{-1} &= \psi_{\pm, C_{3z}\mathbf{r}}^\dagger \begin{pmatrix} e^{\pm i \sigma_z \pi/3} & \\ & e^{\pm i \sigma_z \pi/3} \end{pmatrix} \otimes e^{-i \frac{s_z}{2} \frac{2\pi}{3}} \\ \overline{C}_{2z} \mathcal{T} \psi_{\pm, \mathbf{r}}^\dagger (\overline{C}_{2z} \mathcal{T})^{-1} &= \psi_{\pm, -\mathbf{r}}^\dagger \begin{pmatrix} \sigma_x & \\ & \sigma_x \end{pmatrix} \otimes (-i s_x) \\ \overline{C}_{2x} \psi_{\pm, \mathbf{r}}^\dagger (\overline{C}_{2x})^{-1} &= \psi_{\pm, C_{2x}\mathbf{r}}^\dagger \begin{pmatrix} & -\sigma_x \\ -\sigma_x & \end{pmatrix} \otimes (-i s_x) \\ \mathcal{T} \psi_{\pm, \mathbf{r}}^\dagger (\mathcal{T})^{-1} &= \psi_{\mp, \mathbf{r}}^\dagger \begin{pmatrix} \sigma_0 & \\ & \sigma_0 \end{pmatrix} \otimes i s_y, \end{aligned} \quad (D5)$$

where $K_\theta = \frac{4\pi}{3a_0}(\cos(\theta), \sin(\theta))^T$. The Moiré reciprocal lattice vectors spanned by the linear combinations of $\mathbf{b}_{M,1} = \sqrt{3}k_D(\frac{1}{2}, \frac{\sqrt{3}}{2})$ and $\mathbf{b}_{M,2} = \sqrt{3}k_D(-\frac{1}{2}, \frac{\sqrt{3}}{2})$. The Moiré Brillouin zone (MBZ) is centered at $\Gamma_M = 0$ and has two inequivalent corners $K_M = -\mathbf{q}_3$ and $K'_M = \mathbf{q}_2$.

Throughout the work, the realistic parameter values for the MATBG [3, 5] are chosen as

$$\theta \in [1.05^\circ, 1.15^\circ], w_0/w_1 = 0.8, v_0 = 5817\text{meV} \cdot \text{\AA}, w_1 = 110\text{meV}, a_0 = 2.46\text{\AA}. \quad (\text{D6})$$

$w_0 = 0$ is called the chiral limit [57], which is of great theoretical interests, and thus we will sometimes extend the range of w_0/w_1 and

$$\theta \in [1.05^\circ, 1.15^\circ], w_0/w_1 \in [0, 0.8], v_0 = 5817\text{meV} \cdot \text{\AA}, w_1 = 110\text{meV}, a_0 = 2.46\text{\AA}. \quad (\text{D7})$$

The BM model can be numerically solved by choosing cutoff in the reciprocal lattice. Specifically, we will adopt the scheme in Ref. [5], meaning that \tilde{H}_\pm can be expressed in the matrix representation as

$$\tilde{H}_\pm = \sum_{\mathbf{k} \in \text{MBZ}} \sum_{\mathbf{Q}, \mathbf{Q}', \sigma, \sigma', s, s'} \psi_{\pm, \mathbf{k}, \mathbf{Q}}^\dagger [\tilde{h}_\pm(\mathbf{k})]_{\mathbf{Q}\mathbf{Q}', \sigma\sigma'} [s_0]_{ss'} \psi_{\pm, \mathbf{k}, \mathbf{Q}', \sigma', s'} \quad (\text{D8})$$

with

$$\psi_{\pm, \mathbf{k}, \mathbf{Q}, \sigma, s}^\dagger = \frac{1}{\sqrt{\mathcal{V}}} \int d^2r e^{i(\mathbf{k}+\mathbf{Q}) \cdot \mathbf{r}} \psi_{\pm, l_{\mathbf{Q}}^\pm, \mathbf{r}, \sigma, s}^\dagger, \quad (\text{D9})$$

where $\mathbf{Q} \in Q_{+,t} \cup Q_{+,b} = Q_{-,t} \cup Q_{-,b}$, $Q_{+,t} = Q_{-,b} = \mathbf{q}_3 + \{\mathbf{G}_M\}$, $Q_{+,b} = Q_{-,t} = -\mathbf{q}_2 + \{\mathbf{G}_M\}$, $l_{\mathbf{Q}}^\pm = t$ for $\mathbf{Q} \in Q_{\pm,t}$, $l_{\mathbf{Q}}^\pm = b$ for $\mathbf{Q} \in Q_{\pm,b}$, and \mathbf{G}_M is the Moiré reciprocal lattice vector. For numerical simplicity, we choose $|\mathbf{Q}| \leq 2\sqrt{7}k_D$ for the current work.

As exemplified in Fig. 5(a), the BM model has two doubly degenerate nearly flat bands in each valley. The projected effective models that capture the normal-state nearly flat bands are

$$H_\pm = \sum_{\mathbf{k} \in \text{MBZ}} c_{\pm, \mathbf{k}}^\dagger h_\pm(\mathbf{k}) \otimes s_0 c_{\pm, \mathbf{k}}, \quad (\text{D10})$$

where $c_{\pm, \mathbf{k}}^\dagger = (\dots, c_{\pm, \mathbf{k}, a, s}^\dagger, \dots)$, $c_{\pm, \mathbf{k}, a, s}^\dagger = \sum_{\mathbf{Q}, \sigma} \psi_{\pm, \mathbf{k}, \mathbf{Q}, \sigma, s}^\dagger [V_{\pm, a}(\mathbf{k})]_{\mathbf{Q}, \sigma}$ stands for the creation operator for the Bloch basis of the nearly flat bands in valley \pm , $V_\pm(\mathbf{k}) = (V_{\pm, 1}(\mathbf{k}), V_{\pm, 2}(\mathbf{k}))$ are orthonormal linear combination of eigenvectors of $\tilde{h}_\pm(\mathbf{k})$ (Eq. (D8)) for the nearly flat bands, and

$$h_\pm(\mathbf{k}) = V_\pm^\dagger(\mathbf{k}) \tilde{h}_\pm(\mathbf{k}) V_\pm(\mathbf{k}). \quad (\text{D11})$$

The set of two nearly flat bands are isolated from other bands from other bands by a gap at least 15meV as shown in Fig. 5(b-c), and it has Euler number equalling to 1. Based on the expression of the BM model and the numerical results, we verify that the normal state satisfies the Asm. 1-6 for Eq. (D7), setting the stage for the study of the Euler obstructed pairing.

2. Euler Obstructed Cooper Pairing in MATBG

For the study of superconductivity, we will assume that the superconductivity in MATBG is given by the mean-field Cooper pairs of normal-state electrons. Under this assumption, we will include the nearly flat bands over the entire MBZ, instead of just the modes at the Fermi energy, for pairing operator. The reasoning is the following. In the standard mean-field theory of superconductivity, there is a superconductivity cutoff ϵ_c , and only normal-state electrons with energies in $[\mu - \epsilon_c, \mu + \epsilon_c]$ experience effectively attractive interaction, while normal-state electrons with energies outside the range cannot form Cooper pairs that condensate at zero temperature [69]. In other words, only the normal-state electrons with energies in $[\mu - \epsilon_c, \mu + \epsilon_c]$ are allowed to have nonzero matrix elements in the pairing operator, and need to be included in the study of superconductivity in general.

In the normal state, we know μ lies in the nearly flat bands, but the value of ϵ_c varies with underlying mechanism that accounts for the pairing. Nevertheless, owing to the large gap above and below the nearly flat bands, we will assume ϵ_c is small enough such that modes outside the nearly flat bands can be neglected. Then, if ϵ_c is larger than the small bandwidth of the nearly flat bands, we should include the nearly flat bands over the entire MBZ in the pairing operator. Even if ϵ_c is smaller than the bandwidth of the nearly flat bands, we can still define the pairing

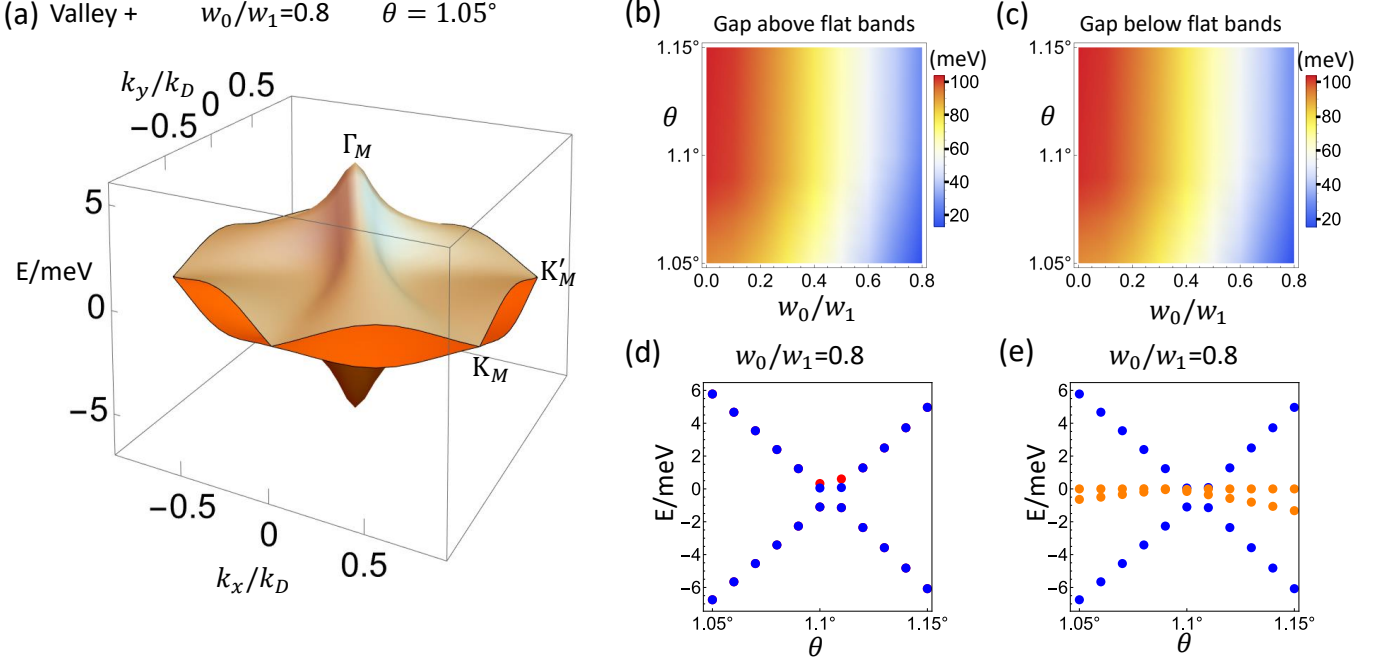


FIG. 5. Numerical calculation for the BM model with Eq. (D7). (a) show the isolated set of two nearly flat bands in valley + for the BM model for $\theta = 1.05^\circ$ and $w_0/w_1 = 0.8$. (b) and (c) show the minimum of the direct gaps above and below the isolated set of nearly flat bands, respectively. In (d), we show the top and bottom of the isolated set of near flat bands as red dots, and show the energies of the two nearly flat bands at Γ_M at blue dots. In most cases, the red dots and blue dots coincide and the blue dots exactly cover the red dots, meaning that the top and bottom of the isolated set of near flat bands are typically at Γ_M . We can see that the band width of the isolated set of two nearly flat bands is about $2 \sim 15$ meV. In (e), we show the energies of the two nearly flat bands at Γ_M at blue dots, and show the normal-state chemical potentials for 2 and 3 holes per Moiré unit cell as the orange dots. We can see when there are 2 \sim 3 holes per Moiré unit cell, the normal-state chemical potential lies in the energy range bounded by the energies of the two nearly flat bands at Γ_M . We caution that given a fixed filling, the chemical potential in the superconducting phase can be different from that in the normal state due to the correction brought by the pairing order parameter.

operator for the nearly flat bands over the entire MBZ by just keeping the pairing matrix vanishing for the electrons beyond ϵ_c . In doing so, we should avoid discontinuous structures (like step function) for electrons at ϵ_c and try to use the corresponding smooth versions (like tanh).

The discussion of the Euler obstructed Cooper pairing is done at zero temperature. The pairing that we consider is the intervalley $C_{2z}\mathcal{T}$ -invariant mean-field pairing operator with form

$$H_{\text{pairing}} = \sum_{\mathbf{k} \in \text{MBZ}} c_{+,\mathbf{k}}^\dagger \Delta(\mathbf{k}) \otimes \Pi c_{-,-\mathbf{k}}^\dagger + h.c., \quad (\text{D12})$$

where MBZ stands for the Moiré Brillouin zone, $c_{\pm,\mathbf{k}}^\dagger = (\dots, c_{\pm,\mathbf{k},a,s}^\dagger, \dots)$ stands for the creation operator for the Bloch basis of the nearly flat bands in valley \pm , $s = \uparrow, \downarrow$ labels the spin index, $a = 1, 2$ since there are two spin-doubly-degenerate nearly flat bands in each valley, $\Delta(\mathbf{k})$ is the spinless part of the pairing with $\Delta(\mathbf{k} + \mathbf{G}_M) = \Delta(\mathbf{k})$ and \mathbf{G}_M the Moiré reciprocal lattice vector, and Π is the spin part of the pairing. The global charge $U(1)$ in $U(2) \times U(2)$ of the normal state is spontaneously broken. Owing to the global spin $SU(2)$ symmetry in $U(2) \times U(2)$ of the normal state, we can consider the spin-singlet and spin-triplet channels separately, and choose the spin part in each channel to be momentum independent as

$$\begin{aligned} \Pi &= is_y \text{ for spin-singlet} \\ \Pi &= s_0 \text{ for spin-triplet.} \end{aligned} \quad (\text{D13})$$

The remaining global $U(2)$ symmetry in $U(2) \times U(2)$ of the normal state makes the spin-singlet and spin-triplet to have the same superconducting critical temperature [24]; we assume that the remaining $U(2)$ is spontaneously broken at zero temperature, and therefore, we will still study the spin-singlet and spin-triplet channels separately. Furthermore, Eq. (D12) can always be viewed as the projection of the pairing in the original basis ψ in Eq. (D1), and since the

pairing in basis ψ is always smooth, we know $\sum_{a,a'} |u_{+, \mathbf{k}, a}\rangle |u_{-, -\mathbf{k}, a'}\rangle [\Delta(\mathbf{k})]_{aa'}$ is always smooth. Therefore, Eq. (D12) satisfies Asm. 7, meaning that $\Delta(\mathbf{k})$ in Eq. (D12) can be split into two channels, a trivial one and a Euler obstructed one as shown in Eq. (B25), and the pairing gap function of the Euler obstructed channel always has zeros as shown in Eq. (B35). In the remaining of this section, we will always imply that the pairing has the form in Eq. (D12).

3. Symmetry Classification of the Pairing in Eq. (D12)

To prepare for the study of the nodal superconductivity, we need to consider more symmetry properties of the pairing. As we have used the $U(2) \times U(2)$, we need to consider the rest of the symmetries. Since we have chosen the pairing to be $C_{2z}\mathcal{T}$ -symmetric and invariant under the Moiré lattice translations and the spin part of all rotation symmetries have been included in $U(2) \times U(2)$, we only need to care about the remaining C_{2z} and C_{3z} , where

$$\begin{aligned} C_{2z} &= \bar{C}_{2z} [\bar{C}_{2z}^{spin}]^{-1} \text{ with } C_{2z} \psi_{\pm, \mathbf{r}}^\dagger (C_{2z})^{-1} = \psi_{\mp, -\mathbf{r}}^\dagger \begin{pmatrix} \sigma_x & \\ & \sigma_x \end{pmatrix} \otimes s_0 \\ C_{3z} &= \bar{C}_{3z} [\bar{C}_{3z}^{spin}]^{-1} \text{ with } C_{3z} \psi_{\pm, \mathbf{r}}^\dagger C_{3z}^{-1} = \psi_{\pm, C_{3z}\mathbf{r}}^\dagger \begin{pmatrix} e^{\pm i\sigma_z \pi/3} & \\ & e^{\pm i\sigma_z \pi/3} \end{pmatrix} \otimes s_0 \end{aligned} \quad (\text{D14})$$

which form the point group C_6 . Owing to the $C_{2z}\mathcal{T}$ -invariant of the pairing, we can only consider the real irreducible representations (irreps) of C_6 , which are (i) C_{2z} -even A irrep, (ii) C_{2z} -odd A irrep, (iii) C_{2z} -even E irrep, and (iv) C_{2z} -odd E irrep. Here A means the irrep is C_{3z} -invariant, while E is a 2D real irrep under C_{3z} .

We will split the pairing according to the real irreps of C_6 , and study them separately. Since the symmetry irrep, $|\Delta_b|$ and the BdG nodes are gauge-invariant properties, we will choose a Chern gauge for the normal-state basis that satisfies Asm. 8 and

$$\begin{aligned} C_{2z} |u_{+, \mathbf{k}}^{Ch}\rangle &= |u_{-, -\mathbf{k}}^{Ch}\rangle \\ C_{3z} |u_{\pm, K_M}^{Ch}\rangle &= |u_{\pm, C_{3z}K_M}^{Ch}\rangle e^{i\tau_z \frac{2\pi}{3}} \\ C_{3z} |u_{\pm, K'_M}^{Ch}\rangle &= |u_{\pm, C_{3z}K'_M}^{Ch}\rangle e^{i\tau_z \frac{2\pi}{3}} \\ C_{3z} |u_{\pm, \Gamma_M}^{Ch}\rangle &= |u_{\pm, \Gamma_M}^{Ch}\rangle, \end{aligned} \quad (\text{D15})$$

and we have numerically checked that the such a Chern gauge is allowed for the BM model with Eq. (D6). Then, for C_{2z} , we have

$$\begin{aligned} [\Delta^{Ch}(\mathbf{k})]^T &= \Delta^{Ch}(\mathbf{k}) \text{ if the pairing is parity-even} \\ [\Delta^{Ch}(\mathbf{k})]^T &= -\Delta^{Ch}(\mathbf{k}) \text{ if the pairing is parity-odd,} \end{aligned} \quad (\text{D16})$$

where the C_{2z} eigenvalue is the same as (opposite to) the parity for spin-singlet (spin-triplet) pairing according to the expression of chosen Π in Asm. 7. Then combined with Eq. (B43), we know that parity-odd pairing has $|\Delta_{\parallel}(\mathbf{k})| = 0$ for all $\mathbf{k} \in \mathbb{R}^2$.

For parity-even pairing, we know $|\Delta_{\parallel}(\mathbf{k})|$ can be non-vanishing at certain momenta and is required to have zeros. The distribution of zeros of $|\Delta_{\parallel}(\mathbf{k})|$ is influenced by the A/E irrep of the parity-even pairing. In the case of A irrep, we combine Eq. (D15) with Eq. (B43) and get

$$d_{\parallel}(K_M/K'_M) e^{-i4\pi/3} = d_{\parallel}(K_M/K'_M) \Rightarrow |\Delta_{\parallel}(K_M/K'_M)| = 0. \quad (\text{D17})$$

Then, the simplest nodal structure of $|\Delta_{\parallel}(\mathbf{k})|$ in A irrep contains and only contains two zeros at K_M and K'_M with winding number 1.

In the case of E irrep, the pairing would be the linear combination of the two component of E , which spontaneously breaks C_{3z} symmetry and thus is called spontaneously nematic pairing. Specifically,

$$\begin{aligned} H_{pairing} &= a_1 H_{pairing,1} + a_2 H_{pairing,2} \\ C_{3z}(H_{pairing,1} H_{pairing,2}) C_{3z}^{-1} &= (H_{pairing,1} H_{pairing,2}) e^{-i\tau_y \frac{2\pi}{3}}. \end{aligned} \quad (\text{D18})$$

where $a_1, a_2 \in \mathbb{R}$ and $H_{pairing,1}$ and $H_{pairing,2}$ also satisfy Asm. 7. Then, combined with Eq. (D15) and Eq. (B43), we get

$$\begin{pmatrix} d_{\parallel,1}(\Gamma_M) & d_{\parallel,2}(\Gamma_M) \end{pmatrix} = \begin{pmatrix} d_{\parallel,1}(\Gamma_M) & d_{\parallel,2}(\Gamma_M) \end{pmatrix} e^{-i\tau_y \frac{2\pi}{3}} \Rightarrow d_{\parallel,1}(\Gamma_M) = d_{\parallel,2}(\Gamma_M) = 0, \quad (\text{D19})$$

which means $|\Delta_{\parallel}(\Gamma_M)| = 0$. Then, the simplest nodal structure of $|\Delta_{\parallel}(\mathbf{k})|$ is to have two zeros with winding number 1 and at least one of them is at Γ_M .

Here, when we count the number of zeros of Δ_{\parallel} , we always mean the smallest number of zeros with winding ± 1 . So, if we have a winding-2 zero, then we would say we have two winding-1 zeros at the same momentum.

4. General Discussion on the Possible Nodal Superconductivity

In this part, we will present a general discussion on the possible nodal superconductivity.

First of all, the mean-field Hamiltonian reads

$$H_{MF} = H_{BdG,+} + H_{BdG,-} + const. , \quad (D20)$$

where

$$H_{BdG,\pm} = \frac{1}{2} \sum_{\mathbf{k} \in \text{MBZ}} \Psi_{\pm,\mathbf{k}}^{\dagger} h_{BdG,\pm}(\mathbf{k}) \Psi_{\pm,\mathbf{k}} , \quad (D21)$$

$$h_{BdG,+}(\mathbf{k}) = \begin{pmatrix} [h_+(\mathbf{k}) - \mu] \otimes s_0 & \Delta(\mathbf{k}) \otimes \Pi \\ \Delta^{\dagger}(\mathbf{k}) \otimes \Pi^{\dagger} & -[h_-(-\mathbf{k}) - \mu]^T \otimes s_0 \end{pmatrix} , \quad (D22)$$

$$h_{BdG,-}(\mathbf{k}) = \begin{pmatrix} [h_-(\mathbf{k}) - \mu] \otimes s_0 & -\Delta^T(-\mathbf{k}) \otimes \Pi^T \\ -\Delta^*(-\mathbf{k}) \otimes \Pi^* & -[h_+(-\mathbf{k}) - \mu]^T \otimes s_0 \end{pmatrix} , \quad (D23)$$

$\Psi_{+,\mathbf{k}}^{\dagger} = (c_{+,\mathbf{k}}^{\dagger}, c_{-,-\mathbf{k}}^T)$, $\Psi_{-,\mathbf{k}}^{\dagger} = (c_{-,\mathbf{k}}^{\dagger}, c_{+,-\mathbf{k}}^T)$, and μ is the chemical potential. $h_{BdG,-}(\mathbf{k})$ is related to $h_{BdG,+}(\mathbf{k})$ by the particle-hole symmetry as

$$-h_{BdG,-}(\mathbf{k}) = \rho_x \tau_0 s_0 h_{BdG,+}^*(-\mathbf{k}) \rho_x \tau_0 s_0 , \quad (D24)$$

which means the gapless nodes of $h_{BdG,-}(\mathbf{k})$ are completely determined by those of $h_{BdG,+}(\mathbf{k})$ and vice versa.

For spin-singlet pairing, we have

$$h_{BdG,+}(\mathbf{k}) = \begin{pmatrix} h_+(\mathbf{k}) - \mu & & \Delta(\mathbf{k}) \\ & h_+(\mathbf{k}) - \mu & -\Delta(\mathbf{k}) \\ & -\Delta^{\dagger}(\mathbf{k}) & -[h_-(-\mathbf{k}) - \mu]^T \\ \Delta^{\dagger}(\mathbf{k}) & & -[h_-(-\mathbf{k}) - \mu]^T \end{pmatrix} \sim \begin{pmatrix} \mathcal{H}(\mathbf{k}) & \\ & \rho_z \tau_0 \mathcal{H}(\mathbf{k}) \rho_z \tau_0 \end{pmatrix} , \quad (D25)$$

where \sim means differing by a \mathbf{k} -independent unitary transformation and

$$\mathcal{H}(\mathbf{k}) = \begin{pmatrix} h_+(\mathbf{k}) - \mu & \Delta(\mathbf{k}) \\ \Delta^{\dagger}(\mathbf{k}) & -[h_-(-\mathbf{k}) - \mu]^T \end{pmatrix} . \quad (D26)$$

For spin-triplet pairing, we have

$$h_{BdG,+}(\mathbf{k}) = \begin{pmatrix} h_+(\mathbf{k}) - \mu & & \Delta(\mathbf{k}) \\ & h_+(\mathbf{k}) - \mu & \Delta(\mathbf{k}) \\ \Delta^{\dagger}(\mathbf{k}) & & -[h_-(-\mathbf{k}) - \mu]^T \\ & \Delta^{\dagger}(\mathbf{k}) & -[h_-(-\mathbf{k}) - \mu]^T \end{pmatrix} \sim \begin{pmatrix} \mathcal{H}(\mathbf{k}) & \\ & \mathcal{H}(\mathbf{k}) \end{pmatrix} . \quad (D27)$$

where we used Eq. (D13). We can see for both spin-singlet and spin triplet pairings, $h_{BdG,+}(\mathbf{k})$ can be decomposed into two blocks, where each block is either equal to or similar to $\mathcal{H}(\mathbf{k})$ in Eq. (D26), meaning that the dispersion of $h_{BdG,+}(\mathbf{k})$ is just the double copy of that of $\mathcal{H}(\mathbf{k})$. Therefore, the gapless nodes of $h_{BdG,+}(\mathbf{k})$ are completely determined by those of $\mathcal{H}(\mathbf{k})$. So we only need to study the gapless nodes of $\mathcal{H}(\mathbf{k})$ in the following.

Since we care about the nodal superconductivity related to the Euler obstructed Cooper pairing, we will only study the parity-even pairing. Therefore, in the remaining of this part, we will always adopt the following condition unless specified otherwise.

Assumption 10. *The pairing is parity-even, and $|\Delta_{\parallel}(\mathbf{k})|$ is not globally vanishing (i.e., $|\Delta_{\parallel}(\mathbf{k})| \neq 0$ holds for at least one \mathbf{k} points).*

Since the band structure of $\mathcal{H}(\mathbf{k})$ is gauge invariant, we can choose any gauge to study it. Let us first choose a generic gauge for $c_{\pm, \mathbf{k}}^{\dagger}$ such that

$$C_{2z} c_{+, \mathbf{k}}^{\dagger} C_{2z}^{-1} = c_{-, -\mathbf{k}}^{\dagger}, \quad (\text{D28})$$

In this gauge, Eq. (D26) becomes

$$\mathcal{H}(\mathbf{k}) = \begin{pmatrix} h_+(\mathbf{k}) - \mu & \Delta_{\perp}(\mathbf{k}) + \Delta_{\parallel}(\mathbf{k}) \\ \Delta_{\perp}^{\dagger}(\mathbf{k}) + \Delta_{\parallel}^{\dagger}(\mathbf{k}) & -[h_+(\mathbf{k}) - \mu]^T \end{pmatrix}. \quad (\text{D29})$$

$\mathcal{H}(\mathbf{k})$ has the spinless $C_{2z}\mathcal{T}$ symmetry as

$$U_{BdG}(\mathbf{k}) \mathcal{H}^*(\mathbf{k}) U_{BdG}^{\dagger}(\mathbf{k}) = \mathcal{H}(\mathbf{k}), \quad (\text{D30})$$

where

$$U_{BdG}(\mathbf{k}) = \begin{pmatrix} U_+(\mathbf{k}) & \\ & U_+^*(\mathbf{k}) \end{pmatrix}, \quad (\text{D31})$$

and $U_+(\mathbf{k}) = \langle u_{\mathbf{k},+} | C_{2z} \mathcal{T} | u_{\mathbf{k},+} \rangle$. Moreover, since the pairing is parity-even, $\mathcal{H}(\mathbf{k})$ has a chiral symmetry as

$$C(\mathbf{k}) \mathcal{H}(\mathbf{k}) C^{\dagger}(\mathbf{k}) = -\mathcal{H}(\mathbf{k}) \quad (\text{D32})$$

with

$$C(\mathbf{k}) = \begin{pmatrix} & U_+(\mathbf{k}) \\ -U_+^*(\mathbf{k}) & \end{pmatrix}. \quad (\text{D33})$$

We can diagonalize $C(\mathbf{k})$ as

$$U_C^{\dagger}(\mathbf{k}) C(\mathbf{k}) U_C(\mathbf{k}) = \begin{pmatrix} i & & \\ & i & \\ & & -i \\ & & & -i \end{pmatrix} \quad (\text{D34})$$

with

$$U_C(\mathbf{k}) = \frac{1}{\sqrt{2}} \begin{pmatrix} 1 & 1 \\ iU_{+, \mathbf{k}}^* & -iU_{+, \mathbf{k}}^* \end{pmatrix}. \quad (\text{D35})$$

Then, $U_C(\mathbf{k})$ can make $\mathcal{H}(\mathbf{k})$ offdiagonal as

$$U_C^{\dagger}(\mathbf{k}) \mathcal{H}(\mathbf{k}) U_C(\mathbf{k}) = \begin{pmatrix} h_+(\mathbf{k}) - \mu - i\Delta(\mathbf{k})U_{+, \mathbf{k}}^* & \\ h.c. & \end{pmatrix}. \quad (\text{D36})$$

In particular, the complex $\det[h_+(\mathbf{k}) - \mu - i\Delta(\mathbf{k})U_{+, \mathbf{k}}^*]$ is independent of the gauge choices, as long as the gauges satisfy Eq. (D28). This quantity is the key to the stable nodal superconductivity, as discussed in the following.

To show this, we can choose a gauge such that Eq. (D28) holds and $|u_{\pm, \mathbf{k}}\rangle$ is globally-smooth, where the existence of such gauge is guaranteed by the zero total Chern number of $|u_{\alpha, \mathbf{k}}\rangle$ [67]. Then, $\det[h_+(\mathbf{k}) - \mu - i\Delta(\mathbf{k})U_{+, \mathbf{k}}^*]$ is globally smooth in this gauge, and thus has interger U(1) winding along any closed loop γ if $\det[h_+(\mathbf{k}) - \mu - i\Delta(\mathbf{k})U_{+, \mathbf{k}}^*] \neq 0 \forall \mathbf{k} \in \gamma$. This winding number is called the chiral symmetry protected winding number [58], or in short chirality in

this work. If the chirality is nonzero, then $\det[h_+(\mathbf{k}) - \mu - i\Delta(\mathbf{k})U_{+, \mathbf{k}}^*]$ must have zero(s) inside γ , and thus $\mathcal{H}(\mathbf{k})$ must have zero-energy gapless node(s) inside γ . Indeed, since $[C(\mathbf{k})]^2 = -1$ and $U_{BdG}(\mathbf{k})C^*(\mathbf{k}) = C(\mathbf{k})U_{BdG}(\mathbf{k})$, $\mathcal{H}(\mathbf{k})$ in this smooth gauge belongs to the CI nodal class proposed in Ref. [58], which can support stable zero-energy gapless points. The stable zero-energy gapless nodes are indeed protected by the nonzero chiralities. Since the gapless nodes of $\mathcal{H}(\mathbf{k})$ are always at zero energy, so does H_{BdG} ; H_{BdG} is gapless (or equivalently the superconductivity is nodal) if and only if $\mathcal{H}(\mathbf{k})$ has zero-energy gapless nodes. In particular, if we smoothly vary

$$\mu, P_{h,+}(\mathbf{k}) = |u_{+, \mathbf{k}}\rangle h_+(\mathbf{k}) \langle u_{+, \mathbf{k}}|, P_{\parallel}(\mathbf{k}), P_{\perp}(\mathbf{k}), \quad (\text{D37})$$

$\mathcal{H}(\mathbf{k})$ would change smoothly, and the zero-energy gapless nodes of $\mathcal{H}(\mathbf{k})$ would change continuously. Note that the chirality can be evaluated in any gauge that satisfies Eq. (D28), since $\det[h_+(\mathbf{k}) - \mu - i\Delta(\mathbf{k})U_{+, \mathbf{k}}^*]$ is independent of the gauge choices as long as the gauges satisfy Eq. (D28).

5. Nodal Superconductivity Guaranteed by Sufficiently-Dominant Δ_{\parallel} in MATBG

In the last part, we have shown that \mathcal{H} or H_{BdG} can be stably nodal in certain cases. The remaining question is what the relation between a gapless $\mathcal{H}(\mathbf{k})$ and the dominance of the Euler obstructed Δ_{\parallel} is. In this part, we will study the nodal superconductivity guaranteed by sufficiently-dominant Δ_{\parallel} in MATBG under Asm. 1-7 and Asm. 10.

First, nodal superconductivity enforced by a sufficiently-dominant Δ_{\parallel} is defined as the following.

Definition 1. For any choice of $(\mu, P_{h,+}(\mathbf{k}), P_{\parallel}(\mathbf{k}))$, nodal superconductivity is enforced by a sufficiently-dominant Δ_{\parallel} if and only if there exists $\lambda > 0$ such that $\mathcal{H}(\mathbf{k})$ has gapless nodes for all choices of symmetry-preserving $P_{\perp}(\mathbf{k})$ with $\max(|\Delta_{\perp}(\mathbf{k})|) < \lambda$.

To look for the nodal superconductivity enforced by a sufficiently-dominant Δ_{\parallel} , we will use the Chern gauge that satisfies Asm. 8 and Eq. (D15), since $|\Delta_{\parallel}(\mathbf{k})|$ and the gapless nodes of $\mathcal{H}(\mathbf{k})$ are gauge invariant. Then, $\mathcal{H}(\mathbf{k})$ becomes

$$\mathcal{H}(\mathbf{k}) = \begin{pmatrix} h_{Ch,+}(\mathbf{k}) - \mu & \Delta_{\perp}^{Ch}(\mathbf{k}) + \Delta_{\parallel}^{Ch}(\mathbf{k}) \\ [\Delta_{\perp}^{Ch}(\mathbf{k}) + \Delta_{\parallel}^{Ch}(\mathbf{k})]^{\dagger} & -h_{Ch,+}^T(\mathbf{k}) + \mu \end{pmatrix}, \quad (\text{D38})$$

where $h_{Ch,+}(\mathbf{k}) = \epsilon(\mathbf{k}) + \text{Re}[f(\mathbf{k})]\tau_x + \text{Im}[f(\mathbf{k})]\tau_y$.

Let us first study the case where $|\Delta_{\perp}(\mathbf{k})| = 0$, and label $\mathcal{H}(\mathbf{k})$ with $|\Delta_{\perp}(\mathbf{k})| = 0$ as $\mathcal{H}^{(0)}(\mathbf{k})$. We care about $\mathcal{H}^{(0)}(\mathbf{k})$ because of the following proposition.

Proposition 1. Under Asm. 1-7 and Asm. 10, for any choice of $(\mu, P_{h,+}(\mathbf{k}), P_{\parallel}(\mathbf{k}))$, nodal superconductivity is enforced by a sufficiently-dominant Δ_{\parallel} if $\mathcal{H}^{(0)}(\mathbf{k})$ has at least one isolated gapless node with nonzero chirality.

The reasoning for the above proposition is the following. The bands of $\mathcal{H}(\mathbf{k})$ are

$$\pm \sqrt{|d_{\parallel}|^2 + (\epsilon - \mu)^2 + |f|^2 + |d_{\perp}(\mathbf{k})|^2 \pm 2\sqrt{|d_{\perp}|^2|d_{\parallel}|^2 + 2d_{\perp}(\epsilon - \mu)\text{Re}(d_{\parallel}f^*) + |\text{Im}(fd_{\parallel}^*)|^2 + |f|^2(\epsilon - \mu)^2}}, \quad (\text{D39})$$

where \mathbf{k} -dependence of f , d_{\parallel} , d_{\perp} and ϵ is implicit and we have used that d_{\perp} is real for parity-even pairing. Then, $\mathcal{H}(\mathbf{k})$ is gapless at \mathbf{k} iff

$$a_0(\mathbf{k}) + a_1(\mathbf{k})d_{\perp}(\mathbf{k}) + a_2(\mathbf{k})d_{\perp}^2(\mathbf{k}) + d_{\perp}^4(\mathbf{k}) = 0, \quad (\text{D40})$$

where

$$\begin{aligned} a_0(\mathbf{k}) &= [|d_{\parallel}(\mathbf{k})|^2 + (\epsilon_{\mathbf{k}} - \mu)^2 + |f(\mathbf{k})|^2]^2 - 4[|\text{Im}(f(\mathbf{k})d_{\parallel}^*(\mathbf{k}))|^2 + |f(\mathbf{k})|^2(\epsilon_{\mathbf{k}} - \mu)^2] \\ a_1(\mathbf{k}) &= -8\text{Re}(d_{\parallel}^*(\mathbf{k})f(\mathbf{k}))(\epsilon_{\mathbf{k}} - \mu) \\ a_2(\mathbf{k}) &= 2(-|d_{\parallel}(\mathbf{k})|^2 + |f(\mathbf{k})|^2 + (\epsilon_{\mathbf{k}} - \mu)^2) \end{aligned} \quad (\text{D41})$$

are all smooth in \mathbb{R}^2 .

Consider that \mathbf{k}_0 is an isolated gapless node of $\mathcal{H}^{(0)}(\mathbf{k})$ with nonzero chirality. There exists a circle γ_0 surrounding \mathbf{k}_0 such that $\mathcal{H}^{(0)}(\mathbf{k})$ is gapped on γ_0 and has nonzero chirality along γ_0 . According to Eq. (D43), $a_0(\mathbf{k}) > 0$ for all

$\mathbf{k} \in \gamma_0$. Since $a_{0,1,2}(\mathbf{k})$ is smooth and γ_0 is closed, we have $\bar{a}_0 = \min_{\mathbf{k} \in \gamma_0} [a_0(\mathbf{k})] > 0$, and $\bar{a}_{1,2} = \max_{\mathbf{k} \in \gamma_0} [a_{1,2}(\mathbf{k})]$ is finite. Then, we define

$$\lambda = \min \left[\left(\frac{\bar{a}_0}{6} \right)^{1/4}, \left(\frac{\bar{a}_0}{6\bar{a}_2} \right)^{1/2}, \frac{\bar{a}_0}{6\bar{a}_1} \right] > 0 \quad (\text{D42})$$

where we choose $1/\bar{a}_{1,2} = +\infty$ if $\bar{a}_{1,2} = 0$. As a result, for all $\mathbf{k} \in \gamma_0$, $|d_\perp(\mathbf{k})| < \lambda$ infers $a_0(\mathbf{k}) + a_1(\mathbf{k})d_\perp(\mathbf{k}) + a_2(\mathbf{k})d_\perp^2(\mathbf{k}) + d_\perp^4(\mathbf{k}) > \bar{a}_0/2 > 0$, meaning that $\mathcal{H}(\mathbf{k})$ is gapped at \mathbf{k} .

Then, for any symmetry-preserving $P_\perp(\mathbf{k})$ such that $\max(|\Delta_\perp(\mathbf{k})|) < \lambda$, we have $\mathcal{H}(\mathbf{k})$ gapped on γ_0 . Since any $P_\perp(\mathbf{k})$ such that $\max(|\Delta_\perp(\mathbf{k})|) < \lambda$ can be smoothly deformed to 0 while keeping $\max(|\Delta_\perp(\mathbf{k})|) < \lambda$, $\mathcal{H}(\mathbf{k})$ can be smoothly deformed to $\mathcal{H}^{(0)}(\mathbf{k})$ in the globally smooth gauge while staying gapped on γ_0 . Therefore, $\mathcal{H}(\mathbf{k})$ must have nonzero chirality along γ_0 and thus must be gapless for any symmetry-preserving $P_\perp(\mathbf{k})$ such that $\max(|\Delta_\perp(\mathbf{k})|) < \lambda$. So Prop. 1 holds.

Now we can see that Prop. 1 based on $\mathcal{H}^{(0)}$ gives us a sufficient condition for nodal superconductivity enforced by sufficiently-dominant Δ_\parallel . Furthermore, for any choice of $(\mu, P_{h,+}(\mathbf{k}), P_\parallel(\mathbf{k}))$, if $\mathcal{H}^{(0)}$ is fully gapped, then nodal superconductivity cannot be enforced by a sufficiently-dominant Δ_\parallel , since \mathcal{H} is gapped for $P_\perp = 0$. Therefore, the nodal structure of $\mathcal{H}^{(0)}$ is crucial in our consideration.

To facilitate later discussions, let us present some general results on the possible nodal structure of $\mathcal{H}^{(0)}$. $\mathcal{H}^{(0)}(\mathbf{k})$ has the four bands, which read

$$\pm \sqrt{|d_\parallel(\mathbf{k})|^2 + (\epsilon_{\mathbf{k}} - \mu)^2 + |f(\mathbf{k})|^2} \pm 2\sqrt{|Im(f(\mathbf{k})d_\parallel^*(\mathbf{k}))|^2 + |f(\mathbf{k})|^2(\epsilon_{\mathbf{k}} - \mu)^2}, \quad (\text{D43})$$

meaning that a gapless node appears at \mathbf{k} if and only if

$$Re(f^*(\mathbf{k})d_\parallel(\mathbf{k})) = 0 \text{ and } \mu = \epsilon(\mathbf{k}) \pm \sqrt{|f(\mathbf{k})|^2 - |d_\parallel(\mathbf{k})|^2} \text{ and } |f(\mathbf{k})| \geq |d_\parallel(\mathbf{k})| \quad (\text{D44})$$

Since $f^*(\mathbf{k})d_\parallel(\mathbf{k})$ and $|f(\mathbf{k})|^2$ are independent of the choice of the Chern gauge that satisfies the requirement, they are smooth in \mathbb{R}^2 . $|d_\parallel(\mathbf{k})|^2 = |\Delta_\parallel(\mathbf{k})|^2$ is also smooth in \mathbb{R}^2 . Then, the solution set of $Re(f^*(\mathbf{k})d_\parallel(\mathbf{k})) = 0$ and $|f(\mathbf{k})| \geq |d_\parallel(\mathbf{k})|$ consists of isolated points or lines without fine tuning. Combined with the fact that $d_\parallel(\mathbf{k} + \mathbf{G}_M) = d_\parallel(\mathbf{k})$ and $f(\mathbf{k} + \mathbf{G}_M) = f(\mathbf{k})$, we only need to care about the solution set of $Re(f^*(\mathbf{k})d_\parallel(\mathbf{k})) = 0$ and $|f(\mathbf{k})| \geq |d_\parallel(\mathbf{k})|$ in MBZ, labeled as Σ . Σ is not empty since the zeros of $\Delta_\parallel(\mathbf{k})$ are definitely in it. We further define

$$E(\Sigma) = \left\{ \epsilon(\mathbf{k}) + \sqrt{|f(\mathbf{k})|^2 - |d_\parallel(\mathbf{k})|^2} \mid \mathbf{k} \in \Sigma \right\} \cup \left\{ \epsilon(\mathbf{k}) - \sqrt{|f(\mathbf{k})|^2 - |d_\parallel(\mathbf{k})|^2} \mid \mathbf{k} \in \Sigma \right\}, \quad (\text{D45})$$

and we know $\mu \in E(\Sigma)$ is equivalent to that $\mathcal{H}^{(0)}(\mathbf{k})$ has zero-energy gapless nodes.

An alternative expression of Σ is useful for the following discussions. The useful alternative expression is based on the fact that $|d_\parallel(\mathbf{k}) \pm isf(\mathbf{k})|^2$ with $s \in [0, 1]$ is smooth in \mathbb{R}^2 , and we label the solution set of $|d_\parallel(\mathbf{k}) \pm isf(\mathbf{k})|^2 = 0$ as $\Sigma_\pm(s) \subset \text{MBZ}$. Then, we have

$$\Sigma = \bigcup_{s \in [0, 1]} [\Sigma_+(s) \cup \Sigma_-(s)] \quad (\text{D46})$$

since $|d_\parallel(\mathbf{k}) + isf(\mathbf{k})|^2 = 0$ or $|d_\parallel(\mathbf{k}) - isf(\mathbf{k})|^2 = 0$ is equivalent to $Re(f^*(\mathbf{k})d_\parallel(\mathbf{k})) = 0$ and $|d_\parallel(\mathbf{k})| = s|f(\mathbf{k})|$. Since $|d_\parallel(\mathbf{k}) \pm isf(\mathbf{k})|^2$ are smooth functions of (s, \mathbf{k}) , we know the zeros of $|d_\parallel(\mathbf{k}) \pm isf(\mathbf{k})|^2$ are moving continuously in MBZ as s continuously varies if we view MBZ as a torus. Then, Σ is nothing but the paths of zeros of $|d_\parallel(\mathbf{k}) \pm isf(\mathbf{k})|^2$ as s increases from 0 to 1 continuously. Crucially, unless invoking fine tuning, $d_\parallel(\mathbf{k}) \pm isf(\mathbf{k})$ always have zeros in MBZ for $s \in [0, 1]$ and the total winding number of the zeros is independent of s and is equal to 2, where the winding number for a zero of $d_\parallel(\mathbf{k}) \pm isf(\mathbf{k})$ is defined by the winding of $\arg[d_\parallel(\mathbf{k}) \pm isf(\mathbf{k})]$ along a small circle around that zero.

The ultimate goal is to specify whether nodal superconductivity guaranteed by a sufficiently-dominant Δ_\parallel can exist for C_{3z} -invariant and spontaneously nematic pairings. To do so, we will impose the following assumption in this part

Assumption 11. $\mu \in [E_1(\Gamma_M), E_2(\Gamma_M)]$, where $E_1(\mathbf{k})$ and $E_2(\mathbf{k})$ are the lower and upper nearly flat bands of $h_+(\mathbf{k})$, respectively. Δ_\parallel only has two zeros with winding 1 in MBZ.

Using the terms in Eq. (D38), we have $E_1(\mathbf{k}) = \epsilon_{\mathbf{k}} - |f(\mathbf{k})|$ and $E_2(\mathbf{k}) = \epsilon_{\mathbf{k}} + |f(\mathbf{k})|$. In the normal state, $\mu \in [E_1(\Gamma_M), E_2(\Gamma_M)]$ is typically true for $2 \sim 3$ holes per Moiré unit cell, since the top and bottom of the set of nearly flat bands are typically at Γ_M , as shown in Fig. 5(d-e). However, we caution that given a fixed filling, the

chemical potential in the superconducting phase can be different from that in the normal state due to the correction brought by the pairing order parameter. Thus, since we care about the zero-temperature superconducting phase, $\mu \in [E_1(\Gamma_M), E_2(\Gamma_M)]$ in Asm. 11 should be tested when applying to specific superconducting phase with specific pairing. Note that we do *not* require the pairing order parameter to be much smaller than the gap between two nearly flat bands at the Fermi surfaces.

On the other hand, recall that when we count the zeros of Δ_{\parallel} , we would treat a zero with winding $\pm n$ as n zeros with winding ± 1 at the same momentum. The reason for requiring Δ_{\parallel} to only have two zeros with winding 1 in MBZ in Asm. 11 is that the least number of zeros for Δ_{\parallel} tends to be physically favored since more zeros of Δ_{\parallel} typically require a more complex structure of the pairing, which tends to be physically suppressed.

In the following, we will discuss the nodal superconductivity guaranteed by sufficiently-dominant Δ_{\parallel} for both C_{3z} -invariant and spontaneously nematic pairings. We will use Prop. 1, Eq. (D46), and Asm. 11.

a. C_{3z} -Invariant

Recall that we work under Asm. 1-7 and Asm. 10-11. The main result for the nodal superconductivity for the C_{3z} -invariant pairing is the following.

Proposition 2. *Under Asm. 1-7 and Asm. 10-11, for C_{3z} -invariant pairing (A irrep), nodal superconductivity is not always guaranteed by sufficiently dominant Δ_{\parallel} , even if fine-tuned cases are ruled out.*

The proposition is true as long as we can find a codimension-0 subregion of choices of $(\mu, P_h, P_{\parallel})$ with C_{3z} -invariant not-globally-vanishing P_{\parallel} , in which nodal superconductivity is not guaranteed by sufficiently dominant Δ_{\parallel} . To find the codimension-0 region, we will use the Chern gauge that satisfies Asm. 8 and Eq. (D15).

Consider a special $(P_{h,+}, P_{\parallel}) = (\tilde{P}_{h,+}, \tilde{P}_{\parallel})$ such that $f(\mathbf{k}) = 10d_{\parallel}(\mathbf{k})$, $\epsilon_{\Gamma_M} + |f(\Gamma_M)| > 1\text{meV}$ and $\epsilon_{K_M/K'_M} = 0$. For this special choice, Λ only contains K_M and K'_M , and $E(\Lambda) = \{0\}$. Since any infinitesimal derivation of $(P_{h,+}, P_{\parallel})$ from $(\tilde{P}_{h,+}, \tilde{P}_{\parallel})$ can only change $E(\Lambda)$ and $\epsilon_{\Gamma_M} + |f(\Gamma_M)|$ infinitesimally, there exists a codimension-0 region X of $(P_{h,+}, P_{\parallel})$ that contains $(\tilde{P}_{h,+}, \tilde{P}_{\parallel})$ such that $E(\Lambda) \subset [-0.5\text{meV}, 0.5\text{meV}]$ and $\epsilon_{\Gamma_M} + |f(\Gamma_M)| > 1\text{meV}$ for all $(P_{h,+}, P_{\parallel}) \in X$. Then, for any $(\mu, P_{h,+}, P_{\parallel})$ in the codimension-0 $(0.5\text{meV}, 1.0\text{meV}) \times X$, $\mu \notin E(\Lambda) \Rightarrow \mathcal{H}^{(0)}$ is gapped. In the codimension-0 $(0.5\text{meV}, 1.0\text{meV}) \times X$, nodal superconductivity is certainly not guaranteed by the sufficiently dominant Δ_{\parallel} since $\mathcal{H}^{(0)}(\mathbf{k})$ is gapped everywhere. So Prop. 2 holds.

b. Spontaneously Nematic Pairing

Now we turn to the spontaneously nematic pairing, which spontaneously breaks the C_{3z} symmetry. It means that the pairing is the linear combination of two components of the E irrep, or in short belongs to the E irrep. Recall that we work under Asm. 1-7 and Asm. 10-11. The main result for the nodal superconductivity for the E pairing is the following.

Proposition 3. *Under Asm. 1-7 and Asm. 10-11, for spontaneously nematic pairing (E irrep), nodal superconductivity is always guaranteed by sufficiently dominant Δ_{\parallel} , if fine-tuned cases are ruled out.*

The reasoning is the following. Since zeros of $d_{\parallel}(\mathbf{k}) \pm isf(\mathbf{k})$ can only be created in pairs with zero total winding, there exist at least two zeros of Δ_{\parallel} that persist through the continuous change of s from 0 to 1 and becomes two zeros of $d_{\parallel}(\mathbf{k}) \pm isf(\mathbf{k})$, in order to carry the total winding number 2. Here, recall that when we count the zeros of Δ_{\parallel} , we would treat a zero with winding $\pm n$ as n zeros with winding ± 1 at the same momentum. The paths of the two zeros of Δ_{\parallel} definitely connects the two zeros of Δ_{\parallel} to zeros of $d_{\parallel}(\mathbf{k}) \pm isf(\mathbf{k})$.

Since P_{\parallel} belongs to the E irrep, we know at least one of the two zeros of Δ_{\parallel} is at Γ_M . Then, there exists a continuous path $\gamma \subset \Sigma$ (continuous when treating MBZ as a torus) such that it connects Γ_M to \mathbf{k}_0 that satisfies $d_{\parallel}(\mathbf{k}_0) + if(\mathbf{k}_0) = 0$ or $d_{\parallel}(\mathbf{k}_0) - if(\mathbf{k}_0) = 0$, unless invoking fine tuning. Finally, we have

$$[\epsilon_{\Gamma_M} - |f_{\Gamma_M}|, \epsilon_{\Gamma_M} + |f_{\Gamma_M}|] \subset E(\Sigma) . \quad (\text{D47})$$

since as \mathbf{k} goes from Γ_M to \mathbf{k}_0 through γ , $\epsilon(\mathbf{k}) \pm \sqrt{|f(\mathbf{k})|^2 - |d_{\parallel}(\mathbf{k})|^2}$ changes from $\epsilon_{\Gamma_M} \pm |f_{\Gamma_M}|$ to $\epsilon_{\mathbf{k}_0}$ continuously. It means that for all choices of $(\mu, P_h, P_{\parallel})$ with not-globally-vanishing P_{\parallel} belonging to the E irrep, $\mathcal{H}^{(0)}(\mathbf{k})$ is always nodal, unless invoking fine tuning. Since a gapless $\mathcal{H}^{(0)}(\mathbf{k})$ has at least one isolated gapless node unless invoking fine tuning, Prop. 1 suggests that the nodal superconductivity is always guaranteed by sufficiently dominant Δ_{\parallel} for all

choices of $(\mu, P_h, P_{||})$ with not-globally-vanishing $P_{||}$, if the pairing is spontaneously nematic and if fine-tuned cases are ruled out. So Prop. 3 holds.

Ref. [27] provides an alternative way for nematic pairing to give the nodal superconductivity. The mechanism proposed in Ref. [27] does not require a sufficiently-dominant Euler obstructed pairing channel and thus is different from our mechanism presented above. On the other hand, the mechanism proposed in Ref. [27] requires the pairing order parameter to be much smaller than the gap between the two nearly flat bands on the Fermi “surface” so that the pairing order parameter can be projected to the Fermi surface and become scalar; this condition is not required here by our mechanism. We note that for MATBG, the pairing order parameter is not always much smaller than the gap between the two nearly flat bands on the Fermi “surface”. In Appendix. E, we will present such an example where the mechanism proposed in Ref. [27] failed but our mechanism presented above works.

6. Bounded Zero-temperature superfluid weight in MATBG

In this part, we will discuss the applicability of the bounded zero-temperature superfluid weight in Eq. (C37) to MATBG.

As discussed before, Eq. (C37) is derived from Eq. (C12) under Asm. 1-7 and Asm. 9. We already know that Asm. 1-6 are satisfied in the normal state of MATBG based on the BM model, and we have always imposed Asm. 7. Then, the extra assumptions for Eq. (C37) to hold in this part would be (i) Eq. (C12) is valid, and (ii) choosing the normal-state flat bands exactly flat and choosing $\mu \neq 0$ in Asm. 9.

Let us first discuss the validity of Eq. (C12). Eq. (C12) is valid for gapped superconductors. Owing to the $C_{2z}\mathcal{T}$ symmetry, the superconductor might be nodal as discussed above. For the 2D $C_{2z}\mathcal{T}$ -invariant pairing model discussed above, Eq. (C12) will also hold for nodal superconductors unless invoking fine tuning. It is because, unless invoking fine tuning, the nodal superconductors only have isolated gapless point nodes with linear dispersion, and then these nodes cannot contribute to the superfluid weight and can be directly neglected, since they cannot give Dirac-delta-like integrands in Eq. (C12). In other words, we can directly neglect all the nodal points in the superconductors unless invoking fine tuning, which means Eq. (C12) is valid unless invoking fine tuning.

Now let us discuss the extra assumptions in Asm. 9. $\mu \neq 0$ is true unless invoking fine-tuning. Choosing the normal-state flat bands exactly flat was previously adopted in the study of bound of superfluid weight for time-reversal invariant uniform pairings in Ref. [49]. It is not exactly true based on the BM model with realistic parameter values (Eq. (D6)), but it is true for the chiral limit with twist angle exactly at the magic angle [57]. For the nodal superconductivity discussed above, we know the normal-state dispersion is very important, since it determines the range of the zero-temperature chemical potential, in which the superconductor is enforced to be nodal by nematic Euler obstructed pairing as discussed in Asm. 11 and Appendix. D 5 b. Nevertheless, Asm. 9 can be a good approximation for the calculation of the superfluid weight of the pairing model chosen in Asm. 7. By being a good approximation, we mean that the superfluid weight of the pairing model in Asm. 7 does not change dramatically (at least within the same order of magnitude) if we choose the normal-state bands to be exactly flat to satisfy Asm. 9 while keeping the pairing matrix and the filling unchanged. Then, the remaining question is when Asm. 9 is a good approximation. It turns out that Asm. 9 is not always a good approximation, and in general, the Asm. 9 becomes a better approximation if the ratio between the pairing amplitude and the normal-state bandwidth becomes large [70, 71]. As shown in the next section, the Asm. 9 becomes good when the twist angle is very close to 1.1° —for which the normal-state bandwidth is smallest. Then, we know in certain cases, Eq. (C37) can be applied to MATBG.

Appendix E: Euler Obstructed Cooper Pairing Induced by Attractive Local Interaction in MATBG

In this section, we will provide more details on the pairing induced by the local attractive interaction that has the similar form as the attractive interaction given by the electron-acoustic phonon coupling in MATBG proposed in Ref. [26].

According to Ref. [26], we choose the attractive interaction to be local in \mathbf{r} , $U(2) \times U(2)$ -invariant, intralayer, and inter-valley. With these constraints, the form of the interaction is

$$\tilde{H}_{int} = -4 \sum_{\sigma_1, \sigma_2, \sigma_3, \sigma_4, s, s', l} g_l(\sigma_1 \sigma_2 \sigma_3 \sigma_4) \int d^2 r \psi_{+, \mathbf{r}, l, \sigma_1, s}^\dagger \psi_{-, \mathbf{r}, l, \sigma_2, s'}^\dagger \psi_{-, \mathbf{r}, l, \sigma_3, s'} \psi_{+, \mathbf{r}, l, \sigma_4, s}^\dagger, \quad (\text{E1})$$

where $\psi_{\pm, \mathbf{r}, l, \sigma, s}^\dagger$ are the basis of the BM model in Eq. (D1), $l, l' \in \{t, b\}$, $\sigma, \sigma' \in \{A, B\}$, and $s, s' \in \{\uparrow, \downarrow\}$. The

interaction should be Hermitian and is assumed to satisfy $\overline{C}_{2z}\mathcal{T}$, \overline{C}_{3z} , \overline{C}_{2x} and \mathcal{T} symmetries, resulting in

$$\begin{aligned}
h.c. : g_l^* (\sigma_1 \sigma_2 \sigma_3 \sigma_4) &= g_l (\sigma_4 \sigma_3 \sigma_2 \sigma_1) \\
\overline{C}_{2z} \mathcal{T} : g_l^* (\sigma'_1 \sigma'_2 \sigma'_3 \sigma'_4) (\sigma_x)_{\sigma_1 \sigma'_1} (\sigma_x)_{\sigma_2 \sigma'_2} (\sigma_x)_{\sigma_3 \sigma'_3} (\sigma_x)_{\sigma_4 \sigma'_4} &= g_l (\sigma_1 \sigma_2 \sigma_3 \sigma_4) \\
\overline{C}_{3z} : \sum_{\sigma'_1 \sigma'_2 \sigma'_3 \sigma'_4} g_l (\sigma'_1 \sigma'_2 \sigma'_3 \sigma'_4) (e^{i\sigma_z \frac{2\pi}{3}})_{\sigma_1 \sigma'_1} (e^{-i\sigma_z \frac{2\pi}{3}})_{\sigma_2 \sigma'_2} (e^{i\sigma_z \frac{2\pi}{3}})_{\sigma_3 \sigma'_3} (e^{-i\sigma_z \frac{2\pi}{3}})_{\sigma_4 \sigma'_4} &= g_l (\sigma_1 \sigma_2 \sigma_3 \sigma_4) \\
\overline{C}_{2x} : \sum_{\sigma'_1 \sigma'_2 \sigma'_3 \sigma'_4} g_t (\sigma'_1 \sigma'_2 \sigma'_3 \sigma'_4) (\sigma_x)_{\sigma_1 \sigma'_1} (\sigma_x)_{\sigma_2 \sigma'_2} (\sigma_x)_{\sigma_3 \sigma'_3} (\sigma_x)_{\sigma_4 \sigma'_4} &= g_b (\sigma_1 \sigma_2 \sigma_3 \sigma_4) \\
\mathcal{T} : g_l^* (\sigma_2 \sigma_1 \sigma_4 \sigma_3) &= g_l (\sigma_1 \sigma_2 \sigma_3 \sigma_4) .
\end{aligned} \tag{E2}$$

Here we use the \overline{C}_{2x} to simplify the interaction in this example, but the symmetry is not essential for the general discussions in Appendix. D. We can use the above relations to simplify Eq. (E1). To do so, we can define

$$\tilde{O}_{l,j,j_s}(\mathbf{r}) = \psi_{+,r,l}^\dagger \tilde{\sigma}_j \otimes (\tilde{s}_{j_s} i s_y) (\psi_{-,r,l}^\dagger)^T \tag{E3}$$

with $\tilde{s}_0 = s_0$, $\tilde{s}_{x,y,z} = i s_{x,y,z}$, $\tilde{\sigma}_{0,x,y} = \sigma_{0,x,y}$, and $\tilde{\sigma}_z = i \sigma_z$. Then, we get

$$\tilde{H}_{int} = - \sum_{l,j,j_s} g_j \int d^2 r \tilde{O}_{l,j,j_s}(\mathbf{r}) \tilde{O}_{l,j,j_s}^\dagger(\mathbf{r}) , \tag{E4}$$

where

$$g_x = g_y = g_1 . \tag{E5}$$

If we choose $g_0 = g_1 = g_z$, Eq. (E4) becomes the effective attractive interaction mediated by the acoustic phonon derived in Ref. [26]. As shown in Ref. [26, 27], the pairing given by the attractive interaction in general would contain intrasublattice and intersublattice channels simultaneously, but the mixing between them is typically small, meaning that we may study the intrasublattice and intersublattice channels separately. To do so, we will impose

$$g_z = g_0 \tag{E6}$$

but allow $g_1 \neq g_0$ just to study the intra-sublattice and inter-sublattice pairings independently.

However, the interaction in Eq. (E4) has a physical problem—the attractive interaction should happen only to low-energy electrons instead of all electrons with all possible energies, since we need to integrate out high-energy electrons to renormalize the Coulomb interaction. To fix this issue, a more physically reasonable attractive interaction should be obtained by projecting Eq. (E4) to the nearly-flat bands, which gives us

$$H_{int} = - \sum_{l,j,j_s,\mathbf{G}_M} g_j \int_{\text{MBZ}} \frac{d^2 q}{(2\pi)^2} O_{l,j,j_s,\mathbf{G}_M}(\mathbf{q}) O_{l,j,j_s,\mathbf{G}_M}^\dagger(\mathbf{q}) , \tag{E7}$$

where $c_{\pm,\mathbf{k}}^\dagger = (\dots, c_{\pm,\mathbf{k},a,s}^\dagger, \dots)$ stands for the creation operator for the Bloch basis of the nearly flat bands in valley \pm ,

$$O_{l,j,j_s,\mathbf{G}_M}(\mathbf{q}) = \sum_{\mathbf{k} \in \text{MBZ}} c_{+,\mathbf{k}}^\dagger \phi_{l,j,\mathbf{G}_M}(\mathbf{k}, \mathbf{q}) \otimes (\tilde{s}_{j_s} i s_y) (c_{-,-\mathbf{k}+\mathbf{q}}^\dagger)^T , \tag{E8}$$

$$\phi_{l,j,\mathbf{G}_M}(\mathbf{k}, \mathbf{q}) = V_{+,\mathbf{k}}^\dagger \bar{m}_{l,j,\mathbf{G}_M} V_{-,-\mathbf{k}+\mathbf{q}}^* , \tag{E9}$$

$V_\pm(\mathbf{k}) = (V_{\pm,1}(\mathbf{k}), V_{\pm,2}(\mathbf{k}))$ are orthonormal linear combination of eigenvectors of $\tilde{h}_\pm(\mathbf{k})$ (Eq. (D8)) for the nearly flat bands,

$$[\bar{m}_{l,j,\mathbf{G}_M}]_{\mathbf{Q}\mathbf{Q}'} = \tilde{\sigma}_j \delta_{\mathbf{Q}+\mathbf{Q}',+\mathbf{G}_M} \delta_{\mathbf{Q} \in Q_{+,l}} , \tag{E10}$$

$Q_{+,t}$ and $Q_{+,b}$ are defined below Eq. (D8), and \mathbf{Q}, \mathbf{Q}' takes values in $Q_{+,b} \cup Q_{+,t}$ according to the convention in Ref. [5]. The total Hamiltonian is

$$H = H_+ + H_- + H_{int} , \tag{E11}$$

where H_{\pm} are the projections of \tilde{H}_{\pm} onto the nearly flat bands in Eq. (D10).

We will adopt the mean-field approximation to derive the superconductivity from the interaction by defining the superconductivity mean-field order parameter as

$$\tilde{\Delta}_{l,j,j_s,\mathbf{G}_M}(\mathbf{q}) = -g_j \text{Tr}[O_{l,j,j_s,\mathbf{G}_M}(\mathbf{q})e^{-\beta(H-\mu N)}] / \text{Tr}[e^{-\beta(H-\mu N)}] , \quad (\text{E12})$$

where N is the electron number operator, $\beta = 1/(k_B T)$, and T is the temperature. Since we care about the order parameter that preserves the Moiré lattice translation, we requires

$$\tilde{\Delta}_{l,j,j_s,\mathbf{G}_M}(\mathbf{q}) = \tilde{\Delta}_{l,j,j_s,\mathbf{G}_M}(2\pi)^2 \delta(\mathbf{q}) , \quad (\text{E13})$$

resulting in the mean-field pairing operator as

$$H_{\text{pairing}} = \sum_{l,j,j_s,\mathbf{G}_M} \tilde{\Delta}_{l,j,j_s,\mathbf{G}_M} O_{l,j,j_s,\mathbf{G}_M}(0) + h.c. \quad (\text{E14})$$

and the mean-field Hamiltonian as

$$H_{MF} = H_+ + H_- - \mu N + H_{\text{pairing}} . \quad (\text{E15})$$

Then, the self-consistent equation for the order parameter reads

$$\begin{aligned} \tilde{\Delta}_{l,j,j_s,\mathbf{G}_M} &= -\frac{g_j}{\mathcal{V}} \text{Tr}[O_{l,j,j_s,\mathbf{G}_M}^\dagger(\mathbf{0})e^{-\beta H_{MF}}] / \text{Tr}[e^{-\beta H_{MF}}] \\ &= -\frac{g_j}{\mathcal{V}} \sum_{\mathbf{k} \in \text{MBZ}} \text{Tr} \left[\begin{pmatrix} 0 & 0 \\ [\phi_{l,j,\mathbf{G}_M}(\mathbf{k},0) \otimes \tilde{s}_{j_s} i s_y]^\dagger & 0 \end{pmatrix} \frac{1}{\exp[\beta h_{BdG,+}(\mathbf{k})] + 1} \right] , \end{aligned} \quad (\text{E16})$$

where \mathcal{V} is the volume of the system,

$$h_{BdG,+}(\mathbf{k}) = \begin{pmatrix} (h_+(\mathbf{k}) - \mu) \otimes s_0 & M(\mathbf{k}) \\ M^\dagger(\mathbf{k}) & -(h_-(-\mathbf{k}) - \mu)^T \otimes s_0 \end{pmatrix} , \quad (\text{E17})$$

and

$$M(\mathbf{k}) = \sum_{l,j,j_s,\mathbf{G}_M} \tilde{\Delta}_{l,j,j_s,\mathbf{G}_M} \phi_{l,j,\mathbf{G}_M}(\mathbf{k},0) \otimes \tilde{s}_{j_s} i s_y . \quad (\text{E18})$$

Nontrivial solutions (*i.e.*, $\tilde{\Delta}_{l,j,j_s,\mathbf{G}_M}$ has nonzero components) of Eq. (E16) are pairing order parameters of the pairing. In particular, there always exists solutions (might be trivial) to Eq. (E16) such that

$$\tilde{\Delta}_{l,j,j_s,\mathbf{G}_M} = -\tilde{\Delta}_{l,j,\mathbf{G}_M} \delta_{j_s y} \quad (\text{E19})$$

with real $\tilde{\Delta}_{l,j,\mathbf{G}_M}$, and if these solutions are nontrivial, they will naturally lead to the $C_{2z}\mathcal{T}$ -invariant pairing in Eq. (D12) that satisfied Asm. 7 with

$$\begin{aligned} \Delta(\mathbf{k}) &= \sum_{l,j,\mathbf{G}_M} \tilde{\Delta}_{l,j,\mathbf{G}_M} \phi_{l,j,\mathbf{G}_M}(\mathbf{k},0) \\ \Pi &= s_0 . \end{aligned} \quad (\text{E20})$$

In the following, we will focus on solutions that satisfy Eq. (E19). For those solutions, Eq. (E16) can be simplified into

$$\tilde{\Delta}_{l,j,\mathbf{G}_M} = -2g_j \int_{\text{MBZ}} \frac{d^2 k}{(2\pi)^2} \text{Tr} \left\{ U^\dagger(\mathbf{k}) \begin{pmatrix} 0 & 0 \\ \phi_{l,j,\mathbf{G}_M}^\dagger(\mathbf{k},0) & 0 \end{pmatrix} U(\mathbf{k}) \begin{pmatrix} n_F(E_1(\mathbf{k})) & & & \\ & n_F(E_2(\mathbf{k})) & & \\ & & n_F(E_3(\mathbf{k})) & \\ & & & n_F(E_4(\mathbf{k})) \end{pmatrix} \right\} , \quad (\text{E21})$$

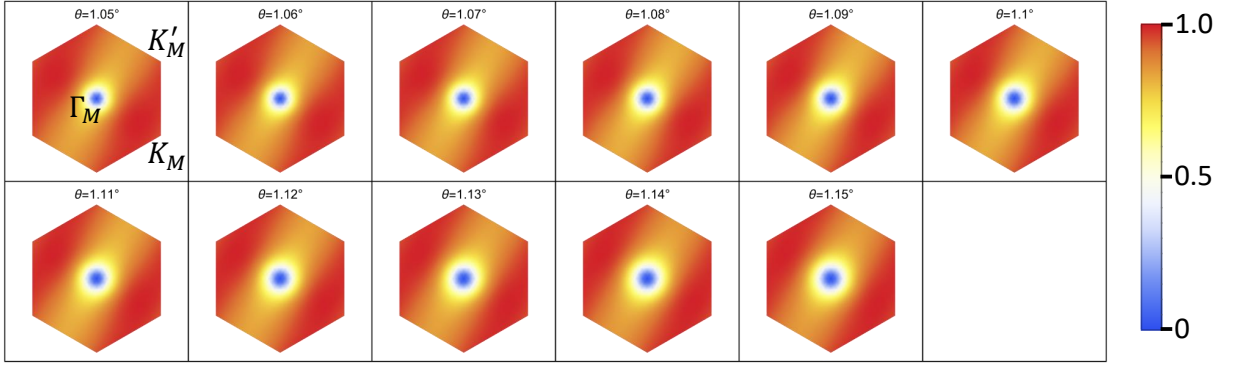


FIG. 6. The plot of $\frac{|\Delta_{||}(\mathbf{k})|}{\max[|\Delta_{||}(\mathbf{k})|]}$ for the intersublattice pairing at zero temperature. The parameter values in Eq. (E23) are adopted.

where $n_F(x) = [e^{\beta x} + 1]^{-1}$, we choose the gauge such that $C_{2z}c_{+,\mathbf{k}}^\dagger C_{2z}^{-1} = c_{-,-\mathbf{k}}^\dagger$, and $U(\mathbf{k})$ is unitary matrix such that

$$U^\dagger(\mathbf{k}) \begin{pmatrix} h_+(\mathbf{k}) - \mu & \Delta(\mathbf{k}) \\ \Delta^\dagger(\mathbf{k}) & -(h_+(\mathbf{k}) - \mu)^T \end{pmatrix} U(\mathbf{k}) = \begin{pmatrix} E_1(\mathbf{k}) & & & \\ & E_2(\mathbf{k}) & & \\ & & E_3(\mathbf{k}) & \\ & & & E_4(\mathbf{k}) \end{pmatrix}. \quad (\text{E22})$$

We solved Eq. (E21) with

$$\begin{aligned} g_0 &= 40 \text{ meV (nm)}^2 \text{ and } g_1 = 0 \text{ for intrasublattice pairing} \\ g_0 &= 0 \text{ and } g_1 = 70 \text{ meV (nm)}^2 \text{ for intersublattice pairing} \\ \theta &\in \{1.05^\circ, 1.06^\circ, \dots, 1.15^\circ\}, \quad w_0/w_1 = 0.8, \quad v_0 = 5817 \text{ meV} \cdot \text{\AA}, \quad w_1 = 110 \text{ meV}, \quad a_0 = 2.46 \text{\AA}, \\ \text{filling} &= 2.5 \text{ holes per Moiré unit cell}, \\ k_B T &\in 10^{-5} + \{0, 0.02, 0.04, \dots, 0.98, 1\} \text{ meV}, \text{ where we approximate } 0 \text{ as } 10^{-5}, \\ |\mathbf{Q}| &\leq 2\sqrt{7}k_D \text{ for the index } \mathbf{Q}, \\ |\mathbf{G}_M| &\leq 2\sqrt{7}k_D \text{ for } \mathbf{G}_M \text{ in } \tilde{\Delta}_{l,j,\mathbf{G}_M}. \end{aligned} \quad (\text{E23})$$

We find nontrivial real solutions to Eq. (E21) for all twisted angles in Eq. (D6) and for both intrasublattice and intersublattice pairing. According to the terminology in Ref. [26], the intrasublattice pairing is f-wave spin-triplet, and the intrasublattice pairing is d-wave spin-singlet. Indeed, the intrasublattice pairing that we numerically got is $C_{2z}\mathcal{T}$ -invariant parity-even C_{3z} -invariant, while the intersublattice pairing that we numerically got is $C_{2z}\mathcal{T}$ -invariant parity-even and belongs to E irrep.

Let us first focus on the zero temperature. In Fig. 6, we show the $|\Delta_{||}(\mathbf{k})|$ for the intersublattice pairing at zero temperature, and we can see they all only have zeros at Γ_M . We numerically check that the total winding number along a circle surrounding Γ_M is 2, and therefore we know there are two zeros with winding number 1 coinciding at Γ_M . In Fig. 7(a), we show that the zero-temperature chemical potential (after including the correction due to the pairing) in Eq. (D26) always lies in the range $[\epsilon_{\Gamma_M} - |f(\Gamma_M)|, \epsilon_{\Gamma_M} + |f(\Gamma_M)|]$ for both intersublattice and intrasublattice pairings. Thus, we know Asm. 11 is satisfied. Therefore, Prop. 3 suggests that the nodal superconductivity should be expected for the intersublattice pairing for all the θ values in Eq. (E23) at zero temperature, as long as its trivial channel is small enough, which is numerically verified as discussed in the main text. In particular, the zero BdG gap for the intersublattice pairing shown in the main text is checked by finding closed loops with nonzero chiralities of the BdG Hamiltonian, which must include zero-energy gapless nodes as discussed in Appendix. D4. On the other hand, as shown in Fig. 7(b) for $\theta = 1.1^\circ$, the normal-state gap between two nearly flat bands at the FS is roughly $0.1 \sim 0.3 \text{ meV}$, which is smaller than the average zero-temperature pairing amplitude ($\sim 0.5 \text{ meV}$, shown in the main text), meaning that the mechanism for nodal superconductivity arising from nematic pairing proposed in Ref. [27] does not always work in this case, while Prop. 3 works.

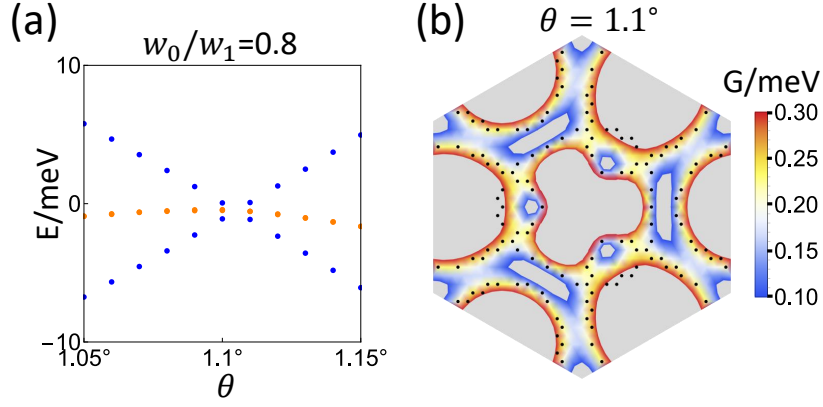


FIG. 7. In (a), we show the energies of the normal-state two nearly flat bands at Γ_M as blue dots, and show the zero-temperature chemical potentials for both intrasublattice and intersublattice pairings with Eq. (E23) as the orange dots. The chemical potential roughly coincide for both intrasublattice and intersublattice pairings at each value of the twist angle. We can see that zero-temperature chemical potential lie in the energy range bounded by the normal-state energies of the two nearly flat bands at Γ_M . In (b), we show the area of the MBZ in which the normal-state gap (G) between two nearly flat bands for $\theta = 1.1^\circ$ is in $[0.1, 0.3]$ meV by the color map, and show the Fermi "surface" as the black dots. We can see the normal-state gap between two nearly flat bands stays roughly in the range $[0.1, 0.3]$ meV at the Fermi "surface".

We further check what are the cases for the MATBG where Asm. 9 is a good approximation for the study of zero-temperature superfluid weight. As shown in Fig. 8(a,c), Asm. 9 is a good approximation for the study of zero-temperature superfluid weight for the intrasublattice and intersublattice pairings derived from Eq. (E21), when the twist angle is very close to 1.1° —for which the normal-state bandwidth is smallest. Therefore, there are cases for the MATBG where Asm. 9 is a good approximation. As shown in Fig. 8(b,d), $\text{Tr}[D_{SF}^{bound}]$ is of the same order of magnitude as $\text{Tr}[D_{SF}]$ evaluated under Asm. 9 for both intrasublattice and intersublattice pairings derived in Eq. (E21) for MATBG.

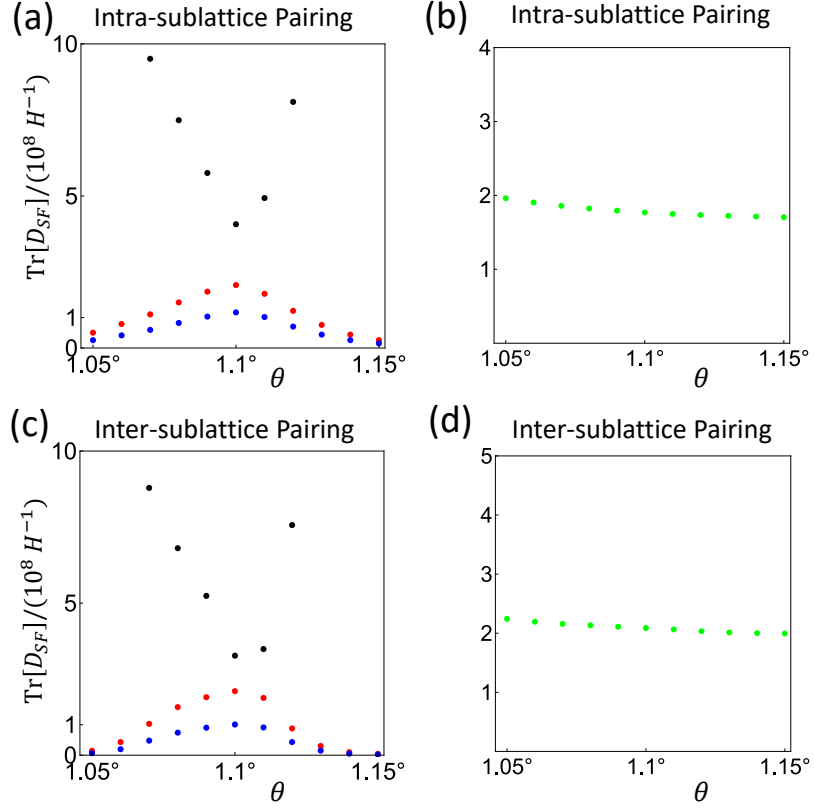


FIG. 8. The superfluid weight has been converted to SI unit in this figure, and is in the zero temperature. (a-b) are for the intrasublattice pairings derived from Eq. (E21) for MATBG, and (c-d) are for the intersublattice pairings derived from Eq. (E21) for MATBG. The black dots stand for the trace of the superfluid weight derived from Eq. (C12) for Eq. (E23), which neglects all high-energy bands. For θ values at which the black dots are missing, the trace of the superfluid weight derived from Eq. (C12) is larger than 10^9 H^{-1} . The red, blue and green dots are obtained by artificially limiting the dispersion of the normal-state nearly flat bands to zero, while keeping the normal-state eigenvectors, the pairing matrix and the filling unchanged. Specifically, the red, blue and green dots stand for the trace of the superfluid weight $\text{Tr}[D_{SF}]$ derived from Eq. (C24), the values of the lower bound $\text{Tr}[D_{SF}^{\text{bound}}]$ in Eq. (C37), and $\text{Tr}[D_{SF}]/\text{Tr}[D_{SF}^{\text{bound}}]$, respectively.

As temperature increases, the pairing would eventually reach zero at the mean-field critical temperature. However, the mean-field critical temperature is typically not what is measured in MATBG experiments; it is the Berezinskii–Kosterlitz–Thouless (BKT) temperature that is typically measured since the superconductivity transition in most 2D systems should be the BKT transition [49]. So, we should estimate the BKT temperature from the pairing in order to compare with the experiments. With μ and $\Delta(\mathbf{k})$ derived from Eq. (E21), we can get $D_{SF}(T)$ using Eq. (C12), and then the BKT temperature can be estimated by Eq. (C21) (be aware of different unit systems in Eq. (C12) and Eq. (C21)). In Fig. 9, we plot the T_{BKT} estimated from Eq. (C21) for both intersublattice and intrasublattice. It shows that the $T_{BKT} \in [1, 2] \text{ K}$ for most of the twist angles, roughly coinciding with the experimentally observed values [72].

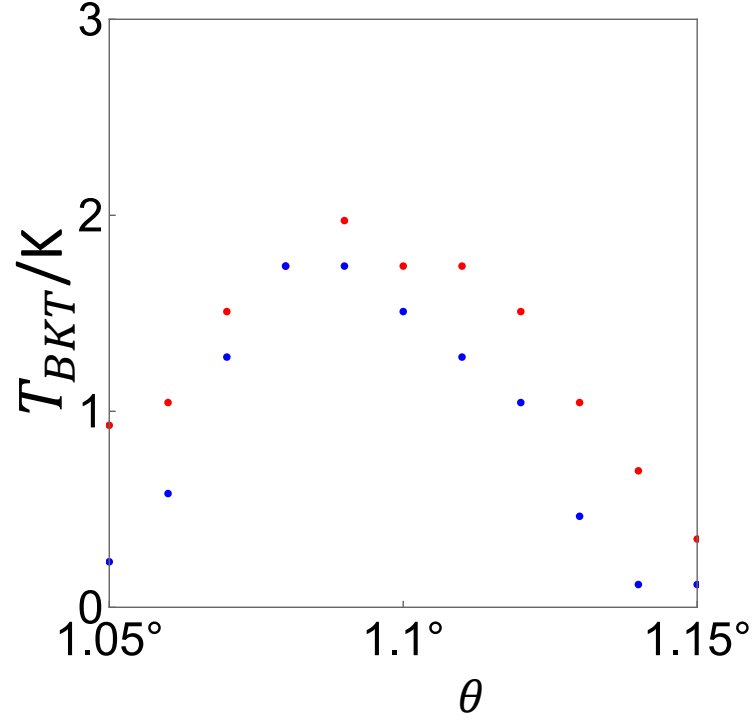


FIG. 9. We show the T_{BKT} estimated from Eq. (C21) with Eq. (E23) for both intrasublattice (blue) and intersublattice (red) pairings.